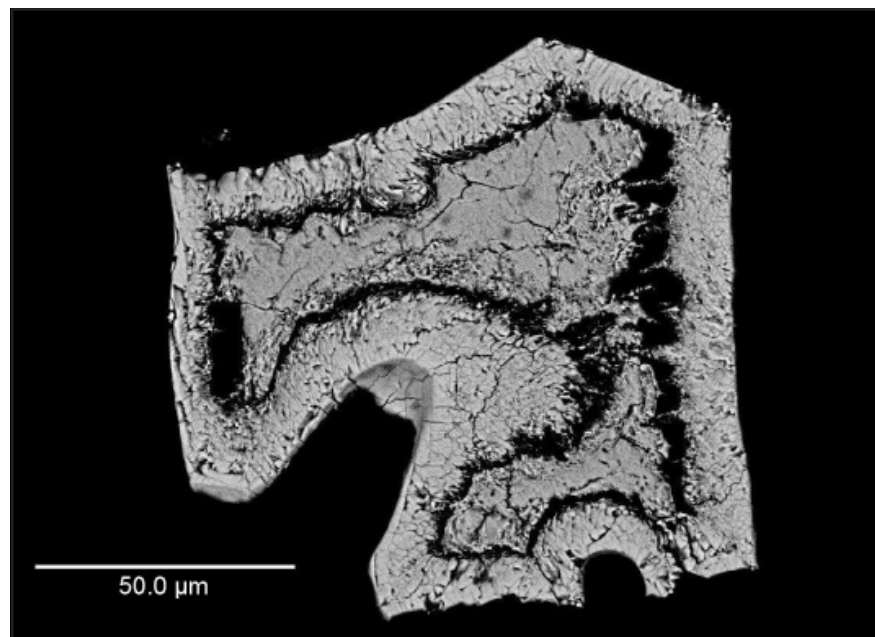


Titanium- and chromium-rich opaque minerals in condensed sediments: chondritic, lunar and terrestrial origins

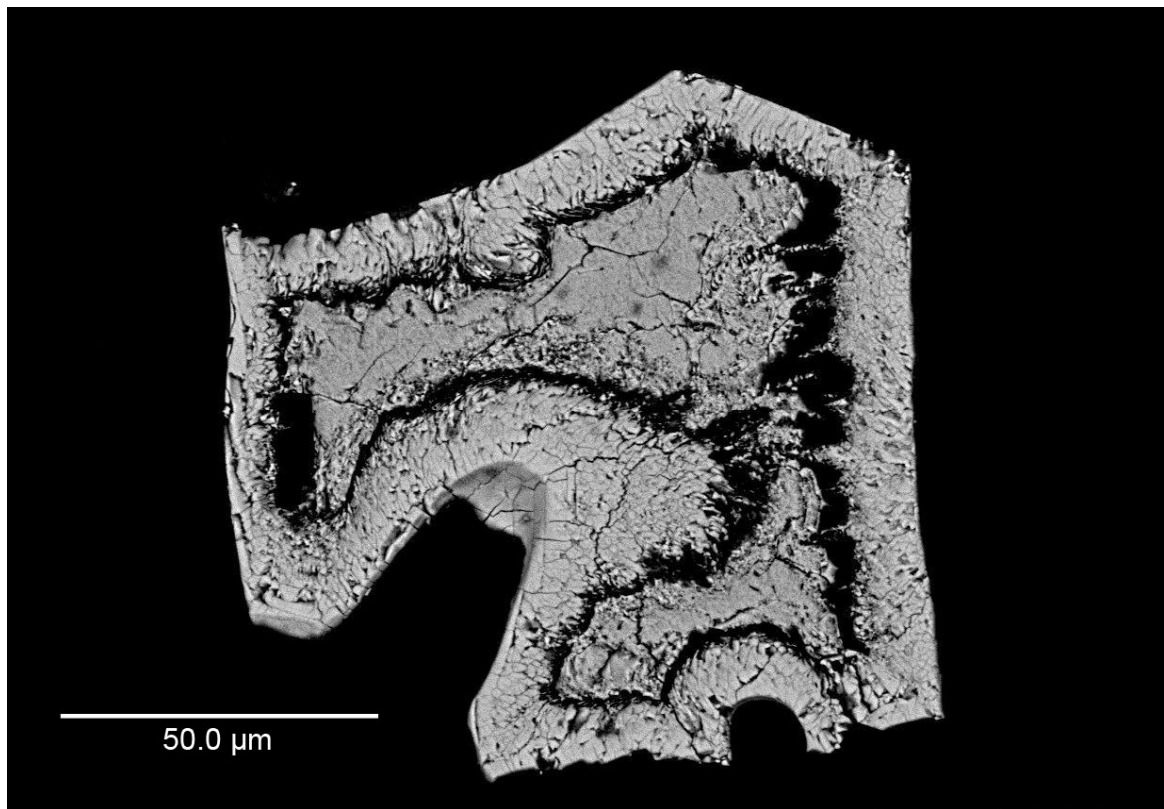
Sanna Holm

Examensarbeten i Geologi vid
Lunds universitet - Berggrundsgeologi, nr. 235
(30 hskp/ECTS)



Geologiska institutionen
Centrum för GeoBiosfärsvetenskap
Lunds universitet
2008

Titanium- and chromium-rich opaque minerals in condensed sediments: chondritic, lunar and terrestrial origins



Master Thesis
Sanna Holm

Department of Geology
Lund University
2008

Contents

1 Introduction	5
2 Sediment-dispersed extraterrestrial chromite grains as tracer for past meteorite flux	6
2.1 A terrestrial concentration mechanism for EC grains and fossil meteorites?	7
3 A lunar origin for the ³He-anomaly in late Eocene sediments?	7
3.1 Delivery of lunar regolith to Earth	8
3.2 How can lunar material be traced in terrestrial sedimentary rocks?	9
4 Mineralogy and composition of ilmenite and Cr-rich spinel	9
4.1 General information about ilmenite and Cr-rich spinel	9
4.1.1 Ilmenite	9
4.1.2 Cr-rich spinel	10
4.2 How to recognize chondritic ilmenite and chromite	10
4.2.1 Chondritic ilmenite	10
4.2.2 Chondritic chromite	12
4.3 How to recognize lunar ilmenite and chrome spinel	12
4.3.1 Lunar ilmenite	12
4.3.2 Lunar Cr-rich spinel	13
4.4 Other Cr-rich spinels (OC)	13
5 Geological Localities	15
5.1 Kinnekulle	15
5.2 Puxi River	15
5.3 Massignano	16
6 Material and Methods	16
7 Results	16
7.1 Kinnekulle	17
7.2 Puxi River	20
7.3 Massignano	23
7.4 Fossil meteorite	23
8 Discussion	24
8.1 Are there any lunar minerals in the sampled sections?	25
8.1.1 Ilmenite alteration	25
8.1.2 Composition of ilmenite from this study and lunar ilmenite	25
8.1.3 Composition of chromite from this study and lunar chrome spinel	26
8.1.4 Possible lunar grains	26
8.1.5 Summary and suggestions for future work	26
8.2 Are there any chondritic minerals in the sampled sections?	27
8.2.1 Possible chondritic ilmenite grains	27
8.3 A terrestrial origin for the ilmenite, OTR and OC grains?	28
8.3.1 The distribution of EC, OC, OTR and ilmenite grains	28
8.3.2 A volcanic origin for the grains?	29
8.3.3 An intrusive source rock?	29
9 Conclusions	31
10 Acknowledgements	31
11 References	31
Appendix	pp. 35-43

Cover Picture: OTR grain recovered from dissolved Orthoceratite Limestone from Kinnekulle, southern Sweden.

Titanium- and chromium-rich opaque minerals in condensed sediments: chondritic, lunar and terrestrial origins

SANNA HOLM

Holm, S., 2008: Titanium- and chromium-rich opaque minerals in condensed sediments: chondritic, lunar and terrestrial origins. *Examensarbeten i geologi vid Lunds universitet*, No. 235, 43 pp. 30 ECTS credits.

Abstract: Evidence from terrestrial sedimentary successions indicate that the amount of extraterrestrial material reaching Earth is not constant, but has been increased during parts of the Phanerozoic. An increase in the flux of extraterrestrial material to Earth has been proposed for the Middle Ordovician and the Late Eocene. These showers of extraterrestrial material on Earth are thought to have resulted from disruption events in the Main Asteroid Belt.

An asteroid shower affecting Earth would also have a great influence on the Moon. A projectile that impacts on the Moon can cause lunar matter to be launched into space, some of which will reach the Earth. Increased amounts of lunar impact ejecta reaching Earth has been proposed to have caused a prominent ^3He anomaly in Late Eocene sediments from Massignano, Italy, as the lunar regolith is extremely enriched in this rare isotope of helium derived from the solar wind. The lunar impact ejecta should not only be preserved in the form of a ^3He anomaly, but minerals representing the ejected matter should also be preserved in terrestrial sediments.

Chrome spinel and ilmenite are resistant minerals that are common in both lunar and terrestrial rocks. These minerals occur in dissolved limestone samples from Kinnekulle, Sweden, eastern Yangtze Gorges area, China, and Massignano, Italy, and their provenance can be discussed based on their chemical composition. Chondritic chromite was confirmed among the grains, but due to the complex overlap in terrestrial and lunar Cr-rich spinel composition, the existence of any lunar chrome spinel could not be definitely confirmed. In order to identify lunar chrome spinel other methods, such as isotope geochemistry, need to be applied.

The study presented in this paper shows that ilmenite is less suitable than Cr-rich spinel when trying to identify lunar minerals in terrestrial sediments. Ilmenite grains are more likely to become altered, which makes provenance studies harder. When comparing the chemical composition of ilmenite grains, which have not been subjected to severe alteration, from this study with the compositions of lunar and chondritic ilmenite it was clear that the grains most likely have a terrestrial origin, even if a few grains have the potential to be of lunar or chondritic origin.

The vast majority of the ilmenite and chrome spinel grains recovered from the dissolved limestone samples come from terrestrial sources. The origin of these grains is discussed in this paper, and the most likely origin for them is erosion of igneous rocks and transportation to the depositional environment by currents.

Keywords: Ilmenite, chrome spinel, ^3He , lunar impact ejecta, source rock, Middle Ordovician, Late Eocene.

Sanna Holm, Department of Geology, GeoBiosphere Science Centre, Lund University, Sölvegatan 12, SE-223 62 Lund, Sweden. E-mail: holm_sanna@hotmail.com

Titan- och kromrika opaka mineral i kondenserade sediment: extraterrestriska och terrestriska ursprung

SANNA HOLM

Holm, S., 2008: Titan- och kromrika opaka mineral i kondenserade sediment: extraterrestriska och terrestriska ursprung. *Examensarbeten i geologi vid Lunds universitet*, Nr. 235, 43 sid. 30 högskolepoäng.

Sammanfattning: Bevis från terrestriska sedimentära lagerföljder att inflödet av extraterrestriskt material till Jorden inte är konstant, utan har varit förhöjt under perioder i fanerozoikum. Ett ökat flöde av extraterrestriskt material till Jorden har föreslagits för mellanordovicium och sen eocen. Orsaken tros vara asteroidskurar orsakade av uppbyggnad av asteroider i asteroidbältet mellan Mars och Jupiter.

En asteroidskur som påverkat Jorden skulle också ha stor påverkan på Månen. En projektil som träffar Månen kan få material att slungas ut i rymden, av vilket en del kommer att nå Jorden. Ökade mängder impaktejekta från Månen har föreslagits vara orsaken till en tydlig ^3He -anomali i sediment från Massignano, Italien, avsatta under sen eocen. Månens regolit är extremt anrikad på den här ovanliga heliumisotopen som kommer från solvinden. Spår av impaktejekta från Månen i terrestriska sediment bör inte bara vara bevarade i form av en ^3He -anomali, utan också i form av bevarade månmineral.

Kromspinell och ilmenit är resistenta mineral som är vanliga i både terrestriska bergarter och på Månen. De här mineralen förekommer i upplösta kalkstensprover från Kinnekulle, Sverige, östra Yangtze Gorges-området i Kina och Massignano, Italien, och deras ursprung kan diskuteras baserat på deras kemiska sammansättningar. Förekomst av kondritisk kromit i proverna kunde bekräftas, men på grund av att sammansättningen hos kromspinell från Månen och terrestrisk kromspinell överlappar kunde inte förekomst av kromspinell från Månen i proverna definitivt bekräftas. För att kunna identifiera kromspinell från Månen måste andra metoder, till exempel isotopgeokemi appliceras.

Studien som presenteras i det här arbetet visar att ilmenit är mindre lämplig att använda än kromspinell när man ska identifiera månmineral i terrestriska sediment. Ilmenitkorn löper större risk att bli omvandlade, vilket försvårar studier av kornens ursprung. När den kemiska sammansättningen hos ilmenitkorn från den här studien, som inte blivit kraftigt omvandlade, jämfördes med sammansättningen hos månilmnit och kondritisk ilmenit blev det klart att kornen sannolikt har ett terrestriskt ursprung, även om några få korn hade potential att vara från Månen eller en kondritisk källa.

Majoriteten av ilmenit- och kromspinellkornen som hittats i de upplösta kalkstensproverna kommer från terrestriska källor. Ursprunget för dessa korn diskuteras i det här arbetet, och det mest sannolika scenariot är att de utgör erosionsrester som förts till depositions miljön av strömmar.

Nyckelord: ilmenit, kromspinell, ^3He , impaktejekta, källbergart, mellanordovicium, sen eocen.

Sanna Holm, Geologiska Institutionen, Centrum för GeoBiosfärvetenskap, Lunds Universitet, Sölvegatan 12, 223 62 Lund, Sverige. E-post: holm_sanna@hotmail.com

1 Introduction

Ever since the formation of the Earth, ~4.6 billion years ago, extraterrestrial material has had an influence on the evolution and development of our planet. The most obvious and spectacular traces of encounters with extraterrestrial matter are impact craters. However, the cratering record on Earth is biased, as the active processes of tectonism and erosion obliterate all evidence of large impacts with time. Due to this lack of a reliable cratering record, and the fact that small extraterrestrial objects do not even form a crater, attention needs to be focused on other sources of information. Information regarding extraterrestrial material reaching Earth can be retrieved from sedimentary successions in the form of Ir-anomalies, shocked quartz and extraterrestrial minerals. Relict extraterrestrial chromite, a resistant common opaque mineral in ordinary chondrites, has been used to determine the flux of extraterrestrial material to the Earth in the past (e.g. Schmitz et al. 2001, 2003; Schmitz & Häggström 2006).

The results of studies of sedimentary successions indicate that the flux of extraterrestrial material to Earth is not constant, but varies significantly and has been increased during periods of the Phanerozoic (e.g. Farley et al. 1998; Schmitz et al. 2001, 2003). There are two main explanations for a varied impact cratering rate: (1) perturbations of the Oort cloud (e.g. Matese et al. 1995), causing increases in the amount of comets with potential Earth-crossing orbits, and (2) break-up events in the inner asteroid belt (e.g. Zappalà et al. 1998).

An increased flux of extraterrestrial matter to Earth has been proposed for the Middle Ordovician and the Late Eocene (e.g. Farley et al. 1998; Schmitz et al. 2001; Fritz et al. 2007). The change in influx of material to Earth has been traced in Ordovician sediments from Kinnekulle, Sweden, by the presence of a remarkably high number of recovered fossil meteorites and sediment-dispersed extraterrestrial chromite grains (e.g. Schmitz et al. 2001, 2003). Also, an anomalously high number of identified craters are of mid-Ordovician age, e.g. the Lockne, Tvären and Granby craters in Sweden.

The Late Eocene is associated with the giant craters Popigai (100 km in diameter; Siberia) and Chesapeake Bay (90 km in diameter; United States), which within age determination uncertainties are given the same age; ~35.5 million years (Koeberl et al. 1996; Bottomley et al. 1997). In addition to these, the period is also known for several smaller impact craters (Montanari et al. 1998) and at least two sedimentary layers of impact debris with microspherules (e.g. microtectites and pancake spherules), Ir-anomalies and shocked quartz found at several places around the world (e.g. Hazel 1989; Molina et al. 1993; Montanari et al. 1993; Clymer et al. 1996; Bodiselsch et al. 2004; Glass et al. 2004). Also, a ^3He -anomaly in a

North Pacific pelagic clay core and in the late Eocene to early Oligocene Massignano section in Italy has been recorded (Farley 1995; Farley et al. 1998).

It has been suggested that an increased cratering rate on Earth also mean that the Moon is more intensely bombarded (Fritz et al. 2007). Fritz et al. (2007) explained that the ^3He -anomaly in the Late Eocene sediments from Massignano reflects an increased infall of ^3He -rich lunar impact ejected material to Earth due to a more intense bombardment of the Moon at that time.

This hypothesis can be tested by searching for lunar minerals that constituted part of the lunar impact ejecta in terrestrial sedimentary rocks. This process is similar to the search for sediment-dispersed extraterrestrial chromite grains in mid-Ordovician limestone (e.g. Schmitz et al. 2003; Schmitz & Häggström 2006). These studies of chromium-rich spinel distribution in limestone from Kinnekulle, southern Sweden, have revealed two groups of grains: chondritic chromite and other chromium-rich spinels (e.g. Schmitz & Häggström 2006). A small fraction of the other chromium-rich spinels may actually come from space (Schmitz et al. 2001; Schmitz & Häggström 2006), but the majority of the grains are terrestrial. The source for the terrestrial grains has been discussed, but no viable explanation has been proposed. As chrome spinel is very resistant, and common in Moon rocks, they will be searched for in this study as well. Ilmenite, the most common lunar opaque mineral, is also resistant and will be searched for. In the previous studies by e.g. Schmitz & Häggström (2006) most of the ilmenite grains were destroyed during the leaching process. With the help from ilmenite grains a potential origin, extraterrestrial or not, for the heavy minerals can be discussed.

The ^3He anomaly, i.e. the potential lunar impact ejecta signal, was detected in sediments from the Late Eocene at Massignano, but the mid-Ordovician limestone at Kinnekulle, or equivalent sections at other localities, is a better place to look for traces of the lunar material. The limestone was deposited during a time when there was a confirmed two orders of magnitude increase in the flux of meteorites to Earth (Schmitz et al. 1996, 2001), most likely due to a break-up event in the inner asteroid belt. The asteroid shower would have caused a major increase in the amount of lunar impact ejecta that was launched into space, and had a chance to reach the Earth.

This paper presents a new perspective on the study of traces of extraterrestrial material in sedimentary rocks, with a pilot study that investigates the possibility of recognizing other extraterrestrial tracers than chondritic chromite in condensed limestones from Kinnekulle, southern Sweden, the eastern Yangtze Gorges area in eastern China and the Massignano section in central Italy. The main purpose of this paper is to attempt to answer these questions:

- Are resistant lunar minerals (ilmenite and chrome spinel) that represent decomposed lunar meteorites and/or dust particles preserved in terrestrial sediments of mid-Ordovician and late-Eocene age, and if so, how can they be recognized?
- With new leaching techniques applied here, allowing also ilmenite to be preserved, can new light be shed on the detailed origin of terrestrial heavy minerals in the limestones?

Aside from these main questions, this paper also presents a review of the background of the search for sediment-dispersed extraterrestrial minerals in mid-Ordovician limestone, which explains why sediments deposited during this period in the Earth's history should have an enhanced content of lunar minerals. A short review of the mineralogy of the Moon is also included.

Studies of the distribution of extraterrestrial tracer minerals in the stratigraphic sections at the chosen localities can give a better understanding of periods when the flux of extraterrestrial matter to Earth was enhanced. Searching for lunar minerals will provide information on how periods of increased cratering rate on Earth has affected the other bodies in the inner Solar System.

2 Sediment-dispersed extraterrestrial chromite grains as tracer for past meteorite flux

Meteorites are extraterrestrial rocks that survived their journey through the Earth's atmosphere and landed on the surface. Traditionally, meteorites are separated into three main groups, each with several further subdivisions; stony meteorites, stony-iron meteorites and iron meteorites. According to a modern classification only two groups are present: undifferentiated (chondrites and primitive achondrites), and differentiated (iron meteorites, stony-iron meteorites and the rest of achondrites).

Chondrites consist of silicates, sulfides and usually metals, and have a chemical composition that approaches that of the volatile-free Sun. Chondrites are remnants of the earliest Solar System and the chemical and isotopic differences among them reflect the heterogeneity in the protoplanetary disk during chondrite parent body accretion. Chondrite classification is primarily based on bulk chemical composition, which differs in the three classes: carbonaceous, ordinary and enstatite. The classes of chondrites are further divided into groups. The ordinary chondrites, which will be in focus in this paper, are separated into three groups based on Fe content: H (high Fe), L (low Fe) and LL (low-Fe, low-metal).

Ordinary chondrites contain, together with, e.g.

silicates such as olivine and pyroxene, also 0.05-0.5 wt. % chromite (Keil 1962). In Ordovician fossil meteorites, the primary mineralogy is almost completely replaced by secondary phases due to magnesium and iron loss. Chromite is the only primary mineral preserved (Thorslund & Wickman 1981). Chondritic chromite retrieved from fossil and recent meteorites has been analyzed in many studies (e.g. Bunch et al. 1967; Thorslund & Wickman 1981; Thorslund et al. 1984; Schmitz et al. 2001; Wlotzka 2005), making the chemical composition of it well known, which allows separating chondritic chromite from its terrestrial equivalent (see below).

The fossil meteorites found in the Ordovician limestone in southern Sweden can be used to interpret the past meteorite influx, but the search for fossil meteorites is time consuming and involves going through thousands of cubic meters of limestone. Instead, the distribution of sediment-dispersed extraterrestrial chromite grains has been used to reconstruct the influx of meteorites to Earth in the past (e.g. Schmitz et al. 2003). Sediment-dispersed chromite grains can be retrieved from acid-dissolved samples of limestone. Chromite is suitable for this purpose as it is very resistant and endures high temperatures and pressures, most acid treatments (including HF), weathering exposure and diagenesis (Schmitz & Håggström 2006).

The limestone beds quarried at the Thorsberg quarry (Fig. 1), southern Sweden, typically contain 1-3 EC grains kg^{-1} (Schmitz et al. 2003; Schmitz & Håggström 2006). The ~5 Myr stratigraphic interval prior to the period of enhanced levels of EC grains and fossil meteorites, contain only 5 grains in 379 kilos of

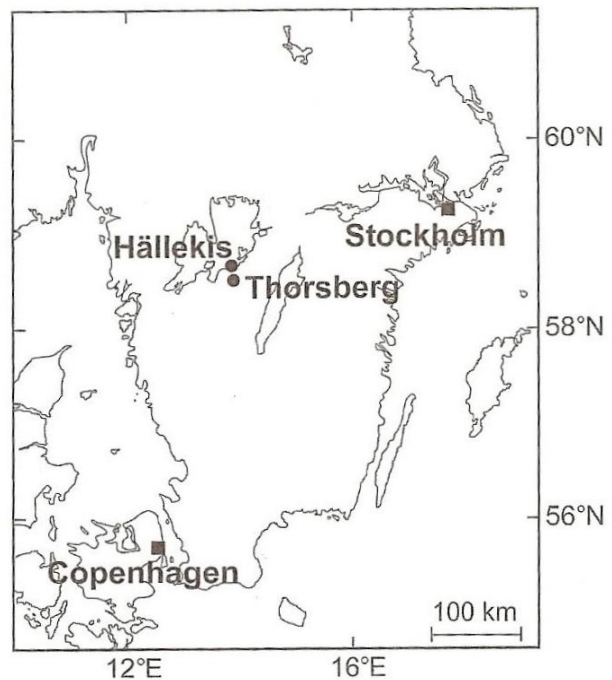


Fig. 1. The location of Hällekis and Thorsberg quarries which are situated on the table mountain Kinnekulle (Schmitz & Håggström 2006).

limestone (~ 0.013 grains kg^{-1} ; Schmitz & Häggström 2006). This is equivalent to a two orders of magnitude increase in the influx of EC grains to Earth (Schmitz et al. 2003). This period of increased flux of extraterrestrial matter to Earth in the Middle Ordovician has been confirmed through the establishment of the influx of extraterrestrial (ordinary chondritic) chromite to Earth during the latest Maastrichtian and Paleocene. In the samples from a section spanning this time interval from Gubbio, Italy, only 6 EC grains were found in 210 kilos (~ 0.03 grains kg^{-1}) of limestone deposited at similar depositional rates as the Kinnekulle Orthoceratite Limestone (Cronholm & Schmitz 2007).

The composition of the chromite grains retrieved from the fossil meteorites from the Kinnekulle limestone suggest that all, or almost all, of the meteorites were L chondrites (Schmitz et al. 2001). According to high-precision ^{40}Ar - ^{39}Ar dating of recent L chondrites, the age of their parent-body disruption is 470 ± 6 Ma. This age falls within the uncertainties of the dating of the beds with fossil meteorites (467.3 ± 1.6 Ma), according to the latest geologic timescale (Korochantseva et al. 2007). Further supporting a common origin for the meteorites is the fact that the amount of cosmic ray-induced ^{21}Ne in the chromite grains increases upwards in the stratigraphy at Kinnekulle (Heck et al. 2004), because the longer time a particle spends in space, the higher its contents of cosmogenic nuclides will be. Thus, the meteorites found at Kinnekulle most likely originate from the same disrupted parent body. The break-up of this asteroid led to the increase in the amount of meteorites, of one to two orders of magnitude, that reached the Earth for a few million years after the event (Schmitz et al. 1996, 2001, 2003).

This information suggests that the mid-Ordovician was a time when an increased amount of lunar impact ejecta would have reached the Earth, as a direct consequence of the enhanced bombardment of the Moon.

2.1 A terrestrial concentration mechanism for EC grains and fossil meteorites?

The fact that the findings of many fossil meteorites and EC grains may be related to some kind of concentration mechanisms rather than an actual increase in the amount of extraterrestrial matter reaching Earth has been discussed by e.g. Schmitz et al. (2003) and Schmitz & Häggström (2006). A concentration mechanism has however been rejected by these authors due to (1): all meteorites and EC grains appear to have a L, or possibly LL, chondritic composition. If a normal, diverse, meteorite population would have been concentrated on the sea floor, the composition would vary among the different meteorites and EC grains. (2): The 40 meteorites which had been recovered by the year of 2001

(Schmitz et al. 2001), represent at least 12 different falls because they have been found on at least 12 different surfaces, separated by hardgrounds. Vertical migration of the meteorites (and EC grains) across hardgrounds after deposition is not likely. (3): The findings of an enhanced amount of L-chondritic meteorites in sediments deposited after a proposed break-up event of an asteroid body of L-chondritic composition (Keil et al. 1994; Bogard 1995), is most likely not a coincidence. The EC grain studies suggest that the disruption event took place right before the deposition of the Arkeologen bed (Schmitz et al. 2001).

3 A lunar origin for the ^3He -anomaly in Late Eocene sediments?

^3He is a rare isotope that can be measured in rock samples and used to detect trace amounts of extraterrestrial matter. ^3He is acquired from the solar wind through bombardment of energetic particles, making extraterrestrial material extremely enriched in this isotope compared to terrestrial material. The solar wind is deflected by the Earth's magnetosphere, and thus terrestrial material is essentially protected from it. The thick regolith layer of the Moon has accumulated ^3He during the past few billion years due to the lack of a lunar magnetic field. Asteroids and comets are not able to retain a thick cover similar to the lunar regolith, as they lack a strong gravitational field. This means that the Moon is richer in ^3He than any comet or asteroid. Actually, approximately seven tons of average lunar regolith contains the annual global average of ^3He that was introduced into marine sediments during the early Oligocene (Fritz et al. 2007; Farley et al. 1998).

Upon atmospheric entry, bodies larger than a few tens of micrometers in diameter are intensely heated and lose their ^3He . Thus, measurements of the ratio between ^3He and ^4He , the only two stable isotopes of helium, in marine sediments can only be used to establish the flux of interplanetary dust particles (IDPs; Farley et al. 1997). These particles, with typical masses of 10^{-12} to 10^{-9} grams, are constantly produced by meteoroid impacts on moons, asteroids and Mars, and by collisions between asteroids. IDPs also originate in periodic comets from the Oort cloud and Kuiper belt.

In a North Pacific pelagic clay core, a prominent ^3He -anomaly close to the Eocene-Oligocene boundary was detected by Farley (1995), but poor age control did not allow for comparison with large known impact structures from the same period. When the late Eocene to early Oligocene Massignano limestone section in Italy was investigated, a correlation between the maxima of a ^3He enhancement lasting 2.5 million years, and the traces of major impact events was discovered (Fig. 2; Farley et al. 1998).

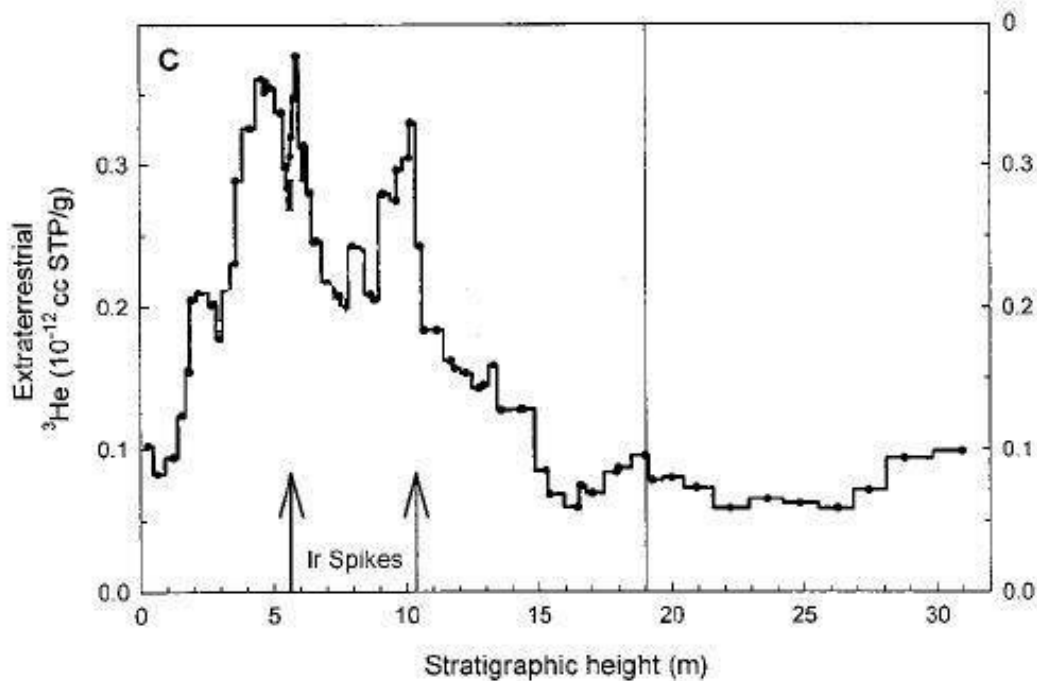


Fig. 2. ^3He concentration in sediments from Massignano, Italy. Stepped curve represent five-point running averages. Vertical line represent Eocene/Oligocene boundary. Cc STP/g, cubic centimeters at standard temperature and pressure per gram (modified from Farley et al. 1998).

The correlation between the impact structures and the enhanced ^3He flux led to speculations regarding a period of enhanced flux of extraterrestrial matter to Earth (Farley et al. 1998), and the ^3He -anomaly was originally interpreted to have been the result of a comet shower triggered by the perturbation of the Oort cloud, e.g. by the passing of a large star (Farley et al. 1998). A comet shower was favored over an asteroid shower e.g. because: (1) the IDP production rate associated with asteroid families decays over hundreds of millions of years, which is much longer than the peak in the late-Eocene sediments lasting only ~ 2.5 million years. (2) The dust formed due to the initial asteroid collision would have arrived to Earth within $\sim 10^4$ years, and thus this cannot explain the long duration of the ^3He anomaly either.

The comet shower theory was rejected by Fritz et al. (2007), who e.g. explained that ^3He -rich particles ejected from long period comets generally are not passing through the Earth's atmosphere at velocities that allow ^3He to be retained because of frictional heating during atmospheric entry. Also, the impact melts of the Popigai (100 km in diameter; Siberia) and Wanapitei (7.5 km in diameter; Canada) craters have platinum group element (PGE) signatures that resembles those of L chondrites currently falling on Earth (Tagle & Claeys 2004, 2005; Tagle et al. 2006). Meteorites are enriched in PGE's compared to crustal rocks, and the PGE signals in the rocks that were melted during impact can be compared to those of known meteorites, and thus give an indication of the impactor origin. Similarly, Cr-isotopic ratios like those in L chondrites have been measured in spherules from

late Eocene sediments (Kyte et al. 2004). Comets are thought to be carbonaceous, and thus they are unlikely to display similar PGE concentrations (Tagle & Claeys 2004) and Cr-isotopic ratios (Kyte et al. 2004) like those of L chondrites. These observations by Tagle & Claeys (2004, 2005), Kyte et al. (2004) and Tagle et al. (2006) are in accordance with the results of a study of cosmic ray exposure ages of recent L chondrites, which showed that a break-up event in the asteroid belt occurred at ~ 40 million years ago (Marti & Graf 1992).

So instead, Fritz et al. (2007) suggested that the cause for the ^3He -anomaly and many late Eocene craters is an asteroid break-up event that led to an increase in the impactor flux in the inner Solar System. Thus, larger amounts of ^3He -rich lunar material would be launched into space after impacts, and have the potential to reach the Earth. This increase in lunar impact ejecta reaching Earth would cause a ^3He -anomaly.

3.1 Delivery of lunar regolith to Earth

The lunar regolith is what separates the solid Moon from space. It is several meters thick and consists of unconsolidated debris that covers the underlying bedrock on almost the entire lunar surface. The regolith has formed due to intensive continuous bombardment of the lunar surface by meteoroids of all sizes and charged atomic particles from the Sun and other stars. The lunar regolith is the source for almost all the information about the Moon presently known to man.

When a projectile impacts on the Moon it can, depending on the angle of impact and speed of impact, cause either projectile mass or target mass, or both, to escape into space (Shuvalov & Artemieva 2006). All meter- to kilometer-sized projectiles are capable of ejecting lunar material equivalent to ~1-4 times the mass of the projectile into space. Impacts that have angles in the range 30°-60° will actually result in a net loss of mass for the Moon (Shuvalov & Artemieva 2006). This process causes some of the ³He-rich lunar regolith to escape into space. High-velocity ejecta will escape as a mixture of melt and vapor due to compression during the impact, but a fraction of the impact ejecta from the uppermost layers of the target material (i.e. the lunar regolith) will escape in a solid state, as lunar meteorites.

According to numerical simulations, 25 to 50 % of ejected lunar material escaping after impact arrives to Earth within 10 Myr. The majority of these particles will arrive within 50 kyr. The fraction of escaping material that does not impact on Earth will either impact on the Moon or escape into heliocentric orbits (Gladman et al. 1995). Today, more than a hundred lunar meteorites have been found on Earth (Meteoritical Bulletin Database; <http://tin.er.usgs.gov/meteor/index.php>), some of which represent the same fall. These meteorites confirm the process of lunar impact ejecta reaching Earth.

3.2 How can lunar material be traced in terrestrial sedimentary rocks?

With a few exceptions, the minerals that make up the lunar rocks and regolith are minerals that are also found on Earth. However, the complete lack of water, common presence of metallic iron and certain trace element ratios are special characteristics of lunar rocks which may be used to distinguish them from terrestrial ones.

As on Earth, silicate minerals dominate the lunar mantle and crust, but on the Moon rarely in the form of quartz. The lunar silicate minerals have slight variations in mineral chemistry compared to terrestrial silicate minerals. Pyroxene, (Ca,Fe,Mg)₂Si₂O₆; plagioclase, (Ca,Na)(Al,Si)₄O₈ and olivine, (Mg,Fe)₂SiO₄, are the most common minerals whereas amphiboles, micas and clays, which are all common on Earth, are absent due to the lack of water. Minerals containing ferric iron are also completely absent as a consequence of the low oxygen fugacity on the Moon.

Oxide minerals are the second most abundant mineral group on the Moon. Some mare basalts contain as much as 20 volume % oxide minerals (Papike et al. 1991), where ilmenite, (Fe,Mg)TiO₃, is the dominating phase. This can be compared to terrestrial basalts, where ilmenite generally does not exceed 5 wt. % (Mason & Melson 1970). The spinel mineral series on the Moon is represented by e.g. chromite, FeCr₂O₄; ulvöspinel, Fe₂TiO₄ and hercynite,

FeAl₂O₄. Also, armalcolite, (Fe,Mg)Ti₂O₅, is frequently found in titanium rich lunar basalts. Less abundant oxide minerals found on the Moon are e.g. rutile, TiO₂, and baddeleyite, ZrO₂.

In contrast to the silicate minerals, the oxide minerals on the Moon display significant differences in composition compared to the composition of terrestrial oxide minerals. This is a consequence of the higher temperatures of formation, the complete lack of water and low oxygen fugacity on the Moon.

The higher temperature of melting and crystallization of igneous rocks on the Moon is a factor that is caused by the lack of water, but alone is not the reason for the significant differences in lunar and terrestrial magmas, as it is only generally about 100° to 150°C higher for melting temperatures around 1200°C. Instead, it is primarily the differences in oxygen fugacity of the Moon and Earth that is the cause for the chemical differences among lunar and terrestrial oxide minerals (Papike et al. 1991 and references therein). The low oxygen fugacity on the Moon prevents any completely oxidized iron (Fe³⁺) from forming and allows e.g. Ti³⁺ and Cr²⁺, which are unusually reduced oxidation states on Earth, to be present in lunar minerals (Papike et al. 1998).

Lunar minerals to look for in terrestrial sediments would be resistant opaque minerals. The silicate minerals are generally very similar to the terrestrial ones whereas the opaque minerals reflect the different environments of formation. The opaques are easily separated from the fraction remaining after acid treatments, and several opaque minerals are resistant and endure acid treatment and diagenetic processes. Ilmenite, the most common opaque lunar mineral, and chromium spinels, which have been frequently reported from dissolved limestone samples from southern Sweden (e.g. Schmitz et al. 2003; Schmitz & Häggström 2006) will be in focus in this paper.

4 Mineralogy and composition of ilmenite and Cr-rich spinel

4.1 General information about ilmenite and Cr-rich spinel

4.1.1 Ilmenite

Ilmenite, with the ideal formula FeTiO₃, is a hexagonal oxide mineral consisting of alternating layers of Ti- and Fe-containing octahedra defined by oxygen atoms (Fig. 3). Terrestrial ilmenite is a common accessory mineral in igneous rocks. It always contains some Fe³⁺, whereas lunar ilmenite never does (see above). In most ilmenite some Mg substitute for Fe, a feature which arises due to the solid solution that exists between ilmenite (FeTiO₃), and geikielite (MgTiO₃). The amount of magnesium in the ilmenite crystal

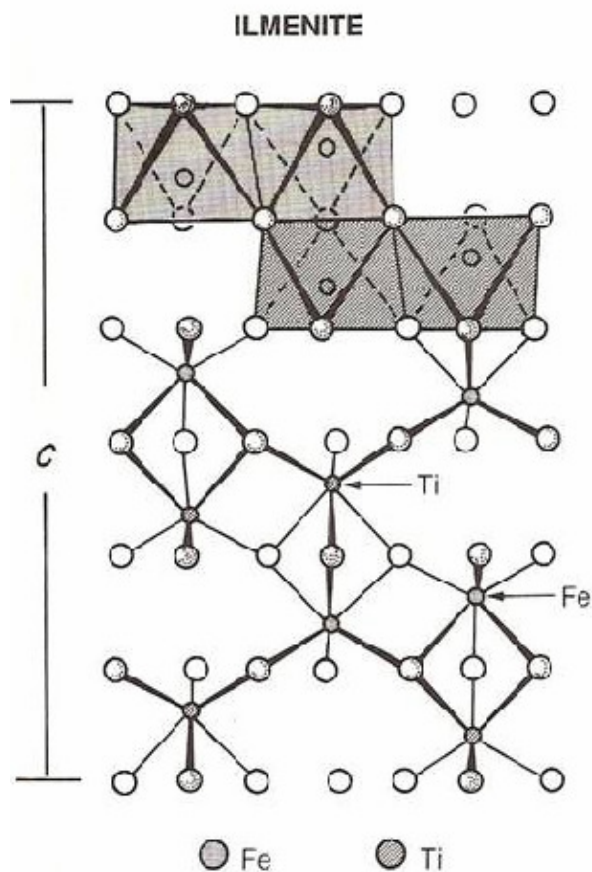


Fig. 3. Crystal structure of ilmenite along c-axis. Oxygen atoms define octahedra which contain the cations, here shown as Ti^{4+} and Fe^{2+} (Modified from Papike et al. 1991).

usually stays below 3 wt. %. Higher concentrations of MgO are primarily found in ultra-mafic, high-pressure rocks such as kimberlites (Papike et al. 1998), but also occur in e.g. trachytes and basalts (see Table 1). Other elements occurring in minor amounts in ilmenite are aluminum, manganese, vanadium and chromium. Al_2O_3 concentrations vary, but usually stay below 1.0 wt. %, which is similar to the contents of vanadium. Low manganese contents (around 1 wt. %) are common due to the solid solution between ilmenite and pyrophanite ($MnTiO_3$). Ilmenite with MnO concentrations greater than 5 wt. % are rare on Earth (Snetsinger & Keil 1969; Snetsinger 1969). Even though the concentration of chromium in terrestrial ilmenite is very low, <0.1 wt. %, it may be significant in extraterrestrial ilmenite. Chemical compositions of ilmenite from a wide range of terrestrial igneous rocks are presented in Table 1.

4.1.2 Cr-rich spinel

Spinel is a group of oxide minerals with extensive solid solution and cubic crystal symmetry (Fig. 4). The cations in the spinel structure occupy both tetrahedral and octahedral positions found in the cubic array of oxygen atoms. The divalent cation, e.g.

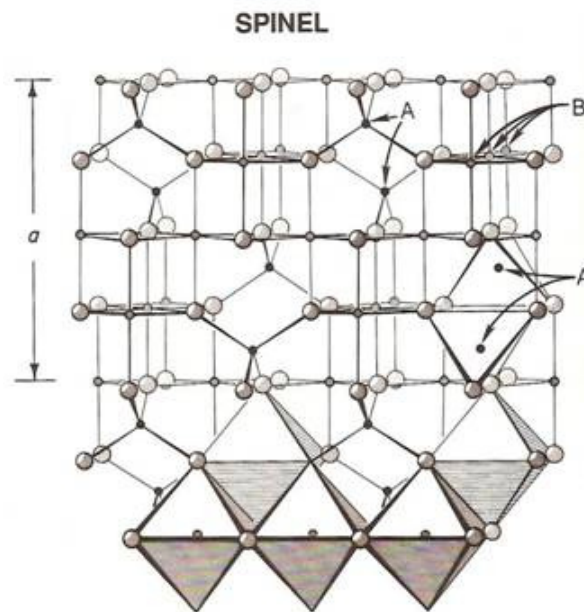


Fig. 4. Crystal structure of spinel along a axis. Oxygen atoms define both tetrahedra (A-site) and octahedra (B-site); modified from Papike et al. 1991).

Fe^{2+} , can occupy both tetrahedral and octahedral positions, whereas the higher-charge cations, e.g. Cr^{3+} , Al^{3+} and Ti^{4+} , are restricted to the octahedral positions. A spinel where the divalent cation occupies both tetrahedral and octahedral positions is called an inverse spinel.

Chromite ($FeCr_2O_4$) is the major ore mineral of chromium on Earth. It is most commonly found in ultra-mafic rocks such as peridotites, but it also occurs in metamorphic rocks. Natural chromite always contains some magnesium substituting for iron due to the solid solution that exists between chromite and magnesiochromite ($MgCr_2O_4$). Aluminum, titanium, vanadium, manganese and zinc are other common minor constituent parts of chromite.

4.2 How to recognize chondritic ilmenite and chromite

4.2.1 Chondritic ilmenite

Snetsinger & Keil (1969) noted that most of the chondritic ilmenite grains they analyzed did not greatly differ from any terrestrial types (Table 2). They do however have mean values of MgO and MnO which are higher than the normal terrestrial ones, above 1.5 wt. % and 1.1 wt. %, respectively. A few grains in Table 2 stand out with unusually high magnesium, manganese, and/or chromium contents.

In contrast to terrestrial ilmenite, which often contain detectable amounts of vanadium, all the analyses presented by Snetsinger & Keil (1969) show concentrations of V_2O_5 that were below the detection limit (100 ppm). The concentration of Al_2O_3 was not determined in some of the grains, and the levels were

Table 1. Representative element concentration (wt. %) of terrestrial ilmenite from different rock types.

Rock type	MgO	Al ₂ O ₃	TiO ₂	V ₂ O ₅	Cr ₂ O ₃	MnO	Fe ₂ O ₃	FeO	SiO ₂	CaO	NiO	ZnO	Total
Granite	0.41	0.68	46.05	0.00	0.00	2.48	10.17	36.62	1.49	1.15	.*	-	99.05
Granite	0.00	0.06	49.10	0.11	0.01	29.60	-	18.20	0.26	0.14	-	-	97.48
Granite	<0.05	-	48.90	-	-	2.70	5.70	41.20	0.10	0.02	-	-	100.00
Granodiorite	-	-	47.31	0.00	0.00	3.16	7.74	40.01	-	-	-	-	98.22
Granodiorite	0.03	0.11	49.00	0.09	0.01	15.20	-	34.00	0.24	0.01	-	-	98.69
Pegmatite	0.48	0.94	46.38	0.00	-	3.60	9.76	36.76	1.07	0.31	-	-	99.30
Pegmatite	0.43	0.55	44.18	0.00	-	5.63	15.72	31.22	1.08	0.10	-	-	98.91
Pegmatite	0.19	1.25	43.25	0.00	-	5.60	15.65	32.25	0.65	0.10	-	-	98.74
Rhyolite	0.31	0.04	49.80	<0.01	<0.01	1.71	5.60	42.50	0.02	0.02	-	<0.01	100.00
Rhyolite	1.93	0.21	41.00	0.15	<0.01	0.72	22.40	33.20	0.02	-	<0.01	0.05	99.80
Pumice	0.40	0.04	48.50	<0.01	<0.01	1.53	8.30	41.30	0.02	0.02	-	<0.01	99.70
Rhyodacite	1.33	0.30	49.80	-	-	0.99	6.70	41.40	-	-	-	-	100.50
Rhyodacite	2.50	0.57	42.80	0.06	<0.01	0.70	17.80	34.20	0.81	0.10	-	<0.01	99.54
Rhyodacite	2.20	0.52	42.20	0.07	<0.01	0.64	18.30	34.20	0.80	0.11	-	<0.01	99.04
Dacite	2.58	0.49	44.40	0.09	0.04	0.41	15.95	34.52	-	0.55	0.02	0.04	99.11
Dacite	2.12	0.28	37.60	0.20	0.03	0.43	29.70	29.60	0.06	0.02	-	<0.01	100.00
Syenite	0.66	1.06	48.36	-	-	0.70	8.91	39.55	0.28	-	-	-	99.66
Syenite	0.14	-	50.85	-	-	7.69	4.15	37.65	-	0.03	-	-	100.51
Syenite	0.05	-	49.40	-	-	1.80	4.10	43.30	0.50	0.01	-	-	99.40
Monzonite	0.07	0.09	48.90	0.12	0.01	3.43	-	45.90	0.19	0.06	-	-	98.77
Monzonite	0.08	0.00	45.43	-	-	2.04	13.60	38.64	-	-	-	-	99.79
Foyaite	0.08	0.00	50.22	-	-	7.86	6.48	37.03	-	0.02	-	-	101.69
Diorite	1.60	0.00	48.79	-	-	2.16	7.94	38.83	-	-	-	-	99.33
Trachyte	3.79	0.36	40.90	0.07	0.01	0.72	24.60	29.30	0.04	0.04	-	<0.01	99.80
Trachyte	3.32	0.00	48.04	-	-	2.32	8.79	34.94	-	-	-	-	97.40
Trachyandesite	4.15	0.57	42.03	-	-	0.00	20.97	30.40	-	-	-	-	98.12
Trachyandesite	1.01	0.41	52.26	-	-	0.81	1.48	44.37	-	-	-	-	100.35
Trachybasalt	0.88	0.04	48.80	-	-	0.79	6.90	41.40	0.13	0.21	-	-	99.30
Trachybasalt	5.64	0.28	49.21	<0.01	-	0.55	10.65	33.64	-	-	-	-	99.97
Tholeiite	1.30	0.15	47.40	0.30	0.00	0.44	9.30	40.00	0.05	0.12	-	0.04	99.10
Tholeiite	0.49	0.02	50.30	0.11	-	0.50	4.40	43.80	0.06	0.07	-	-	99.80
Tholeiite	0.84	0.09	50.48	-	0.02	1.01	4.03	42.87	-	-	-	-	99.34
Basalt	0.69	0.05	49.50	0.21	<0.01	0.70	5.70	42.60	0.14	0.20	-	0.09	99.80
Basalt	4.10	0.80	49.80	-	<0.03	0.80	7.90	36.80	-	-	-	-	100.20
Basalt	1.24	0.15	47.70	0.54	-	0.38	9.40	40.20	0.05	0.14	-	0.07	99.80
Basalt	0.21	0.12	50.53	-	-	0.54	3.70	44.50	-	-	-	-	99.60
Gabbro	1.00	0.37	49.71	<0.01	-	0.85	9.89	38.36	0.08	-	-	-	100.27
Gabbro	2.07	0.42	49.35	0.02	0.05	1.19	6.37	41.08	-	-	-	-	100.55
Gabbro	2.07	0.03	49.58	0.02	0.00	0.92	7.31	40.17	-	-	-	-	100.10
Gabbro	2.31	0.23	48.93	0.01	0.02	2.88	12.17	33.78	-	-	-	-	100.33
Pegmatite	1.10	1.70	44.20	0.10	0.20	2.50	14.70	35.30	0.50	0.10	0.10	-	100.50
Troctolite	2.00	0.60	47.92	0.04	0.11	1.13	8.33	39.76	-	-	-	-	99.89
Troctolite	2.50	0.88	48.55	0.07	0.12	0.94	7.13	39.47	-	-	-	-	99.66
Norite	2.20	0.20	50.10	0.05	-	0.46	5.90	39.90	0.30	0.10	-	0.11	99.40
Norite	0.56	0.40	50.10	0.01	-	0.53	3.90	42.80	0.10	0.10	-	0.13	99.00
Monzonorite	0.66	0.10	51.10	0.02	-	0.53	3.10	43.80	0.20	0.05	-	0.18	99.70
Monzonorite	0.09	0.20	50.10	-	-	0.93	1.80	45.10	0.60	0.07	-	0.13	99.00

* Below detection limit or not analyzed for. Data from Haggerty (1976).

Table 2. Element concentration (wt. %) of ilmenite from ordinary chondrites.

Group	MgO	TiO ₂	Cr ₂ O ₃	MnO	FeO	Total
H3	1.50	54.40	0.06	2.30	41.10	99.36
H4	4.70	53.10	0.07	2.60	40.40	100.87
H5	4.30	51.40	0.11	2.80	41.70	100.31
H5	4.00	51.00	0.09	3.10	41.60	99.79
H5	3.90	52.80	0.12	3.30	40.30	100.44
H5	2.80	51.80	0.12	9.80	35.40	99.92
H6	4.30	51.70	0.04	3.70	39.80	99.54
L4	3.00	52.60	0.08	1.40	41.90	98.98
L4	2.80	53.40	0.03	1.40	42.10	99.73
L5	6.60	52.90	1.04	0.60	38.30	99.44
L5	3.40	52.80	0.09	1.40	41.80	99.49
L6	3.00	52.50	0.04	5.70	38.70	99.94
L6	3.40	52.30	1.40	1.00	41.00	99.10
L6	3.10	52.60	0.53	1.50	41.90	99.63
LL4	2.30	53.10	0.03	1.10	43.30	99.93
LL6	2.50	52.80	0.08	3.80	41.70	100.88
LL6	1.60	51.30	0.56	1.10	43.70	98.26
LL6	2.00	52.10	0.06	1.10	44.60	99.86

Data from Snetsinger & Keil (1969)

below detection limit in the grains where the concentration was determined.

4.2.2 Chondritic chromite

Chondritic extraterrestrial chromite (EC) can be distinguished and separated from terrestrial chrome spinel on the basis of a well defined chemical composition (Schmitz & Haggström 2006). In order for a grain to be classified as EC it has to have Cr₂O₃ concentrations of ~55-60 wt. %, FeO concentrations of ~25-30 wt. %, Al₂O₃ concentrations in the range ~5-8 wt%, and MgO concentrations of ~1.5-4 wt. %. Also, the concentrations of V₂O₃ and TiO₂ have to be in the ranges ~0.6-0.9 wt. % and ~2.0-3.5 wt. %, respectively (see Table 3). If the concentration of any element, one is enough, is significantly outside these defined ranges the grain cannot be classified as chondritic.

4.3 How to recognize lunar ilmenite and chrome spinel

4.3.1 Lunar ilmenite

The most discriminative feature of lunar ilmenite is the

complete lack of Fe₂O₃. However, lunar ilmenite that has settled on Earth may have been subdued to oxidation when meeting a new environment in which it was not stable, and therefore contain Fe₂O₃. In this study, the contents of FeO and Fe₂O₃ have not been used as an indicator of mineral origin.

In contrast to ordinary chondritic ilmenite, which is quite homogeneous (Table 2), lunar ilmenite has a wide variety of compositions (Table 5). This complicates the development of guidelines that are needed in order to identify lunar ilmenite in terrestrial sediments. Table 5 lists compositions of lunar ilmenite from several different rock types.

Many lunar ilmenite crystals have high MgO values (>3 wt. %; Papike et al. 1998). Similar MgO contents can be found in terrestrial ilmenite found in high-pressure rocks (Papike et al. 1998). However, on the Moon, Mg-rich ilmenite is generally not associated with high pressure formation, but are found in rocks that have high Mg contents (Papike et al. 1998). Other elements present in minor to trace amounts in lunar ilmenite (<1 wt. %) are Cr, Mn, Al and V. For example, Mason & Melson (1970) reported minor and trace element concentrations in the range 0.1-0.3 wt. % for Al₂O₃, 0.3-0.6 wt. % for MnO, 0.1-1.3 wt. % for Cr₂O₃ and <0.1-0.2 wt. % for V₂O₃ in ilmenite crystals from Apollo 11 rocks.

The element concentrations presented in Mason & Melson (1970) are similar to those in Table 5, which confirm that lunar ilmenite generally has low Al₂O₃ concentrations (<0.20 wt. %). One grain stands out at 1.13 wt. % Al₂O₃, indicating that a high aluminum content does not rule out a lunar origin. The general pattern for lunar ilmenite is to also have low manganese concentrations at <0.50 wt. % (El Goresy 1981 and references therein; Table 5).

The concentrations of V₂O₃ in lunar ilmenite presented in the analyses by Papike et al. (1998; Table 5) are without exceptions low (<0.10 wt. %). The consistently low concentrations among these grains indicate that this might be something that can be used

Table 3. The average element concentration (wt. % and standard deviation) of EC grains.

	MgO	Al ₂ O ₃	TiO ₂	V ₂ O ₃	Cr ₂ O ₃	MnO	FeO	ZnO
EC grains from one fossil meteorite from Thorsberg quarry, Kinnekulle, 47 grains, this study.	2.60±0.40	6.48±0.29	2.58±0.23	0.79±0.05	59.28±1.40	0.92±0.19	26.13±2.00	1.61±1.47
EC grains from 26 meteorites from Thorsberg quarry, Kinnekulle, 594 grains (Schmitz et al. 2001).	2.57±0.83	5.53±0.29	2.73±0.40	0.73±0.03	57.60±1.30	1.01±0.33	26.94±3.89	1.86±2.43
Chromite from 11 recent H5/6 group chondrites, 261 grains (Alwmark & Schmitz 2007).	2.98±0.23	6.44±0.14	2.20±0.17	0.73±0.02	56.64±0.37	1.00±0.08	29.27±0.67	0.33±0.05
Chromite from 10 recent L5/6 group chondrites, 209 grains (Alwmark & Schmitz 2007).	2.93±0.97	5.97±0.43	2.68±0.40	0.75±0.02	56.00±0.65	0.83±0.10	30.22±2.23	0.30±0.07
Chromite from 13 recent H4-6 group chondrites (Wlotzka 2005).	3.40±0.18	6.64±0.41	1.96±0.29	0.65±0.03	57.1±1.10	0.88±0.07	28.90±0.60	0.28±0.14
Chromite from 6 recent L4-6 group chondrites (Wlotzka 2005).	2.52±0.21	5.90±0.19	2.67±0.44	0.70±0.06	56.10±0.80	0.63±0.08	30.90±0.60	0.34±0.06
Chromite from 4 recent LL3-7 group chondrites (Wlotzka 2005).	1.85±0.14	5.52±0.17	3.40±0.57	0.67±0.10	55.8±0.56	0.51±0.04	31.60±0.62	-*

* Below detection limit or not analyzed for.

Table 4. Rock types and corresponding abbreviations for Tables 5 and 6.

Rock type	Symbol
Mare basalts	
High-Ti (>9% TiO ₂)	
Apollo 11	
high-K (>0.3 K ₂ O)	A-11 HK
low-K (<0.11% K ₂ O)	A-11 LK
Apollo 17	A-17
Low-Ti (1.5-9% TiO ₂)	
Apollo 12	
pigeonite (<10% MgO, <5% TiO ₂)	A-12 pig
olivine (>10% MgO, <5% TiO ₂)	A-12 ol
ilmenite (<10% MgO, >5% TiO ₂)	A-12 ilm
Apollo 15	A-15
olivine (>10% MgO, <5% TiO ₂)	A-15 ol
Meteorite	Met
Aluminous, Low-Ti (>10% Al ₂ O ₃ , 2-5% TiO ₂)	
Apollo 14	A-14 Al
Highland Igneous and Monomict Rocks	
Mg-rich Rocks (variable plagioclase, high-Mg pyroxene)	Mg Rock
Highland Polymict Rocks	
Glassy Melt Breccias (glass with some fragments)	Glassy br
Clast-poor Impact Melt Rocks (crystallized melt with rare fragments)	Melt rock
Soil (single crystals in soil, from unknown rock types)	Soil

Modified from Papike et al. (1998).

to recognize lunar ilmenite, together with the concentrations of Cr₂O₃. Chromium in ilmenite occurs in all the analyses presented in Table 5, in concentrations that are higher than for terrestrial ilmenite (0.2-0.6 wt. % compared to b.d. for the majority of the terrestrial grains; Table 1).

4.3.2 Lunar Cr-rich spinel

Spinel is the second most abundant opaque mineral on the Moon, making up almost 10 volume % of some basalts. Among lunar spinels, the composition can generally be found within the three-component system FeCr₂O₄-FeFeTiO₄(inverse spinel)-FeAl₂O₄. Most compositions fall between chromite and ulvöspinel

(Papike et al. 1991).

Unlike chondritic chromite, lunar chrome spinel has a wide variety of compositions (Table 6). Lunar chrome spinel is lower in Cr₂O₃ (~37-52 wt. %) and higher in Al₂O₃ (~9-18 wt. %) than chondritic chromite and it often contains appreciable amounts of ulvöspinel in solid solution, i.e. it has a high titanium content (El Goresy 1981). The concentrations of MgO and FeO vary significantly among the presented analyzes, in contrast to chondritic chromite (Table 6). It is not clear whether the concentration of vanadium was not determined, or if concentrations were below detection limit in the studies where no such values are presented (see Table 6). The concentration of vanadium was probably not determined, since the values for the other lunar samples are high (>0.70 wt. %), and chromite from other extraterrestrial sources (chondrites and other types of meteorites; Bunch & Keil 1971) almost always contain vanadium. Papike et al. (1991) concluded that chrome spinel from the Apollo 12 lunar samples has relatively high contents of V₂O₃ (~0.7-1.0 wt. %), values that match those in the results of El Goresy et al. (1971), Taylor et al. (1971), Nehru et al. (1974) and Anand et al. (2006).

The lack of consistency in lunar chrome spinel composition makes it hard to give any guidelines for how to separate lunar chrome spinel from certain terrestrial Cr-rich spinels, which may have very similar compositions (see Barnes & Roeder 2001).

4.4 Other Cr-rich spinels (OC)

During the searches for EC grains in dissolved limestone samples, chromium-rich spinels that do not

Table 5. Element concentration (wt. %) of lunar ilmenite.

Rock type*	MgO	Al ₂ O ₃	TiO ₂	V ₂ O ₃	Cr ₂ O ₃	MnO	FeO	ZrO ₂
A-11 HK	1.39	<0.03	52.22	-**	0.53	0.15	44.38	-
A-11 HK	1.14	<0.03	54.53	-	0.53	0.02	44.84	-
A-11 LK	0.75	-	53.00	-	0.52	0.45	45.10	-
A-12 ol	5.14	0.02	53.80	0.07	0.51	0.42	40.50	-
A-11 ol	2.28	0.03	53.00	0.04	0.75	0.41	44.10	-
A-12 pig	0.47	0.04	52.25	-	0.18	0.30	46.74	-
A-12 ilm	0.39	0.28	52.34	-	0.24	0.34	45.16	-
A-12 pig	0.01	1.13	52.91	-	0.19	0.31	46.30	-
A-12 ilm	0.10	0.42	53.90	0.04	0.39	0.36	45.40	-
A-12 ol	0.09	0.12	52.70	0.06	0.23	0.37	46.70	-
Mg Rock	8.20	0.19	51.70	-	0.58	0.20	37.70	-
Glassy br	3.85	0.6	59.35	-	0.85	-	34.30	-
Melt rock	0.83	0.1	52.66	-	0.38	0.32	44.62	-
A-14 Al	0.72	0.09	53.24	-	0.35	0.47	45.30	0.05
A-15 ol	0.27	0.09	50.70	-	0.23	0.52	46.84	-
A-17 basalt	0.72	0.15	53.10	-	0.39	0.44	45.70	0.04
Luna 16 soil	0.86	0.17	52.00	-	0.58	0.50	44.70	-
Luna 20 soil	8.00	-	53.70	-	0.39	0.36	37.10	-

* See Table 4.

** Below detection limit or not analyzed for.

Data from Papike et al. (1998).

Table 6. Element concentration (wt. %) of lunar chrome spinel.

Rock Type* and Reference	MgO	Al ₂ O ₃	TiO ₂	V ₂ O ₃	Cr ₂ O ₃	MnO	FeO	SiO ₂	CaO	CoO	Total
Met (Anand et al. 2006).	3.60	11.90	5.24	0.78	43.90	0.24	33.30	0.06	0.03	-**	99.10
A-12 ilm (Taylor et al. 1971).	3.40	10.60	8.71	0.99	40.00	0.58	36.30	-	0.03	0.05	100.70
	2.26	10.30	9.22	0.86	38.30	0.38	39.00	-	0.04	0.04	100.40
	1.89	11.10	6.74	0.97	42.20	0.40	36.60	-	0.05	0.04	100.00
A-12 ol (Taylor et al. 1971).	3.30	10.10	8.89	0.87	39.60	0.59	36.90	-	<0.02	0.05	100.30
	4.58	11.50	4.66	0.98	48.50	0.42	30.00	-	0.03	0.06	100.70
	3.29	11.70	5.13	0.95	47.90	0.38	30.70	-	0.04	0.06	100.20
Luna 16 soil (Haggerty 1972a).	6.67	14.48	0.92	-	51.49	0.46	25.85	0.76	0.38	-	101.01
	6.43	14.37	0.77	-	50.72	0.46	25.87	0.68	0.30	-	99.60
	7.75	17.70	0.83	-	49.52	0.53	23.58	0.37	0.20	-	100.48
	6.77	17.52	1.06	-	49.16	0.63	25.63	0.06	0.21	-	101.04
	7.05	17.36	0.83	-	49.00	0.53	25.33	0.41	0.20	-	100.71
	7.48	17.05	0.95	-	48.85	0.53	24.01	0.34	0.20	-	99.01
	8.00	18.09	0.95	-	47.98	0.50	24.11	0.36	0.17	-	100.16
	3.63	17.87	0.77	-	46.14	0.38	30.97	0.22	0.17	-	100.15
	1.32	10.11	5.69	-	43.80	0.52	37.33	0.58	0.32	-	99.67
	1.76	12.16	5.25	-	43.54	0.42	36.97	0.29	0.16	-	100.55
	1.01	9.55	6.14	-	43.07	0.55	37.81	0.57	0.35	-	99.05
	1.06	9.48	6.27	-	42.99	0.59	37.97	0.52	0.35	-	99.23
	1.09	9.46	6.38	-	42.93	0.46	37.85	0.52	0.35	-	99.04
A-15 (Nehru et al. 1974).	2.01	12.00	3.70	1.03	44.30	0.31	34.20	1.00	0.51	-	99.06
A-15 ol (Haggerty 1972b).	2.35	11.76	4.10	-	46.28	0.44	35.21	0.19	0.03	-	100.37
	6.10	12.65	4.58	-	43.79	0.49	30.74	0.56	0.11	-	99.01
	3.35	11.35	6.10	-	42.79	0.46	34.35	0.41	0.20	-	99.01
A-12 ol (El Goresy et al. 1971).	2.01	9.66	10.01	-	37.69	0.41	40.29	0.19	0.03	-	100.30
A-12 ilm (El Goresy et al. 1971).	5.89	11.70	5.29	0.98	46.50	0.29	30.10	-	-	-	100.75
A-12 ilm (El Goresy et al. 1971).	3.94	11.00	10.80	0.92	34.90	0.20	37.80	-	-	-	99.56
A-12 ilm (El Goresy et al. 1971).	3.92	11.00	6.27	0.74	43.80	0.27	33.30	-	-	-	99.30
A-12 ol (El Goresy et al. 1971).	3.43	11.70	4.27	0.95	46.00	0.24	32.30	-	-	-	98.89

* See Table 4.

** Below detection limit or not analyzed for.

represent chondritic chromite have been frequently recovered (e.g. Schmitz & Häggström 2006; Schmitz et al. in press). These are referred to as other chromium-rich spinels (OC) and primarily represent terrestrial chromium-rich spinels, but a small portion may also represent Cr-rich spinels from other extraterrestrial sources (Schmitz et al. 2001; Schmitz & Häggström 2006), with a different composition than in chondritic material.

The OC grains show a wide compositional range (Table 7 and 8, in appendix), where e.g. the Al_2O_3 concentrations vary between 4 and 42 wt. %, and the Cr_2O_3 concentrations vary between 19 and 64 wt. %. The main differences from the EC grains lie in the generally lower TiO_2 , Cr_2O_3 , V_2O_5 and MnO concentrations and higher Al_2O_3 and MgO concentrations.

5 Geological Localities

5.1 Kinnekulle

Kinnekulle is a 306 meter high table mountain situated south of Lake Vänern in Sweden. The mountain consists mainly of sedimentary rocks of Cambrian to Silurian age that have been protected by a horizontal dolerite sill. The sediments of Ordovician age are dominated by the Orthoceratite Limestone, where the fossil meteorites and sediment-dispersed chromite grains have been found (e.g. Schmitz et al. 1996, 2001; Schmitz & Häggström 2006). The limestone was deposited mainly during the Arenigian and Llanvirnian, at an average sedimentation rate of one to a few millimeters per one thousand years, in a vast epicontinental sea that covered large parts of the Baltoscandian Shield (Lindström 1971, 1979). Hardgrounds are abundant, and they represent periods of 100 to 1000 years when currents prevented fine detritus from settling on the sea floor (Lindström 1979). The color of the limestone varies between red to brown/red with a 1.4 meter thick gray section deposited during a period of limited sea floor oxygen availability in the depositional environment (Fig. 5). The limestone beds are horizontal and have not been subjected to any tectonism or metamorphism.

At Kinnekulle, the limestone beds are exposed at two quarries, Thorsberg and Hällekis (Fig. 1). The beds have been given traditional names from the quarrying industry (Fig. 5). Arkeologen is the bed where the majority of the fossil meteorites have been found, and also the bed which has the highest concentration of EC grains per kilo of limestone ($3.3 \text{ grains kg}^{-1}$ in the lower middle part of the bed; Schmitz & Häggström 2006).

5.2 Puxi River

The limestone of the Lower to Middle Ordovician Guniutan (Kuniutan) Formation in the eastern Yangtze

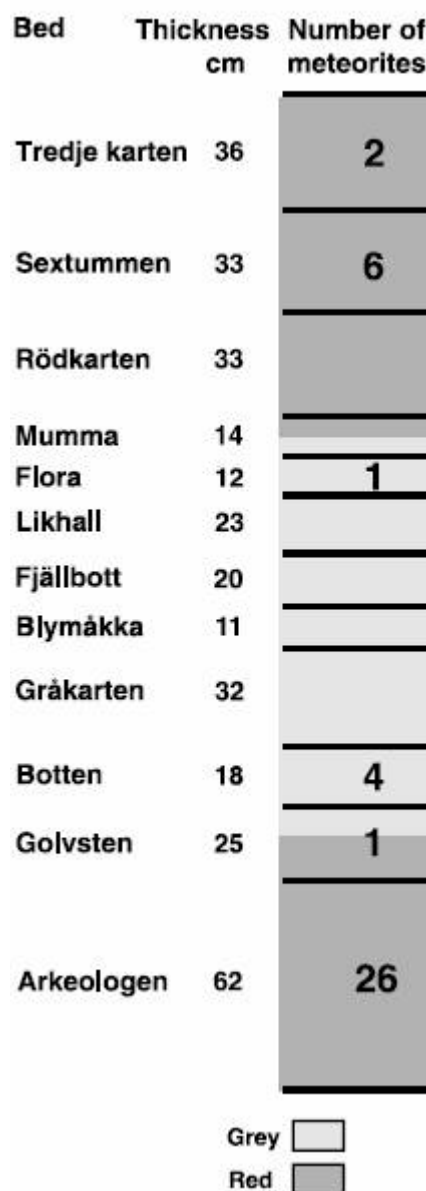


Fig. 5. Meteorite distribution in quarried beds at Thorsberg quarry (modified from Schmitz et al. 2003).



Fig. 6. Outline map of China showing Yangtze platform (grey area). The black dot marks the Yangtze Gorges area (Lindström et al. 1991).

Gorges area in eastern China (Fig. 6) is very similar to the Orthoceratite Limestone at Kinnekulle, and the other localities in northern Europe where the Orthoceratite Limestone can be found, with respect to facies, stratigraphic development and conodont biostratigraphy (Lindström et al. 1991). The Guniutan formation consists of nodular and bedded limestone with alternating layers of marl and shale. The locality that was sampled for this study is called Puxi River (section described in Schmitz et al. 2008).

5.3 Massignano

The Massignano section in central Italy (Fig. 7) is a continuous sequence of pelagic marly limestone and calcareous marls, interbedded with several volcano-sedimentary layers, that covers the upper part of the Eocene and the lowermost part of the Oligocene.

The Massignano limestone section is the Global Stratotype Section and Point (GSSP) for the Eocene/Oligocene boundary (Silva & Jenkins 1993). The section contains a thin impact ejecta layer that has been linked to the Popigai crater in Russia (Glass 2002), and three iridium anomalies (Montanari et al. 1993; Bodiselitsch et al. 2004). Two of these have been linked to the impact craters Popigai and Chesapeake Bay, where one is located in the impact ejecta layer at 5.6 m. The ejecta layer also contains e.g. shocked quartz (Clymer et al. 1996) and extraterrestrial Ni-rich spinel found clustered in flattened spheroids (Pierrard et al. 1998). The ^3He anomaly reported by Farley et al. (1998; Fig. 2) covers the stratigraphic interval ~5-10 meters.



Fig. 7. Outline map of Italy showing geographical position of Massignano (outline map modified from <http://geography.about.com/library/blank/blxitaly.htm>).

6 Material and Methods

Five samples, with weights ranging between 4.45 and 17.9 kilos, of limestone from Kinnekulle, Puxi River and Massignano were dissolved for the chrome spinel and ilmenite searches (Table 9). From Kinnekulle, two samples from the Golvsten bed (Fig. 5) were dissolved, one representing the top half and one representing the bottom half of the bed. These are referred to as GOL top and GOL bottom. Two samples were also dissolved from the Puxi River section, Y9 and P6a. The samples come from the same interval as the Kinnekulle section, i.e. the middle Darrwilian (see Schmitz et al. 2008 for details). The Massignano sample comes from the impact ejecta layer, i.e. 5.6 m. In addition to the limestone samples, the opaque mineral content in a fossil meteorite from the Kinnekulle limestone (Thorsberg quarry) was analyzed.

The samples were decalcified in 6 M (1:1) hydrochloric acid at room temperature with occasional stirring, and then sieved at 32 μm . The residue was leached in hydrofluoric acid (7 %) at room temperature for approximately 20 minutes. In previous studies (e.g. Schmitz et al. 2003; Schmitz & Haggström 2006) the samples have been leached in 18 M hydrofluoric acid (1:1) for two days with occasional stirring, which has caused the majority of the ilmenite grains to be destroyed. A few grains might have been preserved due to insufficient stirring, or if they were covered by mud. The acid insoluble fraction was sieved and the fraction 63-355 μm was searched for opaque minerals under a stereomicroscope. Suspected chrome spinel and ilmenite grains were picked with a fine brush. The grains were mounted in epoxy resin and polished flat using a 1 μm diamond slurry. Quantitative elemental analyzes were performed with an energy dispersive spectrometer (INCA x-sight, Oxford Instruments), with a Si detector linked to a Hitachi S-3400N scanning electron microscope. The grains were analyzed at an acceleration voltage of 15 kV, a beam 1-2 μm in diameter and a counting live-time of 80 seconds. Cobalt was used as calibration element. The precision of analyzes was between 1-4 %, with the analytical accuracy controlled by repeated analyzes of the USNM 117075 chromite reference standard (Jarosewich et al. 1980). Each grain was analyzed at 3-5 different points after which a mean value was calculated. All the iron is shown as Fe^{2+} . The content of Fe_2O_3 in the titanium-rich grains was calculated manually for the classification of the grains as either ilmenite or other titanium-rich grains (see below).

7 Results

A total of 68 chromite grains and 193 titanium-rich grains were found in the samples (Tables 10-15, in appendix; Figs. 8-15). The chromites are all referred to

Table 9. The distribution of EC grains, ilmenite grains and OTR grains in the limestone samples.

Sample	Sample size (kg)	EC grains			ILM & OTR grains (kg ⁻¹)	
		No. EC grains	(kg ⁻¹)	No. ILM grains		No. OTR grains
Golvsten top	13.6	6	0.4	11	29	2.9
Golvsten bottom	17.9	6	0.3	48	21	3.9
Y9	4.45	10	2.2	3	-	0.7
P6a	6.15	5	0.8	1	-	0.2
Massignano	10.1	-	-	81	-	8.0
Fossil Met.	-	47	-	-	1	-

as EC grains because they all have compositions within the defined ranges for chondritic chromite (see above). No OC grains were found in the Golvsten samples, but compositions of OC grains from the Arkeologen and Golvsten beds from a previous study (Schmitz & Häggström 2006) are presented in Table 7. The grains from these beds were chosen because they are from the bed where the highest amounts of EC grains have been found (Arkeologen; Schmitz & Häggström 2006), and the bed immediately above, called Golvsten, which has been searched for chrome spinel and ilmenite in this study. Considering the fact that the Arkeologen bed is so rich in EC grains, that bed is where the highest amounts of lunar minerals should be. Similarly, the compositions of 35 OC grains from the Massignano limestone from Schmitz et al. (in press) are presented in Table 8.

The titanium-rich grains are divided into two groups: ilmenite and other titanium-rich (OTR) minerals. The difference between ilmenite and the OTR grains is the tendency for the OTR grains to have higher TiO₂ concentrations at about 53-60 wt. %, compared to about 46-50 wt. % for the ilmenite grains (Fig. 8 and 14), and lower FeO concentrations at about 33 wt. % compared to ~38-41 wt. % for the ilmenite grains. The reason for why the grains are called OTR and not ilmenite is the fact that the TiO₂ concentrations are too high for any normal ilmenite crystals (as determined by compositional stoichiometry).

Magnesium, aluminum, vanadium and manganese were present as minor constituents in chromite and the titanium-rich grains. In addition to these, many of the titanium-rich grains also contain small amounts of Cr₂O₃ (typically ~0.05-0.10 wt. %) at some analysis points, but only one grain had concentrations that were above detection limit for all the analyzed points (Table 11; ILM 6), and a few of these grains contain silica. In the chromite grains, additional minor elements are titanium and zinc. ZnO occurs due to post-depositional alteration, which normally causes some of the iron in the chromite crystal structure to be replaced by zinc.

7.1 Kinnekulle

After searching the Golvsten bed samples, a total of six extraterrestrial chromite grains had been found. Each sample contained three grains (Tables 10 and 11), and another 3 EC grains from each sample had

been sent for oxygen isotopic analysis, meaning that the samples contained 12 EC grains in total. The titanium-rich opaque grains that were separated were far more abundant than the EC grains. 59 ilmenite grains and 50 OTR grains were found (Tables 10 and 11), where the abundance in each sample is 3.9 grains kg⁻¹ for GOL bottom and 2.9 grains kg⁻¹ for GOL top (Table 9).

The titanium-rich grains from Kinnekulle show a wide compositional range, and thus they plot over a large area (Figs. 8 and 9). Similarly, the OC grains also have a wide compositional range and plot over a large area (Fig. 10). This in contrast to the EC grains, which plot close together due to their more narrow compositional range (Figs. 11-13).

Many of the ilmenite grains have wt. % concentrations of TiO₂ that are lower than the total amount of FeO plus Fe₂O₃, or TiO₂ values close to those of FeO plus Fe₂O₃. One example of this is GOL bottom ilmenite ILM 45 (Table 11) with TiO₂ concentrations of 44.05 wt. % and FeO concentrations of 44.89 wt. %. This is in contrast to ideal ilmenite (~52 wt. % TiO₂ and ~47 wt. % FeO), and the extraterrestrial ilmenite grains (Tables 2 and 5), which have TiO₂ concentrations of ~52-54 wt. % and FeO concentrations of ~40-45 wt. %. The “low” titanium values and “high” iron values are probably caused by fine intergrowths of hematite in the ilmenite crystals, and/or post-depositional alteration (see below).

Another common feature among both ilmenite and OTR grains are total wt. % values that are below 97 % (Tables 10 and 11), which is the limit of when an analysis is considered valid. This can be explained by several factors, where one is that the Fe₂O₃ concentration in the grains has not been taken into account. For the grains with total values below ~95 %, the existence of Fe₂O₃ cannot alone explain the low percentage. The spectras were carefully searched for other detected elements, but no others than the ones presented were found. Instead, the phenomenon is most likely caused by alteration of the ilmenite grains, where the existence of more than one phase disturbs the analysis. In addition to this, the altered grains were hard to polish, and even after polishing many grains had irregular surfaces, which also disturbs the analysis.

The majority of the ilmenite and OTR grains from the Golvsten samples show signs of alteration (Figs. 16-19). Grain boundary alteration, common among grains from both samples, generally appears as a

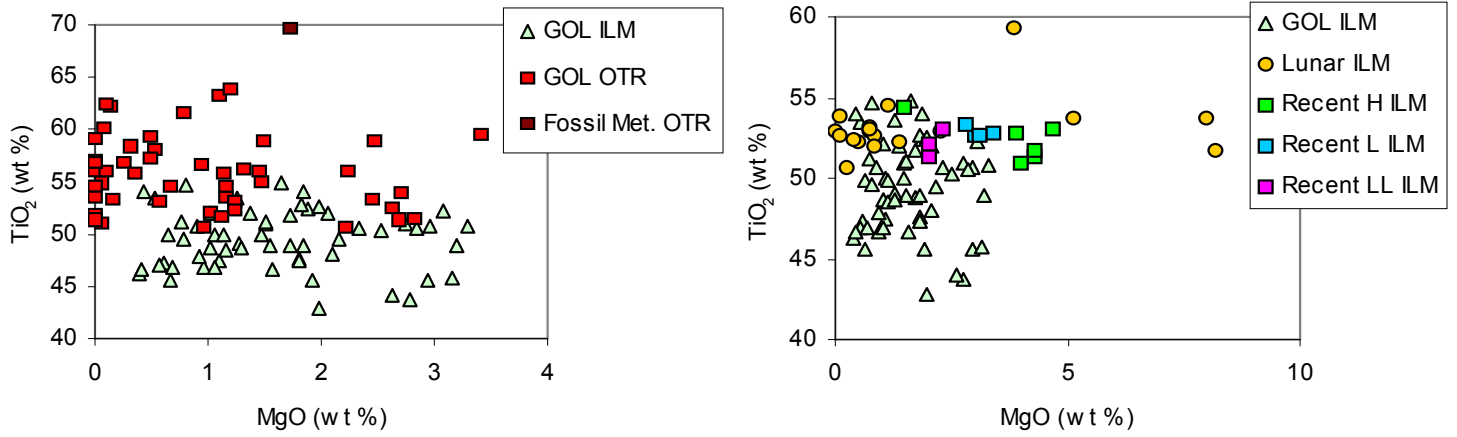


Fig. 8. Chemical composition of individual ilmenite and OTR grains in wt. % (data from Tables 10, 11 and 15). Composition of ilmenite grains from recent H, L and LL chondrites (data from Snetsinger & Keil 1969; Table 2), and lunar ilmenite (data from Papike et al. 1998; Table 5) is also shown.

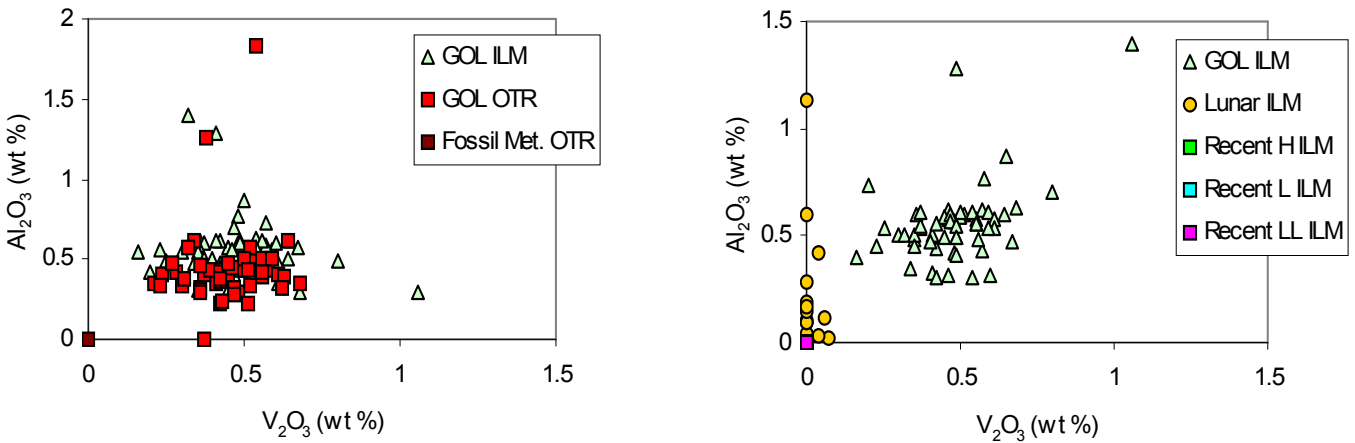


Fig. 9. Chemical composition of individual ilmenite and OTR grains in wt. % (data from Tables 10, 11 and 15). Composition of ilmenite grains from recent H, L and LL chondrites (data from Snetsinger & Keil 1969; Table 2), and lunar ilmenite (data from Papike et al. 1998; Table 5) is also shown.

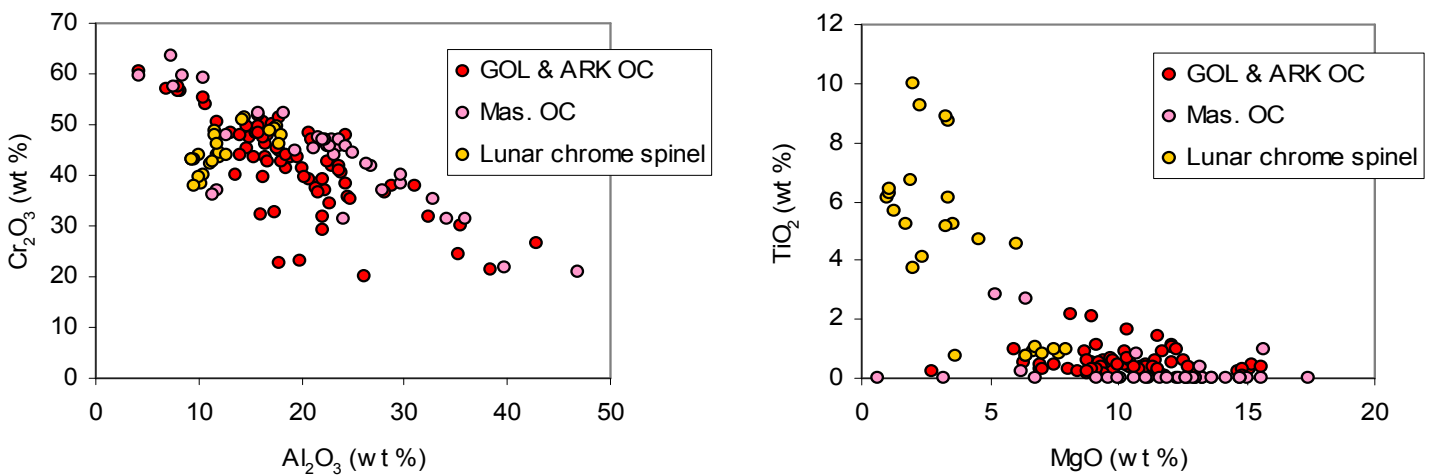


Fig. 10. Chemical composition of individual OC grains (Schmitz & Häggström 2006; Table 7 and Schmitz et al. in press; Table 8) and lunar chrome spinel grains (data and references in Table 6) in wt. %.

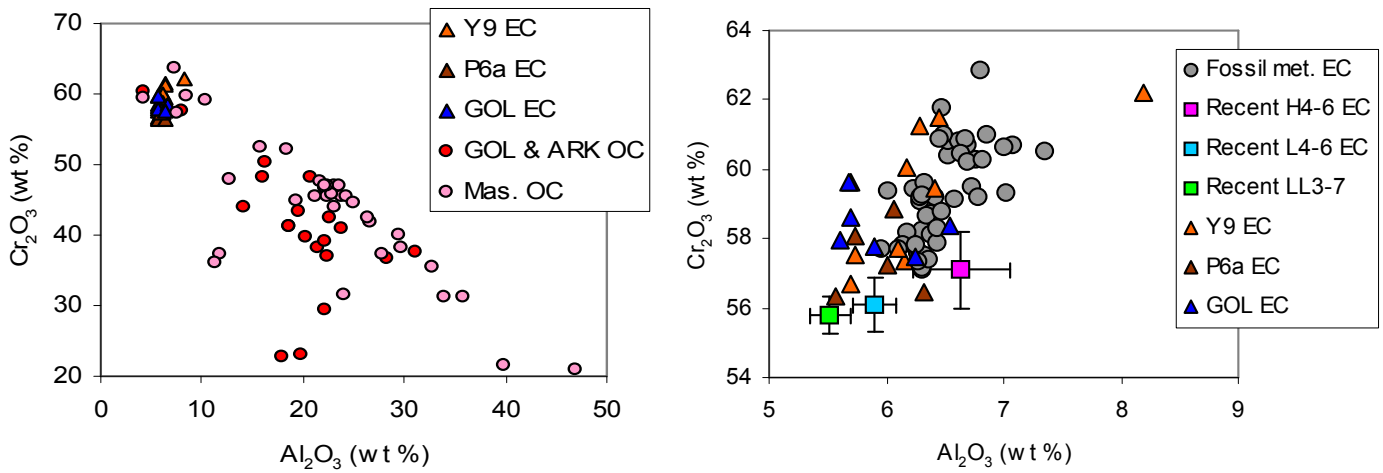


Fig. 11. Chemical composition of individual EC (data from Tables 11-13) and OC grains (data from Schmitz & Häggström 2006; Table 7 and Schmitz et al. in press; Table 8) in wt. %. Average composition, with standard deviation fields, of chromite grains from recent H, L and LL chondrites (data from Wlotzka 2005; Table 3) is also shown.

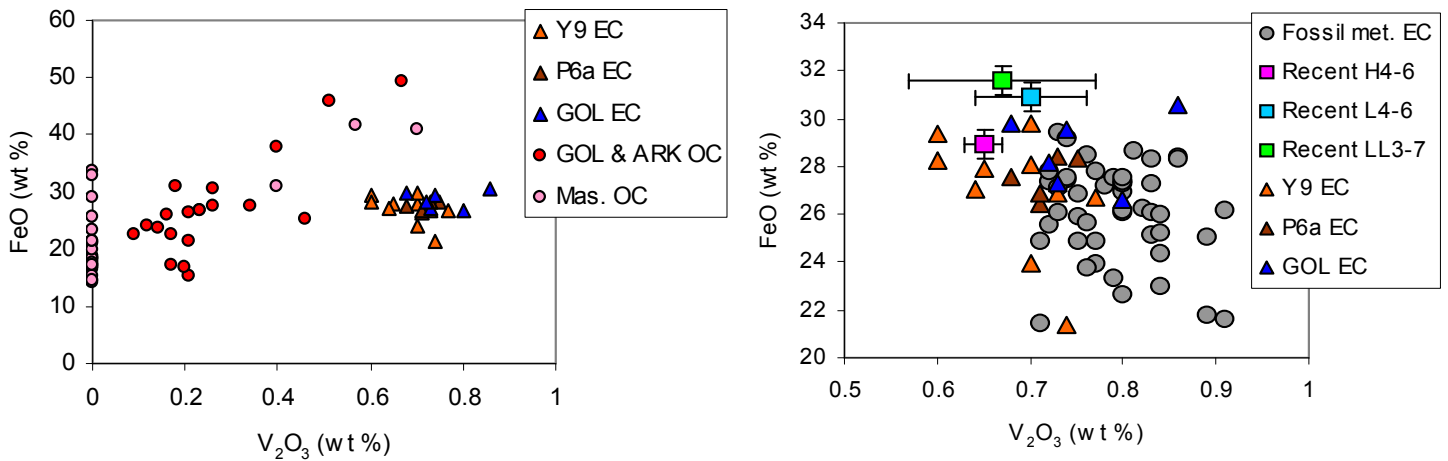


Fig. 12. Chemical composition of individual EC (data from Tables 11-13) and OC grains (data from Schmitz & Häggström 2006; Table 7 and Schmitz et al. in press; Table 8) in wt. %. Average composition, with standard deviation fields, of chromite grains from recent H, L and LL chondrites (data from Wlotzka 2005; Table 3) is also shown.

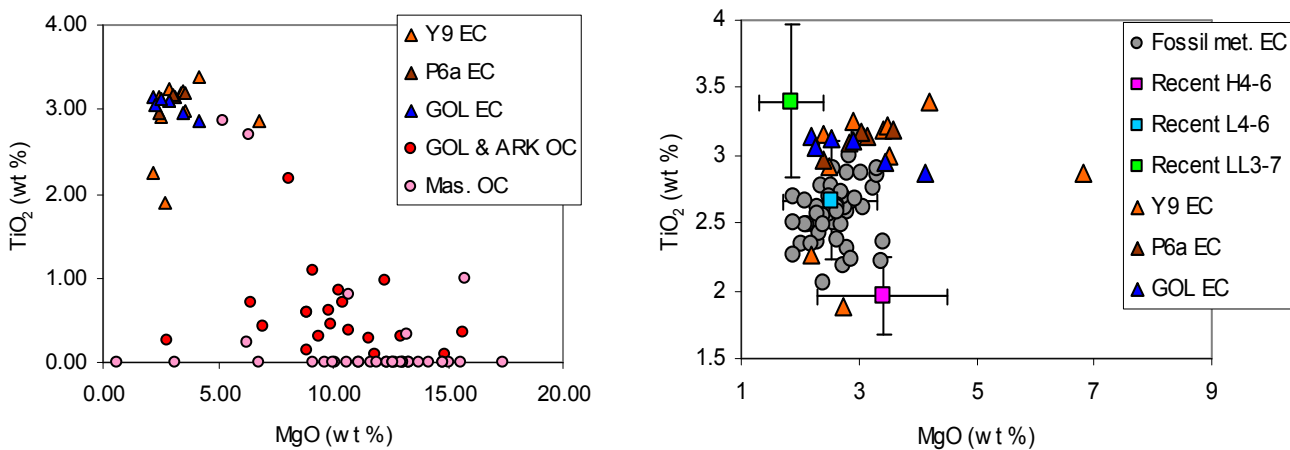


Fig. 13. Chemical composition of individual EC (data from Tables 11-13) and OC grains (data from Schmitz & Häggström 2006; Table 7 and Schmitz et al. in press; Table 8) in wt. %. Average composition, with standard deviation fields, of chromite grains from recent H, L and LL chondrites (data from Wlotzka 2005; Table 3) is also shown.

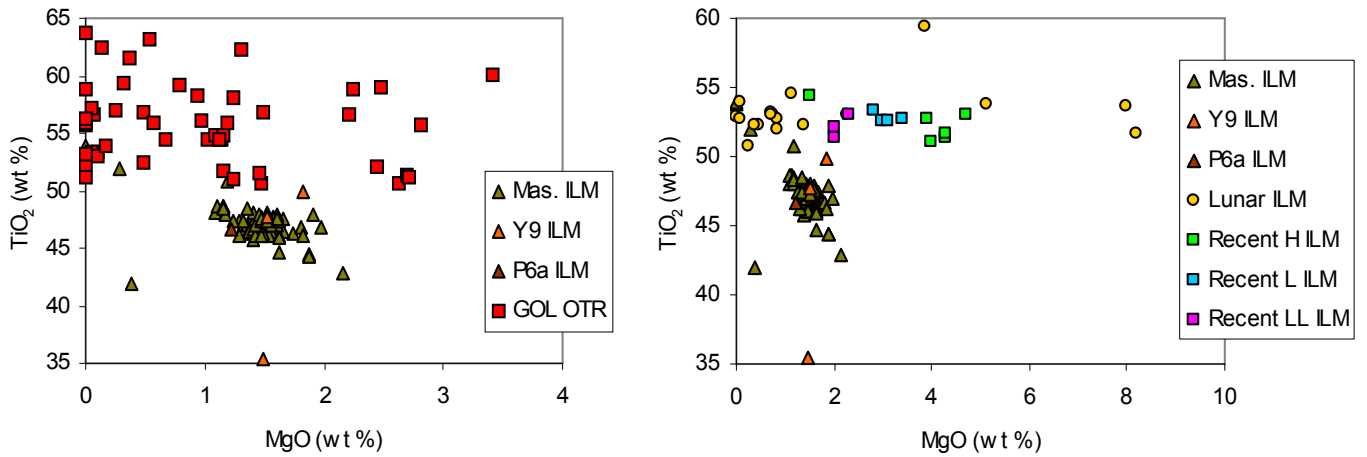


Fig. 14. Chemical composition of individual ilmenite and OTR grains in wt. % (data from Tables 10-14). Composition of ilmenite grains from recent H, L and LL chondrites (data from Snetsinger & Keil 1969; Table 2), and lunar ilmenite (data from Papike et al. 1998; Table 5) is also shown.

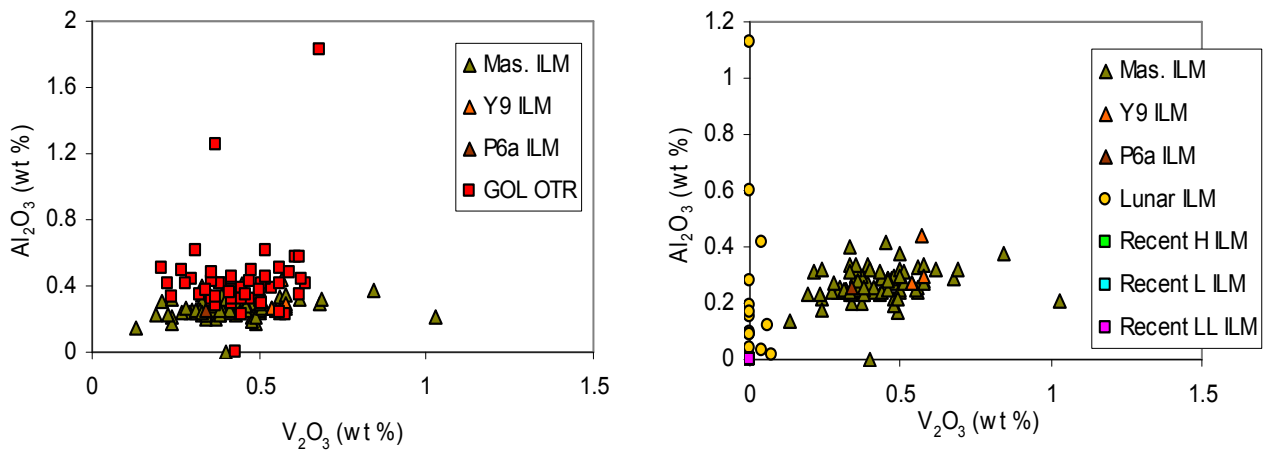


Fig. 15. Chemical composition of individual ilmenite and OTR grains in wt. % (data from Tables 10-14). Composition of ilmenite grains from recent H, L and LL chondrites (data from Snetsinger & Keil 1969; Table 2), and lunar ilmenite (data from Papike et al. 1998; Table 5) is also shown.

porous rim that surrounds the grain (Fig. 17). Inside the porous rim there is a thin section of ilmenite, according to stoichiometry. The dominant, central part of the grain can be found inside this section. In some of the grains the central part consists of more than one phase (Fig. 17), which causes the grain to be enriched in titanium compared to normal ilmenite. Some grains show coexistence of other phases without grain boundary alteration, and others reveal sections inside the grain that appear porous (Fig. 19). In at least one grain (Fig. 19), needle-shaped light areas were observed. The needles were too small to be analyzed (<10 μm long and <1 μm wide), but their lighter color reveal that they contain more heavy elements, most likely FeO, than the surrounding areas of the grain. Many of the grains appear to have been altered from the inside, as they show ilmenite composition at the boundary, but not in the central part of the grain (Fig. 16).

The GOL samples contain, besides the chromite and ilmenite, predominantly pyrite, red feldspar and

quartz together with some iron oxides. The vast majority of these grains are not rounded, which means that they have been transported fast, over a short distance, or both. The only mafic silicates represented in the samples are a few crystals of biotite.

7.2 Puxi River

The Y9 sample contained a total of ten extraterrestrial chromite grains (Table 12; Figs 11-13). Two of these grains (EC 8 and EC 9; Table 12) have chemical compositions that place them just outside the defined ranges for EC, but the variations from the standard are small, and thus they are still considered chondritic. Ten EC grains correspond to 2.2 grains kg^{-1} , as the sample weighed 4.45 kilos (Table 9). This can be compared to the content of terrestrial opaque minerals in the sample, which was much less. Three recovered ilmenite grains correspond to 0.7 grain kg^{-1} (Table 9), which is equivalent to only $\sim 1/3$ of the extraterrestrial input. Two of the ilmenite grains have similar

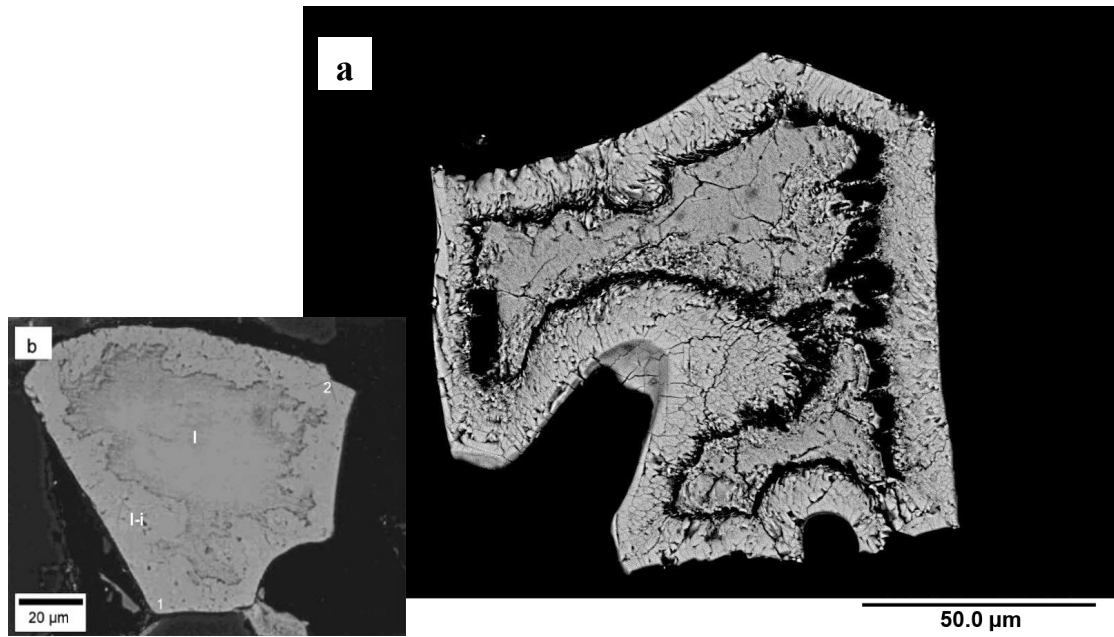


Fig. 16. a. Backscatter image of altered OTR grain from sample GOL bottom. Note the difference between the phase constituting the central part of the grain (leucoxene), and the phase constituting the grain-boundary (less titanium and more iron than the central parts). b. Backscatter image of altered ilmenite grain from a sandstone in Denmark. Note the similarity in appearance to the grain in a. Ignore letters and numbers (Weibel & Friis 2004).

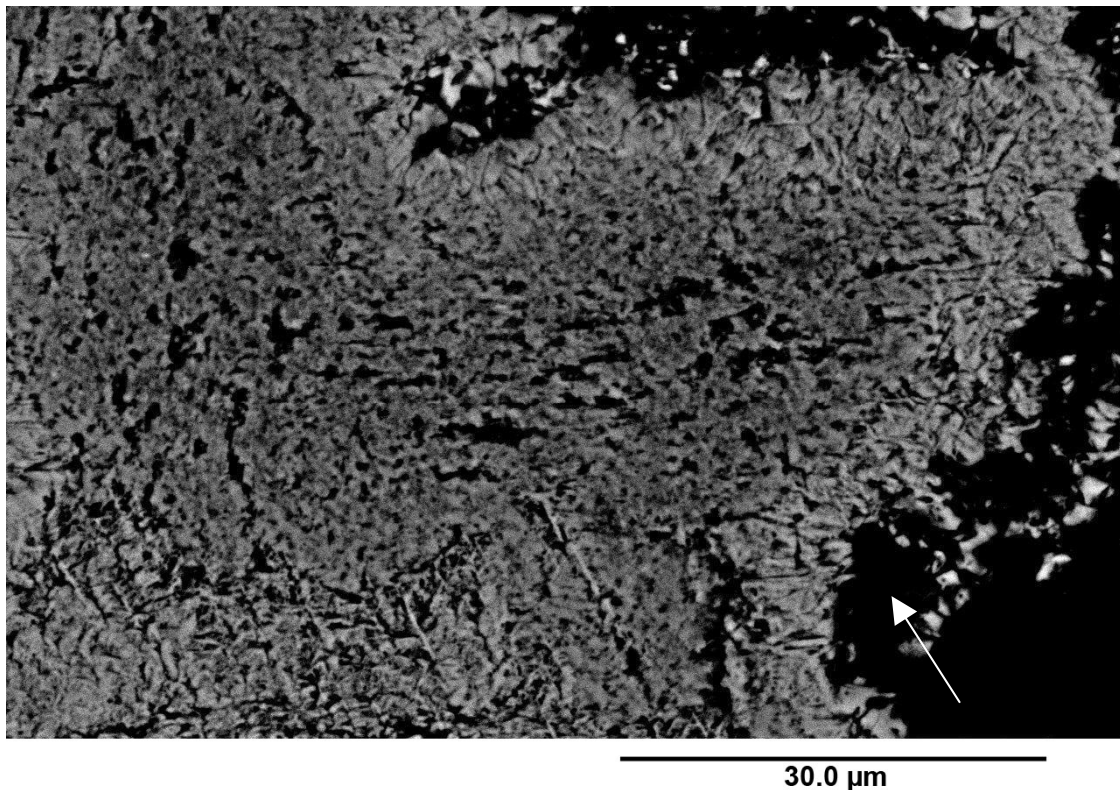


Fig. 17. Backscatter image of altered OTR grain from sample GOL bottom showing coexistence of more than one phase. The phases represent a darker phase that probably contains more TiO_2 , and a lighter phase that probably contains more FeO . Note porous appearance of grain boundary (arrow).



Fig. 18. Backscatter image of altered OTR grain from sample GOL top.

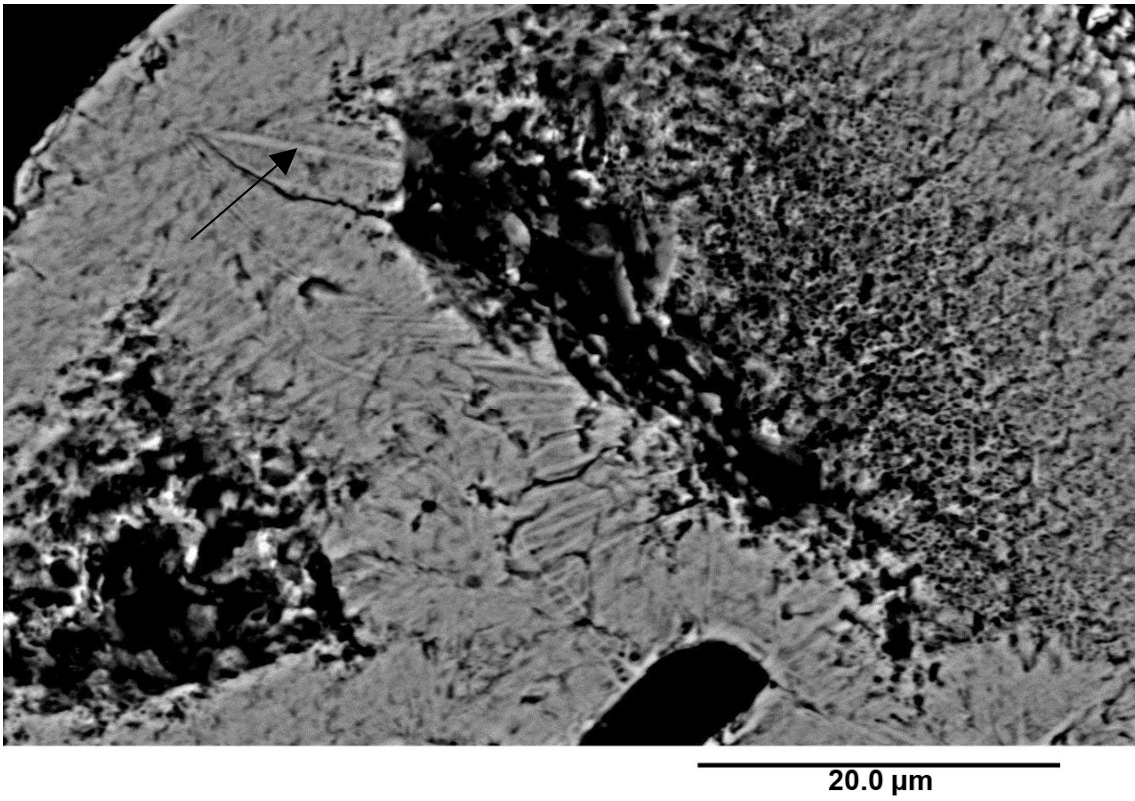


Fig. 19. Backscatter image of altered OTR grain from sample GOL bottom. Note the needle-shaped areas (arrow) of a more FeO-rich mineralogy than the surrounding parts of the grain. Also note porous appearance of the area to the right.

compositions with FeO at ~50-51 wt. % and TiO₂ at ~47-49 wt. % and one has a significantly different composition with FeO at 57.35 wt. % and TiO₂ at 35.43 wt. % (Fig. 14). No OC grains were found in sample Y9 or P6a.

From sample P6a, five extraterrestrial chromite grains and one ilmenite grain were retrieved (Table 13; Figs. 11-13) The chromite grains all have compositions where each element concentration lies within the defined ranges for chondritic chromite. The sample weighed 6.15 kilos, which means that a total of five EC grains is equivalent to 0.8 grain per kilo of limestone (Table 9). The extraterrestrial input of opaque minerals in sample P6a is, like in Y9, bigger than the input of terrestrial opaque minerals. One ilmenite grain corresponds to 0.2 grain kg⁻¹ (Table 9).

The clastic influence in the samples from Puxi River is much less than in the Swedish samples. Y9 contains some feldspars, quartz, pyrite and iron oxides. The grains are not rounded. Mafic silicates are rare in both Y9 and P6a. P6a contains even less clastic material than Y9, and the grain size is generally smaller than in Y9. Angular grains of feldspar and quartz dominate, and pyrite and iron oxides occur in smaller amounts.

7.3 Massignano

The Massignano sample was only analyzed for titanium-rich grains, in which it was very rich. A total

of 82 grains were selected for analysis (Table 14). 81 of these represent real ilmenite, as determined by compositional stoichiometry, in contrast to the Golvsten bed samples where a large fraction of the titanium-rich grains were not true ilmenite. The ilmenite grains have compositions where only a few plot away from the majority (Figs. 14 and 15), similar to the small compositional range for the EC grains. The remaining analyzed grain was an iron oxide.

In contrast to the Kinnekulle limestone ilmenite and OTR grains, the Massignano limestone ilmenite grains are not altered. They do however contain inclusions that have been altered to clay minerals (Fig. 20). The inclusions have varying shapes (most rounded; Fig. 20) and sizes in the range ~2-25 μm. The majority of the inclusions were dominated by silica and aluminum (together constituting ~85-90 wt. %), with minor amounts of Na, Mg, K, Ca, Ti and Fe. Two of the ilmenite crystals contained inclusions of zircon.

The OC grains from Schmitz et al. (in press) are very similar in composition to the Kinnekulle limestone OC grains (Figs. 10-13), and have a wide variety of chemical compositions.

7.4 Fossil meteorite

From the fossil meteorite, a representative portion (48 grains) of the opaque minerals in the sample was collected and analyzed. 47 of these grains consist of

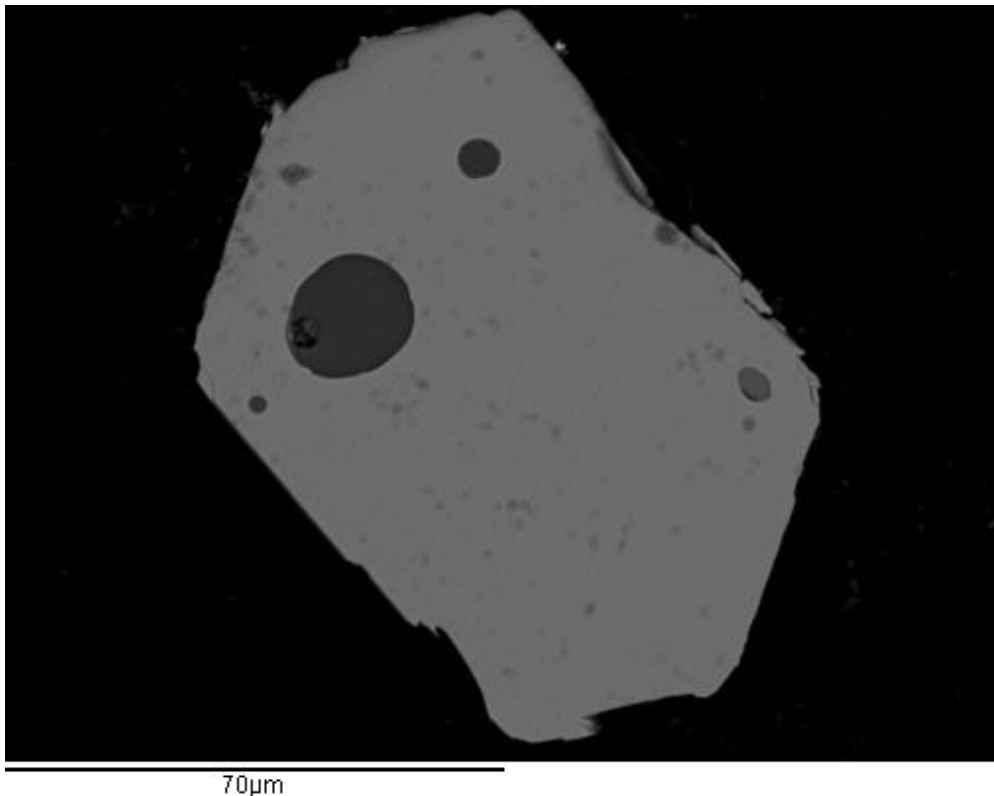


Fig. 20. Backscatter image of ilmenite grain from the Massignano sample with rounded inclusions of clay minerals.

chromite with chondritic composition (Table 15; Figs. 11-13). The concentration of ZnO varies from grain to grain (from 0 to 7 wt. %) due to iron-replacement after deposition, whereas the other elemental concentrations fall within the characteristic narrow ranges for chondritic chromite (Figs. 11-13).

Of the 48 grains analyzed, only one did not represent chondritic chromite (Table 15). This grain is a titanium-rich mineral in which the elemental concentration of titanium is too high for ilmenite, and thus it is classified as OTR. The grain was altered, with two phases of different TiO₂ content alternating. The similarities in composition and alteration between this OTR grain and the other OTR grains suggests that the grain might be from the surrounding bedrock rather than from the actual meteorite.

8 Discussion

Of the approximately 40 000 tons of extraterrestrial material that the Earth captures every year, <1 % is in pieces large enough for recovery. Even though dust that comes from cometary and asteroidal sources is the dominant portion of the captured material (Hutchison 2004), some comes from the Moon. If Fritz et al. (2007) is correct, a period of enhanced flux of extraterrestrial material to the Earth and Moon should be followed by increased amounts of ³He-rich lunar material that will be preserved in the form of a ³He-anomaly in terrestrial sediments of the proper age. Actually, a large impact on the Moon is enough to produce large amounts of launched impact ejecta, which potentially can create a ³He anomaly on Earth. For example, lunar crater Tycho (85 kilometers in diameter and with an age of ~100 Ma; Grier & McEwen 2001), formed when a 6-7 kilometer-diameter projectile collided in an oblique angle, i.e. 30-45°, with the Moon. Shuvalov & Artemieva (2006) calculated that this resulted in the delivery of 25-100 km³ of impact ejected lunar material to the Earth. This would have been enough to uniformly cover the entire planet. The impact that led to the formation of the South Pole-Aitken Basin (~2500 km in diameter), which is the largest known impact crater in the Solar System, would have launched massive portions of the lunar crust into space. However, the impact took place in the pre-Nectarian period, i.e. before 3.9 Ga, and thus none of the impact ejecta that reached the Earth is preserved.

Investigations of the potential extraterrestrial mineral content, and ³He content, in the right sediments of Cretaceous age can hopefully reveal information about whether the Tycho impact actually led to the delivery of lunar impact ejecta to the Earth, if some of the material is still preserved. Sedimentary rocks might lose ³He due to deep burial and heating, and according to Farley et al. (2005), ³He has only been detected in samples older than ~150 Ma in three studies. Thus it would be possible to find ³He in ~100

million year-old sediments.

The increase in the amount of both meteorites and EC grains during part of the Middle Ordovician should be associated with an increase in the amount of impact ejected material from the Moon, both in the form of IDPs and lunar meteorites. When Patterson et al. (1998) measured ³He in limestone samples from the mid-Ordovician at Kinnekulle, ³He was detected, but no ³He-anomaly was found. The amount of ³He preserved was comparable to the estimated average ³He flux for the Cenozoic. This is in contrast to the fact that other evidence suggests a major increase in the flux of extraterrestrial material to Earth during the same period. One could argue that the extraterrestrial matter that fell on Earth during the mid-Ordovician was dominated by material that was too large to retain ³He during atmospheric entry (Patterson et al. 1998). This is however not likely, as a shower of L-chondritic material in a smaller fraction should accompany an asteroid break-up, as it would have caused dust to be released in the initial collision, and dust to be ejected from the lunar surface as it was struck by projectiles originating from the parent body. A more likely explanation is, as Patterson et al. (1998) writes, substantial post depositional ³He loss from the IDPs in the limestone beds.

The question whether lunar impact ejecta even can be transferred to Earth, and thus explain the strong ³He-anomaly in Late Eocene sediments, is of course crucial in this paper, and for the hypothesis presented by Fritz et al. (2007). It is numerical simulations and not empirical evidence that have predicted the delivery of impact ejected lunar material to Earth, and provided the time constraints (e.g. Gladman et al. 1995; Shuvalov & Artemieva 2006). However, the fact that new recent lunar meteorites are being found proves that impact ejected lunar material has always fallen on Earth. These meteorites might have been preserved if the right conditions prevailed, but it is more likely that they decomposed after impact. Schmitz et al. (2003) estimated that as much as 85-90 % of the total mass of meteorites larger than about 0.1 centimeters, which fell on the sea floor that is now lithified at Kinnekulle, decomposed. The chrome spinel crystals from the lunar meteorites, and maybe also other resistant minerals such as ilmenite, is most likely preserved in sedimentary rocks, just like the chondritic chromite. During the part of the Middle Ordovician, which is represented at Kinnekulle, the infall of lunar meteorites was probably higher due to an increased amount of large impacts in the inner Solar System, which means that it is more likely to find traces of lunar matter in those beds than in beds which were deposited during a period of a more "normal" cratering rate.

8.1 Are there any lunar minerals in the sampled sections?

The fact that the ilmenite grains from the Ordovician limestone are altered, and the chromite and OC grains are not, indicate that the ilmenite grains are less stable than the Cr-rich spinels, and thus they are not ideal to use in the search for lunar minerals.

8.1.1 Ilmenite Alteration

The occurrence of sediment dispersed ilmenite grains in all the samples that were searched indicate that ilmenite is more or less stable up to at least ~470 million years, which is the age of the Orthoceratite Limestone. However, the extensive alteration of many of the ilmenite and OTR grains from the Kinnekulle and Puxi River limestones, compared to the unaltered appearance of the Massignano limestone ilmenite grains could indicate that the grains only survive in their original state for a number of million years which is more than ~35 and less than ~470. The explanation could also be that conditions that favored alteration of the grains in the depositional environment for the Kinnekulle and Puxi River limestone did not prevail in the Massignano depositional environment. Alteration due to metamorphism is excluded, as the Orthoceratite Limestone has not been subjected to any metamorphic events.

Diagenetic alteration of ilmenite in sedimentary rocks displaying oxidizing and reducing conditions similar to those of the Orthoceratite Limestone has been observed in other rocks (e.g. Weibel & Friis 2004). The Golvsten bed is located in the Kinnekulle section where the limestone goes from red to grey, which means that it goes from being oxidized to reduced. In a Lower Triassic sandstone from Denmark, Weibel & Friis (2004) observed alteration of ilmenite to leucoxene (alteration product of Fe-Ti oxides, especially ilmenite, consisting mainly of anatase or rutile). This alteration is a result of ilmenite being reduced and/or oxidized and replaced with leucoxene. Oxidized ilmenite grains also showed impregnation of iron oxide needles (Weibel & Friis 2004) at the outer part of the grain, resulting in an appearance that resembles that of some of the grains from this study (compare grains in Fig. 16). In Fig. 19 needle-shaped structures of more Fe-rich mineralogy in an OTR grain from Kinnekulle are visible. Leucoxene has a porous structure in the reduced grains (Weibel & Friis 2004), but this structure was lost when the grains became oxidized (Weibel & Friis 2004). The porous appearance of some of the OTR grains analyzed in this study probably reflects leucoxene alteration, even though it coexists with the needle-shaped structures in one grain (Fig. 19). This alteration to leucoxene explains why the OTR grains from this study are enriched in TiO₂. The grains that only display an apparent grain boundary alteration, and alteration connected to fractures, probably do so due to the fact

that they have not been subjected to the same extensive alteration as the other grains.

Thus, the OTR grains most likely had a stoichiometric composition like that of ilmenite before they were subjected to alteration. The mechanism that has caused some of the grains (i.e. the OTR grains) to show more extensive signs of alteration than the ilmenite grains remain unclear. Even though the OTR grains might originate from extraterrestrial sources, the origin of them cannot be discussed due to the extensive alteration.

8.1.2 Composition of ilmenite from this study and lunar ilmenite

The ilmenite grains from this study have varying chemical compositions, especially the ones from the Golvsten samples. The MgO concentrations in all the samples are generally low, around 1-2 wt. % (Figs. 8 and 14). Occasionally however, they reach 3 wt. %, which is unusual for terrestrial ilmenite according to Papike et al (1998). However, Table 1 implies that MgO concentrations above 3 wt. % are probably not as uncommon as Papike et al. (1998) writes, as five of the ilmenite grains retrieved from non-Kimberlitic rocks, have MgO concentrations above 3 wt. %. Papike et al. (1998) also implied that many lunar ilmenite crystals have high MgO concentrations (>3 wt. %), but according to the analyses of lunar ilmenite from many different sources presented in Papike et al. (1998; Table 5), only four analyses of the 18 presented reveal MgO concentrations above 3 wt. %. Thus, a low MgO concentration of ilmenite does not rule out a lunar origin for the grains from this study, and a high (>3 wt. %) MgO concentration does not automatically mean that the grain is lunar, even if an ultramafic terrestrial parent rock can be excluded.

The Al₂O₃ concentration in ilmenite is generally higher in this study than for lunar ilmenite grains presented by Papike et al. (1998; Figs. 9 and 15). The mean value of the lunar ilmenite grains which had detectable concentrations is 0.19 wt. % (Table 5), compared to ilmenite grains from this study which have mean values of 0.34, 0.26, 0.41, 0.59 and 0.27 wt. % Al₂O₃ (Tables 10-14). These small concentrations of aluminum are however associated with large relative errors due to the few counts during analysis. The only safe conclusion to be drawn from the Al₂O₃ concentrations of the ilmenite grains from this study is that for many grains they are low, which is in accordance with the analyzes of terrestrial and lunar ilmenite presented in Table 1 and 5. Thus, it is not possible to use the concentration of Al₂O₃ in a grain to decide whether the grain is lunar or not, especially not since also lunar ilmenite can have Al₂O₃ concentrations that are higher than ~0.20 wt. % (Figs. 9 and 15).

The ilmenite grains analyzed in this study have V₂O₃ concentrations varying from below 0.20 wt. %

up to about 1.00 wt. %, with the majority having values above 0.30 wt. % (Figs. 9 and 15). This concentration of vanadium in the vast majority of grains is higher than what would be expected in a lunar ilmenite, and thus a lunar origin for the grains is unlikely. However, the error in the V_2O_3 concentration is rather large. The counts of the titanium K_β peak are linked to the counts of the titanium K_α peak. Since the Ti K_β peak and V K_α peaks overlap, the V K_α peak is determined from the difference in counts of the combined peak and the counts attributable to the Ti K_β peak. Thus, the error in the concentration of vanadium is large and depending on the error in the Ti K_α peak. This is not a problem when analyzing chrome spinel due to the low concentration of titanium, but the ilmenite crystals contain ~45-53 wt. % TiO_2 , which causes the error in the calculation of the vanadium K_α top to be significant.

The only grain (ILM6, Table 11) that has acceptable Cr_2O_3 concentrations compared to the lunar grains (i.e. ~0.20 wt. % or higher), is too high in V_2O_3 to be considered lunar. Similarly, all the ilmenite grains that have MgO concentrations above 3 wt. %, which could indicate a lunar origin, all have concentrations of V_2O_3 and/or MnO that are not typical for lunar ilmenite.

8.1.3 Composition of chromite from this study and lunar chrome spinel

The chemical composition of lunar chrome spinel presented in Table 6 differs significantly from that of the EC grains from all samples, and thus it is clear that none of the EC grains are lunar, even though further studies of the chemical composition of lunar chrome spinel need to be performed before this can be definitely confirmed.

The OC grains however, are closer in chemical composition to lunar chrome spinel even if lunar chrome spinel is often higher in titanium and lower in magnesium (Fig. 10). Especially the Massignano limestone OC grains are lower in TiO_2 than lunar chrome spinel (Fig. 10). Lunar chrome spinel also has narrower Cr_2O_3 and Al_2O_3 compositional ranges than the OC grains, which plot over a larger area (Fig. 10). From Barnes and Roeder (2001) it is clear that it is not only the compositions of some of the OC grains from this study that are similar to that of lunar chrome spinel, but terrestrial chrome spinel often has a composition that overlap with the composition of lunar Cr-rich spinel.

8.1.4 Possible lunar grains

Despite the problems with alteration of ilmenite grains, and the overlap between terrestrial and lunar chrome spinel, some grains stand out as at least having potential to be of lunar origin. In Table 16, a comparison between the most “lunar-like” ilmenite grains from this study and some lunar ilmenite grains

is presented. Although grains from this study have chemical compositions that are similar to lunar ilmenite, they are all slightly higher in V_2O_3 and do not contain detectable Cr_2O_3 . However, the concentrations of these elements in both lunar ilmenite and in the ilmenite grains from this study are low, and thus associated with large relative errors because of few counts during analysis. Also, the error in vanadium concentration previously mentioned in section 8.1.2 is present. Some of the grains from this study (Table 16) are too high in MnO, as lunar ilmenite seem to be low in MnO (<0.50 wt. %).

Table 17 presents a comparison of the most “lunar-like” OC grains and actual lunar chrome spinel (OC grains from Schmitz & Haggström 2006 and Schmitz et al. in press). There is only one OC grain from the Orthoceratite Limestone that has a V_2O_3 concentration in the range 0.70-1.0 wt. %, which is the range where the composition of most lunar chrome spinel can be found (Table 6), but the grain is low in Cr_2O_3 (22.66 wt. %). Such low chromium concentrations are more indicative of ulvöspinel, and thus much lower than any of the lunar chrome spinel grains. The best fit of a OC grain from the Kinnekulle limestone, according to a lunar chrome spinel classification, does a grain with V_2O_3 concentrations of 0.56 wt. % have (Table 17). Vanadium contents as low as 0.40 wt. % have been observed in Apollo 12 chrome spinel crystals (see figures 7, 8 and 9 in El Goresy et al. 1971), so the grain has great potential to be of lunar origin according to the ranges of chemical composition for lunar chrome spinel. Among the Massignano limestone OC grains, three present V_2O_3 concentrations that are acceptable for lunar chrome spinel (Table 17). Two of these are especially interesting as they are two of the few grains among the Massignano limestone OC grains that have detectable TiO_2 concentrations (Table 17). They are actually the two grains with the highest TiO_2 concentrations (~2.80 wt. %).

8.1.5 Summary and suggestions for future work

The results of this study have not excluded the occurrence of lunar minerals, i.e. ilmenite or chrome spinel, in the mid-Ordovician and late-Eocene sediment samples dissolved in this study, but it has not definitely confirmed the existence of any such minerals either. The vast majority of the grains are actually almost certainly terrestrial, and the Cr-rich spinel grains that are the most similar in composition to lunar chrome spinel (Table 17), have compositions which can be found among terrestrial Cr-rich spinel as well (see Barnes & Roeder 2001). The lack of apparent lunar minerals might be explained by the fact that the hypothesis that Fritz et al. (2007) presented said that the enhanced levels of lunar material reaching Earth should be in the form of IDPs. If the particles survived the journey to Earth, through the atmosphere and the ~470 million years of being incorporated in the sediments, and then the leaching, the acid insoluble

Table 16. Chemical composition of "lunar-like" ilmenite grains compared to chemical composition of lunar ilmenite.

Type	MgO	Al ₂ O ₃	TiO ₂	V ₂ O ₃	Cr ₂ O ₃	MnO	FeO
Lunar ilmenite*	0.47	0.04	52.25	-**	0.18	0.30	46.74
Lunar ilmenite	0.39	0.28	52.34	-	0.24	0.34	45.16
Lunar ilmenite	0.01	1.13	52.91	-	0.19	0.31	46.30
Lunar ilmenite	0.10	0.42	53.90	0.04	0.39	0.36	45.40
Lunar ilmenite	0.09	0.12	52.70	0.06	0.23	0.37	46.70
Lunar ilmenite	0.72	0.15	53.10	-	0.39	0.44	45.70
Mas. ILM***	1.15	0.31	48.61	0.21	-	0.57	48.53
Mas. ILM	0.29	0.32	52.00	0.24	-	2.57	41.13
Mas. ILM	-	0.14	53.81	0.13	-	2.46	45.12
Mas. ILM	1.43	0.22	46.68	0.24	-	0.78	48.70
GOL ILM****	3.15	0.45	45.71	0.23	-	1.21	44.50
GOL ILM	2.33	0.40	50.62	0.16	-	2.82	36.61

* Data from Papike et al. (1998); Table 5.

** Below detection limit or not analyzed for.

*** Data from this study; Table 14.

**** Data from this study; Table 10 and 11.

Table 17. Chemical composition of "lunar-like" OC grains compared to chemical composition of lunar chrome spinel.

Type	MgO	Al ₂ O ₃	TiO ₂	V ₂ O ₃	Cr ₂ O ₃	MnO	FeO
Lunar chrome spinel*	6.10	12.65	4.58	-**	43.79	0.49	30.74
Lunar chrome spinel	3.63	17.87	0.77	-	46.14	0.38	30.97
OC ARK***	5.92	16.69	1.00	0.56	42.49	0.44	29.22
OC Mas.****	5.20	11.90	2.86	0.70	37.17	-	40.92
Lunar chrome spinel	2.01	9.66	10.01	-	37.69	0.41	40.29
OC Mas.	3.17	4.14	-	0.40	59.44	-	31.04
OC Mas.	6.38	11.30	2.71	0.57	36.13	-	41.59
Lunar chrome spinel	2.01	12.00	3.70	1.03	44.30	0.31	34.20
Lunar chrome spinel	5.89	11.70	5.29	0.98	46.50	0.29	30.10

* Data and references in Table 6. SiO₂, CaO and CoO not included.

** Below detection limit or not analyzed for.

*** Data from Schmitz & Häggström (2006); Table 7.

**** Data from Schmitz et al. (in press); Table 8.

fraction searched for minerals in this study (63-355 µm) might be too big to reveal any IDP particles.

As the overlap in composition between terrestrial and lunar chrome spinel is significant, the classification and identification of lunar chrome spinel in terrestrial sedimentary rocks based on just chemical composition is not enough. The use of isotope geochemistry, e.g. oxygen isotope ratios, might help in identifying lunar minerals after suspected minerals have been identified in dissolved sediments. The oxygen isotopic ratios are heterogeneous in the Solar System and thus a lunar origin might be determined through such a study. However, according to high precision measurements of the oxygen isotopic composition of 31 lunar samples, there is no detectable difference in the oxygen isotopic compositions between the Moon and Earth (Wiechert et al. 2001), and thus other isotope methods must be used.

8.2 Are there any chondritic minerals in the sampled sections?

The finding of the EC grains in the Ordovician

limestone was expected, as the grains have been frequent in previous studies of the same sections (e.g. Schmitz & Häggström 2006; Schmitz et al. 2008). The composition of the EC grains that were found in the Golvsten and Puxi River samples can reveal more about their origin, in addition to that they are chondritic. The TiO₂ concentrations of the EC grains in the GOL samples (3.10 and 2.98 wt. %; Fig. 13), which are very similar to the numbers presented by Schmitz & Häggström (2006; 3.1 wt. %), support an L or LL chondritic parent body for the grains, as the TiO₂ content increases from H to LL chondrites. This also applies for the Y9 and P6a EC grains, which have TiO₂ mean concentrations of 2.91 and 3.11 wt. % (Fig. 13). This supports the hypothesis of an L-chondritic asteroid shower having a global influence. The fossil meteorite is lower in TiO₂, with a mean value of 2.58 wt. %. Despite this, the most likely origin for this meteorite is an L chondritic parent body, because the majority of the chromite grains are closer to the L chondrite reference values than the H chondrite values (Fig. 13). The FeO concentrations may also be used for assigning chromite grains to the different chondrite

classes, as the Fe content increases from H to L to LL chondrites, but iron is susceptible to some diagenetic alteration (Bunch et al. 1967; Schmitz et al. 2003), and is therefore not as reliable as titanium.

Although ilmenite is rare in chondrites it does occur, and thus sediment-dispersed ilmenite grains should occur in the samples.

8.2.1 Possible chondritic ilmenite grains

Chondritic ilmenite generally has higher MgO concentrations than the majority of both lunar and terrestrial ilmenite grains, and ilmenite from this study (Table 2). Thus, a high MgO concentration (>1.50 wt. %) is probably indicative of chondritic ilmenite. The fact that low Al₂O₃ concentrations are also required for a grain to be classified as chondritic, and the low V₂O₃ concentrations that are expected in chondritic ilmenite indicate that chondritic and lunar ilmenite are quite similar in composition. The difference between the two is the higher MnO concentrations in chondritic ilmenite. In Table 16, the ilmenite grain (last grain called GOL ILM) from this study that has high MnO and MgO concentrations can be considered as a potential chondritic grain. The same problem as for the identification of lunar ilmenite in terrestrial sediments is however present: the fact that the ilmenite grains from the Ordovician limestone are altered, making these kinds of classifications difficult.

8.3 A terrestrial origin for the ilmenite, OTR and OC grains?

Almost every ilmenite, OTR and OC grain do most likely not have an extraterrestrial origin. The grains must instead have been brought out to their depositional environment either as a product of erosion of rocks and transportation through current activity, or through volcanic eruptions.

The depositional environment for the limestone at all the localities was marine, but not abyssal. The ilmenite, OTR and OC grains have a high density, and would have been deposited rapidly when in contact with water. The Kinnekulle limestone was deposited far out in a vast epicontinental sea, and the Puxi river limestone section should have been deposited in a similar environment, as they show many common features. The Massignano section contains evidence of volcanic eruptions, and thus volcanism may be the explanation for the findings of many ilmenite grains there.

High MgO concentrations in terrestrial ilmenite can be found in not only high-pressure rocks such as kimberlite, but also in trachyte and trachyandesite, and in the mafic rocks trachybasalt and basalt according to Table 1. Also, e.g. gabbro and dacite can have ilmenite with MgO concentrations close to 3 wt. %, at 2.30-2.50 wt. % (Table 1). The possible source rock for the ilmenite grains with “higher” MgO concentrations

(>1.00 wt. %) can thus be both felsic and mafic. However, a granitic source rock is most likely where the quartz and feldspar come from, together with some of the low-MgO ilmenite and OTR grains. The OC grains from the Kinnekulle and Massignano limestones do not come from a felsic rock, and thus a mafic source, volcanic or plutonic, must have been present in the surroundings. If a mafic rock provided at least some of the heavy minerals, mafic minerals other than the few biotite crystals that were found in the samples, would also have been brought out to the depositional environment. Thorslund & Wickman (1981) reported that in fossil meteorites, all the primary mineral phases (e.g. pyroxene and olivine), except chromite, have been replaced by alteration products. This has probably happened to the mafic minerals that were brought out together with the heavy minerals.

8.3.1 The distribution of EC, OC, OTR and ilmenite grains

The input of heavy opaque minerals most likely representing terrestrial sources, and clastic material such as quartz and feldspar, is much less in the Puxi River samples than in the Kinnekulle samples. In GOL top, the extraterrestrial input is only ~14 % of that of the terrestrial input of heavy titanium-rich opaque minerals. Similarly, in GOL bottom, the extraterrestrial input is only ~7 % of that of the terrestrial input of ilmenite and OTR grains. The abundance of titanium-rich grains in the Golvsten bed samples is also much higher than the abundance of OC grains. Schmitz & Haggström (2006) found five OC grains in the Golvsten sample (Table 7). This can be compared with the 109 ilmenite and OTR grains (i.e. the influence of OC is less than 4 % of the influence of titanium-rich grains).

In samples Y9 and P6a the extraterrestrial input is ~68 % of that of the terrestrial for Y9, and 75 % of that of the terrestrial input of ilmenite and OTR grains for P6a. The reason for this major difference between the Kinnekulle and Puxi River limestones could either be lack of rocks providing terrestrial minerals, or lack of current activity able to transport the heavy minerals out to the depositional environment at Puxi River, which means that it was more of a “closed” environment. The Puxi River limestone is not only rare in ilmenite and OTR grains, but also in OC grains (B. Schmitz, personal communication), which is supported by the fact that no OC grains were found in the samples that were searched in this study. This high abundance of EC grains in especially sample Y9 strengthens the fact that the Kinnekulle EC grains, and thus also most likely OC grains, have not been concentrated, but reflects an increase in the amount of both extraterrestrial material reaching Earth, and terrestrial material reaching the depositional environment at Kinnekulle.

Even though the amount of EC grains recovered

from the Kinnekulle samples in this study is lower than the amount that previously have been discovered (see Schmitz & Haggström 2006), the levels are increased compared to the levels in samples prior to the Arkeologen bed. In this study, the amount of EC grains in the GOL samples are 0.4 and 0.3 grains kg⁻¹, compared to 0 for the majority of the samples taken below the Arkeologen bed (0.1 grains kg⁻¹ is the highest abundance, but only for one of 14 samples; Schmitz & Haggström 2006).

The OC grains in the Kinnekulle samples seem, according to Schmitz & Haggström (2006) to have been brought out to the depositional environment in pulses, and there is no clear correlation between the levels of OC grains compared to the levels of EC grains other than the fact that the OC grains are also enriched compared to the occurrence of such grains prior to the Arkeologen bed (see table 1 in Schmitz & Haggström 2006). The EC grains were introduced as a steady flow, and the levels are increased throughout the entire interval, whereas the OC grains are abundant only in selected sections of the Thorsberg and Hällekis quarries. The only correlation between both EC- and OC-rich intervals is the most EC grain-rich interval in the Arkeologen bed which contains elevated levels of OC grains as well, in both quarries (Schmitz & Haggström 2006).

If some of the OC grains in the Ordovician limestone represent rarer extraterrestrial material (compared to the abundant L-chondritic material retrieved in the sections), such as other chondritic sources, the levels of OC grains are not expected to be increased, as the enhanced levels of infalling extraterrestrial material is L chondritic. However, if they have a lunar origin, the amount should be increased, as the Moon loses more mass during asteroid showers. Considering the fact that most of the OC grains most likely are not lunar, the reason for the dominant part of the increase in OC grains which coincides with the increase in EC, is changes in the surrounding environment, which led to an increased transportation of heavy terrestrial minerals to the depositional environment (see below).

8.3.2 A volcanic origin for the grains?

A possible explanation for the findings of large quantities of dense minerals in the Kinnekulle limestone, without any current activity, is volcanic activity. The formation of the Caledonides was associated with both acid and basic volcanism, and thus both ilmenite and chrome spinel crystals might have been able to crystallize in the magmas. However, any coeval volcanism that would have been able to provide ash material to the depositional environment had to be felsic, or at least intermediate, as mafic magmas have low viscosity and will not produce explosive eruptions. Depending on the composition of a felsic magma, or an intermediate magma, it might have been able to provide all the ilmenite grains, even

the ones with >2 wt. % MgO. Even if the volcanism theoretically can produce ilmenite with high MgO concentrations, the volcanoes were situated off the west coast of what today is Norway. Due to the large grain-size of the particles retrieved in the samples (63-355 µm), and their high density, a scenario where the grains were transported at least ~1500 kilometers to Kinnekulle in the atmosphere is unlikely. The chromium-rich spinels must come from a mafic source, and thus explosive volcanism is excluded. Basic volcanism on the sea floor associated with a subduction zone during the formation of the Caledonides needs to have been close by in order to be able to allow transportation of the heavy minerals to the depositional environment. This is not likely, as the formation of the mountain chain and the related subduction zones were situated too far away.

As mentioned above, the Massignano ilmenite grains could originate from volcanic eruptions. The Mediterranean Ocean area was volcanically active during the Late Eocene, with explosive felsic volcanism. The majority of the ilmenite grains from Massignano have uniform compositions (Figs. 14 and 15), which could be a reflection of a common origin. The grains probably come from the same source, i.e. the same volcano. Some ilmenite grains, maybe the ones with deviant compositions, might have been brought to the depositional environment in another way, together with the Cr-rich spinels, which do not originate from felsic volcanism.

8.3.3 An intrusive source rock?

Schmitz & Haggström (2006) suggested that the source for the OC grains in the Kinnekulle limestone is volcanic related intrusions of mafic dikes on the sea floor. Erosion of these dikes would have led to incorporation of chrome spinels in the sediments. A mafic dike is a likely source rock for ilmenite and OTR and OC grains, but in order for the mafic dike scenario to be plausible, (1) the dikes must have been intruded several times, in pulses, as described by Schmitz & Haggström (2006). Otherwise, they would not have been able to provide the chromium-rich spinel grains and the titanium-rich minerals during several million years during the deposition of the Orthoceratite Limestone, as the dikes would have been covered in sediments with time. (2) The sea floor current activity must have been extensive during long periods of time in order to erode a mafic rock on the sea floor. Normally, no extensive erosion occurs on the sea floor, as agents causing erosion (strong wave and/or current activity) are missing.

If a mafic magma is intruded in the Ordovician sedimentary rocks and reaches the sea floor (which it must do in order to be eroded and provide heavy minerals) it would spread over the sea floor, forming pillow-lava, or a rock with similar features to pillow lava in that it would be extremely fine-grained, or glassy, in the areas that were chilled in contact with

the water. It seems unlikely that the limestone is so homogeneous and that no visible traces of any such dikes/intrusions have been traced over the ~6000 m² (Schmitz & Haggström 2006) quarried area. If the magma was intruded somewhere near the Thorsberg and Hällekis quarries, that would explain why the intrusions have not been recovered during the quarrying of the limestone. However, no mafic intrusions or dike swarms of Middle Ordovician age have been discovered in the surrounding area, even though the area is well studied.

The fine grain-size of a mafic intrusion chilled under water is not in accordance with the size of the recovered Cr-rich spinel or ilmenite grains. Also, even if, although unlikely, the Cr-rich spinel and ilmenite grains originate from mafic intrusive rocks on the sea floor, the quartz and potassium feldspar grains do not. These come from a felsic rock and must have been brought to the depositional environment by currents (most feldspar grains are too big to have been transported from the volcanoes situated off the west coast of Norway to Kinnekulle), which proves that currents brought grains from land out to sea.

In contrast to the complete lack of evidence of mafic intrusions of mid-Ordovician age, several bodies of mafic rocks that are older than the Ordovician limestone can be found on several places around the Kinnekulle area (see SGU mapservice, bedrock). They are potential source rocks for both the Cr-rich spinel and titanium-rich grains, if they were exposed during the part of the Middle Ordovician when the limestone was deposited. The fact that the input of OC grains is less than 4 % of that of the input of titanium-rich grains, is in accordance with the bedrock of Baltoscandia, where mafic bodies occur much less frequently than the dominating rock types granite and gneiss. Many of the ilmenite and OTR grains most likely originate from these dominating rock types, which would have provided a larger fraction of the eroded material to the depositional environment of the Kinnekulle limestone. However, many of the ilmenite grains have wt. % concentrations of MgO that are too high for granites (~1 wt. % and higher). Ilmenite is far more abundant in most mafic rocks than Cr-rich spinel, and thus the titanium-rich grains naturally make up a larger fraction of the eroded material of these rocks. To summarize, the heavy minerals almost certainly originate from an exposed rock on land, and were brought to the depositional environment by currents. This does however not explain why the OC grains appear to have been brought out to the depositional environment in pulses.

The period of enriched levels of OC grains (and thus also EC grains) in the Kinnekulle limestone has been proposed to also be a period of unusual and prominent sea-level changes (e.g. Dronov 2004). Dronov (2004) suggested that a prominent sea-level drop occurred approximately two meters below the Arkeologen bed. With this, igneous mafic rocks

previously situated below water may have been exposed to erosion. A fluctuating sea-level during the period could cause these mafic bodies to be exposed only during limited periods of time, causing erosion, and production of eroded material, to occur in "pulses". Current activity in the ocean, which would have been more pronounced further out in the sea during periods of lower sea-level could have transported the heavy minerals out to the depositional environment. However, the scenario requires strong currents, which would have prevented the small detritus particles, which eventually would have formed the limestone, from settling on the sea floor. The frequently occurring hardgrounds in the Kinnekulle section formed when there was no deposition, most likely due to current activity (Lindström 1979). These periods of non-deposition probably coincide with the periods when heavy minerals were brought out to the location of the formation of the Kinnekulle limestone. The feldspars and quartz, and other light clastic material would have been transported even further away than the Cr-rich spinels and titanium-rich grains due to their lower density, explaining why these minerals are rare in the samples. This scenario explains why the OC grains were brought out in pulses, as they are too heavy to have been transported when the currents were not strong enough, and no material, or at least much less material, would have been eroded during periods when the mafic rocks were below sea-level. The hypothesis would be strengthened if a correlation between hardgrounds and the occurrence of elevated levels of heavy minerals could be made.

Strong currents would have transported the mineral grains fast, and thus it also explains why the clastic material is not rounded. Schmitz et al. (2001) suggested that the meteorites that fell on hardgrounds and were exposed to currents for a long time were decomposed. Thus, the preserved meteorites would represent those that fell on the sea floor during periods when the current activity was less pronounced, and when deposition of fine detritus occurred.

In what today is China, when the Puxi River limestone was deposited, the current activity might not have been strong enough to bring heavy minerals out to the depositional environment. If it was, the reason for why such low amounts of clastic minerals were found, compared to the Kinnekulle limestone, must be that there were no mafic igneous rocks in the surrounding environment that could provide similar amounts of ilmenite and Cr-rich spinel grains to the depositional environment.

The vast majority of chrome spinels recovered in the Massignano limestone must, like the OC grains from the Ordovician limestone, come from a terrestrial mafic source rock. Schmitz et al. (in press) noted that many of the grains have similar compositions to the OC grains retrieved from middle Paleocene sediments in the Bottaccione Gorge section at Gubbio, Italy, by

Cronholm & Schmitz (2007). This suggests that the grains might come from a local source that provided minerals to the depositional environment for a long time. This local source is most likely a large rock body situated above sea-level, as the erosion on the sea-floor is very limited.

The origin of dense chrome spinel, ilmenite and other titanium-rich minerals in the limestone samples is undoubtedly a question that needs to be further investigated. The grains are not all from space, so they must come from somewhere on Earth. Research regarding the compositions of OC grains compared to e.g. chrome spinel from the Moon, and the composition of ilmenite crystals of different origins, will shed some light on this issue. Also, compositional comparisons with surrounding potential source rocks for the grains need to be made, if the source rock has not completely disappeared. When searching for lunar minerals a limestone section that is rich in EC grains, but poor in terrestrial minerals, is the best candidate to sample and dissolve. The Puxi river limestone, and other sections representing the same rock in the eastern Yangtze Gorges area in China, are examples of such limestone sections. The Arkeologen bed from Kinnekulle is thus not an optimal candidate, even though it is very rich in grains that have the potential to be from the Moon or other extraterrestrial bodies. If finding lunar chrome spinel, and not lunar ilmenite, is the main purpose the content of titanium-rich grains in the limestone is not important. In such a study the Golvsten bed from Kinnekulle is suitable to use, as it contains very small amounts of OC grains.

9 Conclusions

- The right lunar minerals to look for in terrestrial sediments are resistant opaque oxide minerals as the lunar oxide minerals differ in composition from the terrestrial ones due to the significantly lower oxygen fugacity of the Moon.
- Besides sediment-dispersed chondritic chromite and other Cr-rich spinel (OC) grains, limestone samples from the Middle Ordovician and Late Eocene also contain resistant opaque titanium-rich minerals (ilmenite and altered ilmenite). The provenance of the ilmenite and OC grains can be discussed through investigations of their chemical compositions.
- A complex overlap in chemical composition between lunar chrome spinel, which can have a wide variety of chemical compositions, and terrestrial chrome spinel prevents any definite identification of lunar chrome spinel grains in terrestrial sediments based on chemical composition.
- In order to confirm the origin of suspected lunar chrome spinel grains other methods must be applied. Isotope geochemistry might be suitable for this purpose.

- Ilmenite is less likely to persist in its original state incorporated in sedimentary rocks than chrome spinel is, and thus chrome spinel is more suitable as a tool when trying to identify lunar minerals in terrestrial sedimentary rocks.
- The vast majority of the recovered heavy minerals from limestone samples from Kinnekulle, Sweden, eastern Yangtze Gorges area, China, and Massignano, Italy, almost certainly have a terrestrial origin.
- The most likely scenario for the transportation of the grains to the depositional environment is by currents, although some of the ilmenite grains from the Massignano limestone might originate from volcanic eruptions. At Kinnekulle, the grains were probably brought out during periods of enhanced current activity caused by changes in sea-level. It is probably during these periods that the currents prevented small detritus particles from settling on the sea floor, resulting in the formation of hardgrounds. The grains probably originate from several igneous rocks, felsic and mafic, present somewhere in the surroundings.
- This study has not excluded the existence of lunar chrome spinel and chondritic and/or lunar titanium-rich minerals in terrestrial sediments, but it has not conclusively confirmed the existence of any such minerals either. Thus, the occurrence of lunar minerals representing impact ejecta in terrestrial sediments, and the hypothesis that lunar impact ejecta is capable of forming ^3He -anomalies in terrestrial sedimentary rocks remains unresolved.

10 Acknowledgements

First of all I would like to thank my head supervisor Birger Schmitz for great commitment to the project, always taking the time to answer questions, and for constructive criticism on the manuscript, and finally for helpful discussions. Thanks to Carl Alwmark, my assistant supervisor, for helpful discussions, help with the SEM, answering questions and for constructive criticism on the manuscript. Thanks to Anders Lindh, assistant supervisor, for always answering questions, taking the time to discuss my ideas with me and for helpful comments on the manuscript. I would like to thank everyone else that has answered questions and discussed my ideas with me. Also, thanks to Anders Cronholm for helpful comments on the manuscript and for help with the SEM.

11 References

Alwmark, C. & Schmitz, B., 2007: Extraterrestrial chromite in the resurge deposits of the early Late Ordovician Lockne crater, central Sweden. *Earth and Planetary Science Letters* 253, 291-303.

- Anand, M., Taylor, L.A., Floss, C., Neal, C.R., Terada, K. & Tanikawa, S., 2006: Petrology and geochemistry of LaPaz Icefield 02205: A new unique low-Ti mare-basalt meteorite. *Geochimica et Cosmochimica Acta* 70, 246-264.
- Barnes, S.J. & Roeder, P.L., 2001: The range of spinel compositions in terrestrial mafic and ultramafic rocks. *Journal of Petrology* 42, 2279-2302.
- Bodiselič, B., Montanari, A., Koeberl, C. & Coccioni, R., 2004: Delayed climate cooling in the Late Eocene caused by multiple impacts: high-resolution geochemical studies at Massignano, Italy. *Earth and Planetary Science Letters* 223, 283-302.
- Bogard, D.D., 1995: Impact ages of meteorites – a synthesis. *Meteoritics* 30, 244-268.
- Bottomley, R., Grieve, R., York, D. & Masaitis, V., 1997: The age of the Popigai impact event and its relation to events at the Eocene/Oligocene boundary. *Nature* 388, 365-368.
- Bunch, T.E., Keil, K. & Snetsinger, K.G., 1967: Chromite composition in relation to chemistry and texture of ordinary chondrites. *Geochimica et Cosmochimica Acta* 31, 1569-1582.
- Bunch, T.E. & Keil, K., 1971: Chromite and ilmenite in non-chondritic meteorites. *The American Mineralogist* 56, 146-157.
- Clymer, A.K., Bice, D.M. & Montanari, A., 1996: Shocked quartz from the late Eocene: Impact evidence from Massignano, Italy. *Geology* 24, 483-486.
- Cronholm, A. & Schmitz, B., 2007: Extraterrestrial chromite in latest Maastrichtian and Paleocene pelagic limestone at Gubbio, Italy: The flux of unmelted ordinary chondrites. *Meteoritics & Planetary Science* 42, 2099-2109.
- Dronov, A.V., 2004: Magnitude of sea-level changes in the Ordovician of Baltoscandia (abstract). *Working group on the Ordovician geology of Baltoscandia-2004*. Tartu: Tartu University Press, pp. 21-22.
- El Goresy, A., Ramdohr, P. & Taylor, L.A., 1971: The opaque minerals in the lunar rocks from Oceanus Procellarum. *Proceedings of the Second Lunar Science Conference* 1, 219-235.
- El Goresy, A., 1981: Oxide minerals in lunar rocks. In D. Rumble (ed.): *Oxide Minerals*, EG1-EG43. Mineralogical Society of America.
- Farley, K.A., 1995: Cenozoic variations in the flux of interplanetary dust particles recorded by ^3He in a deep-sea sediment. *Nature* 376, 153-156.
- Farley, K.A., Love, S.G. & Patterson, D.B., 1997: Atmospheric entry heating and helium retentivity of interplanetary dust particles. *Geochimica et Cosmochimica Acta* 61, 2309-2316.
- Farley, K.A., Montanari, A., Shoemaker, E.M. & Shoemaker, C.S., 1998: Geochemical evidence for a comet shower in the Late Eocene. *Science* 280, 1250-1253.
- Farley, K.A., Ward, P., Garrison, G. & Mukhopadhyay, S., 2005: Absence of extraterrestrial ^3He in Permian-Triassic age sedimentary rocks. *Earth and Planetary Science Letters* 240, 265-275.
- Fritz, J., Tagle, R. & Artemieva, N., 2007: Lunar helium-3 in marine sediments: Implications for a late Eocene asteroid shower. *Icarus* 189, 591-594.
- Gladman, B.J., Burns, J.A., Duncan, M.J. & Levison, H.F., 1995: The dynamical evolution of lunar impact ejecta. *Icarus* 118, 302-321.
- Glass, B.P., 2002: Upper Eocene impact ejecta/spherule layers in marine sediments. *Chemie der Erde Geochemistry* 62, 173-196.
- Glass, B.P., Shaobin, L. & Montanari, A., 2004: Impact ejecta in upper Eocene deposits at Massignano, Italy. *Meteoritics & Planetary Science* 39, 589-597.
- Grier, J.A. & McEwen, A.S., 2001: The lunar record of recent impact cratering. In B. Peucker-Ehrenbrink, & B. Schmitz (eds.): *Accretion of extraterrestrial matter throughout Earth's history*, 403-422. Kluwer Academic/Plenum Publishers.
- Haggerty, S.E., 1972a: Luna 16: An opaque mineral study and a systematic examination of compositional variations of spinels from Mare Fecunditatis. *Earth and Planetary Science Letters* 13, 328-352.
- Haggerty, S.E., 1972b: Solid solution, subsolidus reduction and compositional characteristics of spinels in some Apollo 15 basalts. *Meteoritics* 7, 353-370.
- Haggerty, S.E., 1976: Opaque mineral oxides in terrestrial igneous rocks. In D. Rumble (ed.): *Oxide Minerals*, Hg-101 to Hg-300. Mineralogical Society of America.
- Hazel, J.E., 1989: Chronostratigraphy of Upper Eocene microspherules. *Palaio* 4, 318-329.
- Heck, P.R., Schmitz, B., Baur, H., Halliday, A.N. & Wieler, R., 2004: Fast delivery of meteorites to Earth after a major asteroid collision. *Nature* 430, 323-325.
- Hutchison, R., 2004: *Meteorites: A petrologic, chemical and isotopic synthesis*. Cambridge University Press. 506 pp.
- Jarosewich, E., Nelen, J.A. & Norberg, J.A., 1980: Reference samples for electron microprobe analysis. *Geostandards Newsletters* 4, 43-47.
- Keil, K., 1962: On the phase composition of meteorites. *Planetary and Space Science* 42, 1109-1122.
- Keil, K., Haack, H. & Scott, E.R.D., 1994: Catastrophic fragmentation of asteroids: evidence from meteorites. *Planetary and Space Science* 42, 1109-1122.
- Koeberl, C., Poag, C.W., Reimold, W.U. & Brandt, D., 1996: Impact origin of the Chesapeake Bay structure and the source of the North American

- tektites. *Science* 271, 1263-1266.
- Korochantseva, E.V., Trierlof, M., Lorenz, C.A., Buykin, A.I., Ivanova, M.A., Schwarz, W.H., Hopp, J. & Jessberger, E.K., 2007: L-chondrite asteroid breakup tied to Ordovician meteorite shower by multiple isochron ^{40}Ar - ^{39}Ar dating. *Meteoritics and Planetary Science* 42, 113-130.
- Kyte, F.T., Shukolyukov, A., Hildebrand, A.R., Lugmair, G.W. & Hanova, J., 2004: Initial Cr-isotopic and iridium measurements of concentrates from late-Eocene cpx-spherule deposits. *Lunar and Planetary Science XXXV*. Abstract number 1824.
- Lindström, M., 1971: Vom Anfang, Hochstand und Ende eines Epikontinentalmeeres. *Geologische Rundschau* 60, 419-438.
- Lindström, M., 1979: Diagenesis of lower Ordovician hard grounds in Sweden. *Geologica et Paleontologica* 13, 9-30.
- Lindström, M., Chen, J. & Zhang, J., 1991: Section at Daping reveals Sino-Baltoscandian parallelism of facies in the Ordovician. *GFF* 113, 189-205.
- Marti, K. & Graf, T., 1992: Cosmic-ray exposure history of ordinary chondrites. *Annual Review of Earth and Planetary Sciences* 20, 221-243.
- Mason, B. & Melson, W.G., 1970: *The Lunar Rocks*. John Wiley & Sons, Inc. 179 pp.
- Matese, J.J., Whitman, P.G., Innanen, K.A. & Valtonen, M.J., 1995: Periodic modulation of the Oort cloud comet flux by the adiabatically changing galactic tide. *Icarus* 116, 255-268.
- Molina, E., Gonzalvo, C. & Keller, G., 1993: The Eocene-Oligocene planktic foraminiferal transition – extinctions, impacts and hiatuses. *Geological Magazine* 130, 483-499.
- Montanari, A., Asaro, F., Michel, H.V. & Kennett, J.P., 1993: Iridium anomalies of Late Eocene age at Massignano (Italy), and ODP site-689B (Maud-Rise Antarctic). *Palaios* 8, 420-437.
- Montanari, A., Bagatin, A.C. & Farinella, P., 1998: Earth cratering record and impact energy flux in the last 150 Ma. *Planetary and Space Science* 46, 271-281.
- Nehru, C.E., Prinz, M., Dowty, E. & Keil, K., 1974: Spinel-group minerals and ilmenite in Apollo 15 rake samples. *American Mineralogist* 59, 1220-1235.
- Papike, J.J., Taylor, L. & Simon, S., 1991: Lunar minerals. In G.H. Heiken, D.T. Vaniman & B.M. French (eds.): *Lunar Sourcebook, a User's Guide to the Moon*, 121-182. Cambridge University Press.
- Papike, J.J., Ryder, G. & Shearer, C.K., 1998: Lunar Samples. In J.J. Papike (ed.): *Planetary Materials*, 5-1 to 5-234. Mineralogical Society of America.
- Patterson, D.B., Farley, K.A. & Schmitz, B., 1998: Preservation of extraterrestrial ^3He in 480-Ma-old marine limestones. *Earth and Planetary Science Letters* 163, 315-325.
- Pierrard, O., Robin, E., Rocchia, R. & Montanari, A., 1998: Extraterrestrial Ni-rich spinel in upper Eocene sediments from Massignano, Italy. *Geology* 26, 307-310.
- Schmitz, B., Lindström, M., Asaro, F. & Tassinari, M., 1996: Geochemistry of meteorite-rich marine limestone strata and fossil meteorites from the lower Ordovician at Kinnekulle, Sweden. *Earth and Planetary Science Letters* 145, 31-48.
- Schmitz, B., Tassinari, M. & Peucker-Ehrenbrink, B., 2001: A rain of ordinary chondritic meteorites in the early Ordovician. *Earth and Planetary Science Letters* 194, 1-15.
- Schmitz, B., Häggström, T. & Tassinari, M., 2003: Sediment-dispersed extraterrestrial chromite traces a major asteroid disruption event. *Science* 300, 961-964.
- Schmitz, B. & Häggström, T., 2006: Extraterrestrial chromite in Middle Ordovician marine limestone at Kinnekulle, southern Sweden – Traces of a major asteroid breakup event. *Meteoritics and Planetary Science* 41, 455-466.
- Schmitz, B., Harper, D.A.T., Peucker-Ehrenbrink, B., Stouge, S., Alwmark, C., Cronholm, A., Bergström, S.M., Tassinari, M. & Xiaofeng, W., 2008: Asteroid breakup linked to the Great Ordovician Biodiversification Event. *Nature Geoscience* 1, 49-53.
- Schmitz, B., Cronholm, A. & Montanari, A., in press: A search for extraterrestrial chromite in the late Eocene Massignano section, central Italy. *Geological Society of America Special Papers*.
- Shuvalov, V.V. & Artemieva, N.A., 2006: Impact ejecta escaping the Moon. *Lunar and Planetary Science XXXVII*. Abstract number 1168.
- Silva, I.P. & Jenkins, D.J., 1993: Decision on the Eocene - Oligocene boundary stratotype. *Episodes* 16, 379-381.
- Snetsinger, K.G., 1969: Manganian ilmenite from a sierran adamellite. *The American Mineralogist* 54, 431-436.
- Snetsinger, K.G. & Keil, K., 1969: Ilmenite in ordinary chondrites. *The American Mineralogist* 54, 780-786.
- Tagle, R. & Claeys, P., 2004: Comet or asteroid shower in the late Eocene? *Science* 305, 492.
- Tagle, R. & Claeys, P., 2005: An ordinary chondrite impactor for the Popigai crater, Siberia. *Geochimica et Cosmochimica Acta* 69, 2877- 2889.
- Tagle, R., Claeys, P., Grieve, R.F.A., Schmitt, R.T. & Erzinger, J., 2006: Evidence for a second L chondrite impact in the Late Eocene: Preliminary results from the Wanapitei crater, Canada. *Lunar and Planetary Science XXXVII*. Abstract number 1278.

- Taylor, L.A., Kullerud, G. & Bryan, W.B., 1971: Opaque mineralogy and textural features of Apollo 12 samples and a comparison with Apollo 11 rocks. *Proceedings of the Second Lunar Science Conference vol. 1*, 855-871.
- Thorslund, P. & Wickman, F.E., 1981: Middle Ordovician chondrite in fossiliferous limestone from Brunflo, central Sweden. *Nature* 289, 285-286.
- Thorslund, P., Wickman, F.E. & Nyström, J.O., 1984: The Ordovician chondrite from Brunflo, central Sweden, I. General description and primary minerals. *Lithos* 17, 87-100.
- Weibel, R. & Friis, H., 2004: Opaque minerals as keys for distinguishing oxidising and reducing diagenetic conditions in the Lower Triassic Bunter Sandstone, North German Basin. *Sedimentary Geology* 169, 129-149.
- Wiechert, U., Halliday, A.N., Lee, D.-C., Snyder, G.A., Taylor, L.A. & Rumble, D., 2001: Oxygen isotopes and the Moon-forming giant impact. *Science* 292, 345-348.
- Wlotzka, F., 2005: Cr spinel and chromite as petrogenetic indicators in ordinary chondrites: Equilibration temperatures of petrologic types 3.7 to 6. *Meteoritics and Planetary Science* 40, 1673-1702.
- Zappalà, V., Cellino, A., Gladman, B.J., Manley, S. & Migliorini, F., 1998: Asteroid showers on Earth after family breakup events. *Icarus* 134, 176-179.

Internet addresses:

- <http://geography.about.com/library/blank/blxitaly.htm> (080906).
- Meteoritical Bulletin Database: <http://tin.er.usgs.gov/meteor/index.php> (080910).
- SGU mapservice: http://www.sgu.se/sgu/sv/produkter-tjanster/tjanster/kart-tjanst_start.htm (080929).

Appendix

Table 7. Element concentrations (wt. %) of other chromium-rich spinels (OC) from the Kinnekulle limestone.

Stratigraphic unit	MgO	Al ₂ O ₃	TiO ₂	V ₂ O ₃	Cr ₂ O ₃	MnO	FeO	ZnO
Arkeologen, lower	9.27	17.76	0.18	0.12	44.97	0.39	23.35	0.20
	13.10	32.28	0.22	0.09	31.54	0.15	20.33	0.31
	9.95	16.44	0.36	0.22	46.11	0.35	23.96	0.25
	10.37	24.53	0.41	0.23	35.72	0.45	25.18	0.14
	12.96	20.70	0.30	0.20	48.13	0.23	16.90	0.19
	8.68	16.47	0.90	0.13	43.69	0.23	28.14	0.14
	8.09	14.98	0.33	0.24	47.51	0.45	25.83	0.21
	9.81	24.84	0.48	0.16	35.17	0.41	27.20	0.20
	9.92	22.29	0.46	0.34	36.97	0.23	27.57	0.19
	12.13	22.86	1.10	0.30	34.37	0.33	29.41	0.14
	9.70	23.08	0.41	0.17	41.63	0.24	22.02	0.18
	14.70	35.32	0.23	0.21	24.49	0.18	24.85	0.14
	11.56	15.55	1.40	0.28	48.19	0.32	21.42	0.16
	9.46	20.08	0.56	0.21	41.51	0.25	25.07	0.04
	11.85	16.31	0.09	0.09	50.27	0.30	22.72	0.33
	9.38	14.73	0.40	0.21	45.15	0.26	27.08	0.22
	10.90	17.66	0.38	0.16	45.23	0.41	25.08	0.18
	9.76	26.04	0.69	0.40	19.79	0.39	39.99	0.00
	9.38	21.39	0.30	0.14	38.08	0.31	23.82	0.15
	15.10	35.50	0.27	0.23	29.79	0.39	24.34	0.11
	15.21	20.89	0.44	0.14	47.13	0.15	17.93	0.11
	9.02	19.03	0.53	0.20	43.53	0.42	27.77	0.23
	5.92	16.69	1.00	0.56	42.49	0.44	29.22	0.16
	11.07	21.51	0.48	0.13	37.30	0.32	28.45	0.26
	10.39	20.79	1.61	0.21	38.96	0.23	26.13	0.23
	10.74	23.93	0.32	0.20	40.22	0.32	26.50	0.16
	12.13	24.24	1.01	0.31	38.36	0.32	23.49	0.31
	11.06	21.57	0.36	0.31	36.62	0.33	29.35	0.25
	11.43	24.24	0.61	0.19	47.68	0.25	21.45	0.21
	6.98	16.18	0.28	0.25	32.04	0.57	43.57	0.23
	9.79	20.27	0.62	0.26	39.65	0.41	27.60	0.10
	12.11	28.79	0.49	0.21	38.00	0.33	22.24	0.11
	11.36	16.66	0.40	0.17	48.24	0.44	23.11	0.15
	11.68	23.55	0.13	0.12	41.91	0.33	21.62	0.27
	8.84	18.63	0.60	0.23	41.23	0.31	26.65	0.29
	9.78	15.95	0.21	0.21	51.60	0.44	22.16	0.30
	10.44	13.28	0.39	0.17	48.24	0.36	25.94	0.16
	7.52	15.47	0.47	0.11	43.50	0.52	28.76	0.25

	9.27	17.11	0.55	0.18	50.09	0.23	19.90	0.03
	10.42	11.92	0.35	0.07	50.65	0.37	23.39	0.16
	9.40	18.08	0.35	0.20	42.59	0.39	27.90	0.10
	9.01	17.40	2.07	0.54	32.50	0.48	35.79	0.17
	8.12	17.83	2.17	0.67	22.66	0.37	49.20	0.18
	14.83	38.38	0.29	0.21	21.23	0.27	25.88	0.26
	6.99	14.13	0.43	0.18	43.84	0.31	31.11	0.23
	10.32	14.82	0.46	0.12	49.64	0.39	23.10	0.05
	9.96	15.66	0.48	0.17	48.24	0.52	25.95	0.12
	10.49	18.61	0.63	0.24	43.78	0.26	24.22	0.17
	10.24	22.08	0.86	0.40	29.31	0.40	37.99	0.15
	11.56	16.66	0.20	0.10	47.86	0.24	25.68	0.34
	10.84	14.00	0.29	0.08	47.94	0.24	27.03	0.08
	11.75	22.04	0.89	0.31	31.81	0.25	32.19	0.09
	7.11	8.14	0.27	0.21	56.51	0.48	26.58	0.16
	8.84	8.08	0.15	0.12	57.44	0.47	23.90	0.00
	2.75	19.62	0.26	0.26	43.44	1.32	30.59	1.08
	12.59	16.35	0.62	0.19	47.30	0.13	22.20	0.11
	8.42	6.83	0.24	0.17	56.86	0.36	22.22	0.00
	9.16	13.68	0.33	0.14	40.05	0.48	34.98	0.15
	10.67	23.75	0.38	0.21	40.77	0.19	26.23	0.00
	12.79	17.92	0.38	0.15	51.09	0.41	19.83	0.16
	10.40	22.16	0.70	0.16	39.08	0.32	26.15	0.05
	6.32	16.31	0.50	0.20	39.67	0.34	30.60	0.28
	8.98	15.86	0.27	0.12	49.55	0.43	29.12	0.25
	8.84	10.49	0.21	0.10	55.25	0.30	24.36	0.05
	11.53	15.94	0.29	0.17	48.22	0.22	22.41	0.35
Arkeologen, upper	9.43	8.26	0.14	0.12	56.51	0.39	24.51	0.11
	9.13	10.82	0.07	0.07	53.75	0.25	24.95	0.11
	13.68	42.84	0.00	0.38	26.57	0.07	15.52	0.32
Golvsten, lower	14.9	31.13	0.10	0.21	37.65	0.31	15.24	0.26
Golvsten, upper	15.64	28.22	0.35	0.17	36.7	0.31	17.01	0.02
	9.14	19.83	1.09	0.51	23.11	0.33	45.85	0.12
	12.3	22.62	0.96	0.21	42.4	0.43	21.52	0.03
	6.41	4.24	0.71	0.46	60.36	0.32	25.29	0.22

Data from Schmitz & Haggström (2006).

Table 8. Element concentrations (wt. %) of other chromium-rich spinels (OC) from the Massignano limestone.

MgO	Al ₂ O ₃	TiO ₂	V ₂ O ₃	Cr ₂ O ₃	MnO	FeO	ZnO	Total
13.33	26.70	-*	-	41.88	-	17.51	-	99.40
15.73	39.83	1.00	-	21.56	-	20.99	-	99.10
15.01	35.83	-	-	31.30	-	16.47	-	98.60
11.15	10.45	-	-	59.22	0.51	17.93	-	99.30
10.72	19.35	0.81	-	44.79	-	25.51	-	101.20
3.17	4.14	-	0.40	59.44	-	31.04	0.19	98.40
12.33	23.75	-	-	45.56	-	18.32	-	100.00
9.63	18.34	-	-	52.18	-	18.45	-	98.60
5.20	11.90	2.86	0.70	37.17	-	40.92	-	98.80
12.35	23.00	-	-	46.91	-	17.93	-	100.20
9.14	24.04	-	-	31.42	-	33.77	-	98.40
14.76	32.76	-	-	35.36	-	17.00	-	99.90
13.31	22.16	-	-	46.58	-	17.10	-	99.20
6.82	8.43	-	-	59.72	-	23.39	0.70	99.10
11.63	15.80	-	-	52.29	-	18.62	-	98.30
10.08	22.47	-	-	45.47	-	21.03	0.38	99.40
13.05	23.11	-	-	43.94	-	18.24	-	98.30
17.39	46.82	-	-	21.05	-	14.36	-	99.60
11.90	26.34	-	-	42.29	-	18.75	-	99.30
10.64	21.75	-	-	47.43	-	18.37	-	98.20
0.62	7.64	-	-	57.36	1.53	32.87	0.54	100.60
6.38	11.30	2.71	0.57	36.13	-	41.59	-	98.70
12.73	23.58	-	-	46.94	-	16.84	-	100.10
13.20	27.90	0.34	-	37.16	-	20.05	-	98.70
10.01	21.28	-	-	45.35	0.69	21.56	-	98.90
11.10	7.27	-	-	63.69	-	16.72	-	98.80
12.65	22.84	-	-	45.75	-	17.18	-	98.40
6.24	12.68	0.24	-	48.01	2.09	28.93	-	98.20
14.19	24.25	-	-	45.48	-	15.21	-	99.10
13.01	34.06	-	-	31.21	-	21.42	-	99.70
12.98	24.96	-	-	44.40	-	17.26	-	99.60
13.70	29.70	-	-	38.09	-	17.47	-	99.00
15.58	29.58	-	-	39.97	-	14.06	-	99.20
14.80	22.29	-	-	46.89	0.73	14.51	1.00	100.20
12.65	22.17	-	-	46.90	-	17.35	-	99.10

Data from Schmitz et al. (in press).

* Below detection limit

Table 10. Average element concentration (wt. % and standard deviation (1 σ)) of grains from Kinnekulle sample GOL top.

	MgO	Al ₂ O ₃	TiO ₂	V ₂ O ₃	Cr ₂ O ₃	MnO	FeO	ZnO	Total
GOL TOP EC									
EC1	2.20±0.15	5.70±0.09	3.14±0.39	0.74±0.03	58.62±0.75	0.86±0.18	29.56±1.08	0.04±0.07	100.85±0.52
EC2	2.27±0.09	5.90±0.03	3.06±0.06	0.86±0.12	57.77±0.38	0.89±0.27	30.57±0.28	-*	101.32±0.11
EC3	2.89±0.29	5.61±0.14	3.11±0.10	0.68±0.10	57.94±0.63	0.85±0.10	29.81±0.71	-	100.90±0.52
Mean	2.45±0.38	5.74±0.15	3.10±0.04	0.76±0.09	58.11±0.45	0.87±0.02	29.98±0.53	0.01±0.02	101.02±0.26
Max.	2.89	5.9	3.14	0.86	58.62	0.89	30.57	0.04	101.32
Min.	2.2	5.61	3.06	0.68	57.77	0.85	29.56	-	100.85
SiO₂									
GOL TOP ILM									
ILM 1	1.89±0.09	0.31±0.05	52.44±0.58	0.60±0.12		0.99±0.05	40.42±0.55	-	96.65±0.35
ILM2	1.73±0.52	0.32±0.02	51.72±0.74	0.41±0.18		0.86±0.11	38.15±0.96	-	93.19±1.11
ILM3	1.50±0.10	0.58±0.20	50.88±0.26	0.46±0.28		1.49±0.37	38.70±1.23	-	93.61±0.89
ILM4	1.06±0.03	0.50±0.06	50.03±0.81	0.30±0.10		0.71±0.15	38.09±0.85	0.23±0.09	90.92±0.64
ILM5	1.13±0.92	0.62±0.07	49.90±0.36	0.57±0.22		2.10±1.35	36.44±1.86	0.28±0.07	91.04±0.86
ILM6	2.06±0.19	0.30±0.09	51.98±0.24	0.54±0.15		0.95±0.11	38.39±0.59	-	94.22±0.66
ILM7	0.52±0.04	0.30±0.04	53.48±0.20	0.42±0.20		4.79±0.87	37.52±1.49	-	97.04±0.80
ILM8	2.33±0.18	0.40±0.09	50.62±0.23	0.16±0.27		2.82±0.53	36.61±0.77	-	93.02±0.25
ILM9	2.53±0.21	0.53±0.06	50.25±0.74	0.25±0.16		2.85±0.28	37.96±1.03	-	94.46±0.44
ILM10	2.15±0.29	0.35±0.05	49.49±1.37	0.34±0.15		1.79±0.50	37.55±0.33	-	91.66±0.95
ILM11	1.83±0.51	0.31±0.05	52.73±0.36	0.46±0.16		0.88±0.14	39.11±0.78	-	95.32±0.45
Mean	1.70±0.60	0.41±0.12	51.23±1.31	0.41±0.14		1.84±1.25	38.09±1.12	0.05±0.10	93.74±2.07
Max.	2.53	0.62	53.48	0.60		4.79	40.42	0.28	97.04
Min.	0.52	0.30	49.49	0.16		0.71	36.44	-	90.92
SiO₂									
GOL TOP OTR									
OTR1	0.14±0.08	0.42±0.07	62.37±1.81	0.28±0.24		2.64±0.82	33.99±1.86	-	99.83±3.15
OTR2	0.07±0.04	0.32±0.01	56.69±0.21	0.36±0.23		2.82±0.08	33.19±0.91	0.32±0.09	93.78±1.21
OTR3	0.25±0.33	0.29±0.01	56.91±0.51	0.48±0.07		2.27±0.87	33.33±0.88	0.22±0.12	93.75±0.40
OTR4	-	0.35±0.07	55.79±0.56	0.21±0.21		2.71±0.35	32.02±0.31	0.09±0.04	91.16±0.87
OTR5	0.05±0.05	0.41±0.13	57.19±1.02	0.24±0.32		2.78±0.33	31.16±0.50	-	91.83±0.37
OTR6	1.49±0.75	0.38±0.05	56.73±2.73	0.45±0.07		0.30±0.10	31.33±3.59	0.34±0.14	91.01±0.21
OTR7	-	0.39±0.08	53.17±0.19	0.56±0.33		2.19±0.26	34.22±0.36	0.35±0.12	90.87±0.49
OTR8	-	0.32±0.07	55.86±0.59	0.47±0.10		2.40±0.36	31.94±0.44	0.30±0.08	91.30±1.14
OTR9	-	0.31±0.04	56.23±0.56	0.36±0.30		2.45±0.24	32.01±0.18	-	91.36±0.77
OTR10	0.31±0.28	0.44±0.08	59.36±3.08	0.37±0.19		1.06±1.37	29.90±2.24	-	91.44±0.76
OTR11	0.78±0.04	0.23±0.08	59.14±0.52	0.51±0.30		2.02±0.15	37.11±0.25	-	99.79±0.72
OTR12	2.24±1.04	0.41±0.05	58.77±2.12	0.45±0.07		0.44±0.35	31.65±3.48	-	93.97±0.82
OTR13	0.53±0.32	0.45±0.03	63.20±0.56	0.46±0.18		0.38±0.18	28.17±0.30	-	93.45±0.31
OTR14	0.10±0.03	0.44±0.11	53.42±0.09	0.58±0.29		2.63±0.55	34.55±0.17	-	91.86±0.46
OTR15	0.05±0.05	0.35±0.04	53.44±0.25	0.68±0.10		3.04±0.50	32.77±0.69	0.68±0.26	91.02±0.22
OTR16	1.02±0.20	0.35±0.06	54.44±0.55	0.41±0.10		1.00±0.09	36.50±1.31	0.15±0.09	93.87±0.68
OTR17	1.47±0.47	0.49±0.25	50.56±0.88	0.52±0.10		4.42±0.95	32.58±0.76	-	90.09±1.76
OTR18	2.21±0.20	0.41±0.06	56.56±0.27	0.61±0.27		0.91±0.04	35.94±0.22	-	96.64±0.56
OTR19	2.82±0.19	0.29±0.03	55.78±0.36	0.36±0.15		1.86±0.05	34.59±0.17	-	95.70±0.27
OTR20	-	-	63.75±1.42	0.37±0.31		2.04±0.29	27.56±1.72	0.24±0.14	93.96±0.58
OTR21	-	0.61±0.19	53.00±2.05	0.34±0.10		2.68±0.20	31.47±1.48	-	88.10±3.45
OTR22	0.10±0.06	0.41±0.04	53.05±0.61	0.37±0.33		3.56±0.47	32.24±0.44	0.19±0.03	89.92±0.58
OTR23	-	0.32±0.15	52.21±1.25	0.62±0.12		4.45±0.52	32.28±0.57	0.21±0.09	90.08±1.00
OTR24	-	0.50±0.08	53.14±0.73	0.56±0.18		1.07±0.14	35.66±0.23	1.00±0.13	91.93±0.63
OTR25	1.13±0.40	0.51±0.09	54.45±0.07	0.59±0.22		1.59±1.42	37.12±2.09	0.13±0.13	95.52±0.87
OTR26	0.49±0.65	0.33±0.03	52.38±0.76	0.52±0.08		3.28±0.66	34.19±0.62	0.08±0.04	91.27±0.08
OTR27	-	0.39±0.08	51.15±0.81	0.63±0.21		5.17±0.37	33.60±0.84	0.23±0.15	91.17±0.51
OTR28	0.16±0.09	0.42±0.02	53.82±0.34	0.56±0.07		2.28±0.06	35.59±0.26	0.19±0.08	93.29±0.58
OTR29	1.46±0.17	0.43±0.08	51.57±0.37	0.50±0.20		2.51±0.13	35.94±1.10	0.17±0.07	92.59±1.01
Mean	0.58±0.81	0.38±0.11	55.66±3.48	0.46±0.12		2.31±1.20	33.19±2.41	0.17±0.23	92.78±2.72
Max.	2.82	0.61	63.75	0.68		5.17	37.12	1.00	99.83
Min.	-	-	50.56	0.21		0.30	27.56	-	88.10

* Below detection limit

Table 11. Average element concentration (wt. % and standard deviation (1 σ)) of grains from Kinnekulle sample GOL bottom.

	MgO	Al ₂ O ₃	TiO ₂	V ₂ O ₃	Cr ₂ O ₃	MnO	FeO	ZnO	Total
GOL BOTTOM EC									
EC1	4.14±0.10	6.55±0.23	2.87±0.14	0.73±0.04	58.35±0.60	0.93±0.21	27.28±0.69	0.26±0.27	101.12±0.25
EC2	2.52±0.06	6.25±0.32	3.12±0.15	0.72±0.05	57.46±2.36	0.85±0.19	28.16±0.79	0.41±0.21	99.34±2.45
EC3	3.45±0.24	5.68±0.27	2.95±0.12	0.80±0.19	59.61±0.37	0.81±0.14	26.58±0.90	0.56±0.22	100.45±0.33
Mean	3.37±0.81	6.16±0.44	2.98±0.13	0.75±0.04	58.47±1.08	0.86±0.06	27.34±0.79	0.41±0.15	100.30±0.90
Max.	4.14	6.55	3.12	0.80	59.61	0.93	28.16	0.56	101.12
Min.	2.52	5.68	2.87	0.72	57.46	0.81	26.58	0.26	99.34
								SiO ₂	
GOL BOTTOM ILM									
ILM1	1.38±1.37	0.48±0.03	51.99±0.40	0.35±0.11	-*	0.71±0.34	39.81±1.68	-	94.72±0.88
ILM2	1.72±1.68	0.62±0.03	48.81±0.34	0.46±0.02	-	0.93±0.19	46.31±0.66	-	98.84±2.77
ILM3	1.01±0.07	0.58±0.09	52.10±0.41	0.55±0.08	-	0.74±0.08	44.02±0.75	-	99.17±0.42
ILM4	1.65±1.74	0.61±0.13	54.86±1.58	0.59±0.17	-	0.44±0.38	43.53±1.50	-	101.68±0.76
ILM5	1.26±0.15	0.60±0.05	53.54±0.26	0.36±0.29	-	0.85±0.11	43.98±0.43	0.39±0.06	100.98±0.46
ILM6	0.44±0.27	1.40±1.46	53.98±1.01	1.06±0.24	0.57±0.03	0.77±0.10	42.68±0.99	-	100.91±1.06
ILM7	1.85±1.05	0.63±0.05	53.99±0.48	0.68±0.18	-	0.80±0.05	46.23±0.47	0.21±0.11	104.38±0.53
ILM8	1.48±1.45	0.56±0.04	49.94±1.77	0.55±0.07	-	0.59±0.28	38.83±3.72	-	91.95±0.86
ILM9	1.09±0.22	0.77±0.06	47.53±0.78	0.58±0.06	-	0.59±0.04	40.24±0.29	-	90.81±1.01
ILM10	1.84±0.47	0.58±0.06	49.00±0.26	0.61±0.16	-	0.60±0.06	40.58±0.78	-	95.22±1.37
ILM11	0.60±0.25	0.59±0.16	47.32±0.58	0.45±0.12	-	0.69±0.03	41.61±0.41	-	91.26±0.19
ILM12	1.55±1.07	0.54±0.05	48.94±0.32	0.61±0.07	-	1.05±0.17	42.77±1.87	-	95.45±2.70
ILM14	0.39±0.09	0.87±0.33	46.26±1.31	0.65±0.24	-	0.50±0.16	39.24±1.08	-	87.90±1.03
ILM15	0.96±0.14	0.60±0.06	46.73±0.48	0.51±0.12	-	0.67±0.07	39.39±0.66	-	88.74±1.17
ILM16	1.57±1.37	0.49±0.10	46.66±0.05	0.49±0.16	-	0.86±0.07	40.23±1.27	-	90.29±2.40
ILM17	1.05±1.13	0.54±0.12	46.87±1.45	0.37±0.16	-	0.55±0.30	39.84±1.79	-	89.22±0.87
ILM18	1.99±0.68	0.50±0.07	42.80±4.70	0.32±0.12	-	0.16±0.12	35.38±2.21	-	81.15±2.83
ILM19	0.81±0.28	0.61±0.08	54.61±0.57	0.54±0.04	-	0.73±0.06	43.17±0.57	-	100.46±0.94
ILM20	3.07±0.24	0.53±0.07	52.29±0.33	0.59±0.17	-	0.30±0.11	40.05±0.25	-	96.82±0.31
ILM21	1.51±1.58	0.57±0.08	51.13±2.74	0.48±0.04	-	0.71±0.28	42.80±0.23	-	97.22±1.76
ILM22	3.30±0.19	0.49±0.07	50.78±1.81	0.45±0.14	-	0.50±0.25	42.76±1.40	-	98.27±2.75
ILM23	3.19±0.34	0.50±0.08	48.89±2.08	0.35±0.15	-	1.04±0.16	43.00±0.01	-	96.97±1.67
ILM24	2.97±0.28	0.59±0.08	50.71±0.86	0.50±0.13	-	2.50±2.08	40.45±1.35	-	97.71±2.77
ILM25	1.99±1.25	0.61±0.06	52.58±1.04	0.50±0.08	-	0.49±0.36	41.72±2.13	-	97.89±1.03
ILM26	2.75±0.30	0.57±0.08	50.93±2.96	0.48±0.13	-	0.19±0.14	42.65±3.88	-	97.56±1.60
ILM27	1.01±0.26	0.70±0.13	48.61±0.39	0.80±0.21	-	0.85±0.15	41.41±0.32	0.20±0.03	93.57±0.55
ILM28	1.80±0.58	0.45±0.06	47.59±0.28	0.35±0.17	-	0.79±0.16	42.19±1.37	-	93.17±0.87
ILM29	1.93±0.83	0.61±0.06	45.59±0.28	0.37±0.06	-	0.67±0.10	41.23±0.68	-	90.41±1.25
ILM30	0.64±0.08	0.44±0.07	49.92±0.29	0.42±0.06	-	0.93±0.13	39.36±0.47	-	91.70±0.75
ILM31	0.93±0.32	0.42±0.11	47.90±0.16	0.48±0.18	-	0.96±0.05	42.68±0.88	-	93.38±0.40
ILM32	0.78±0.09	0.41±0.05	49.61±0.11	0.49±0.16	-	0.68±0.15	40.40±0.84	-	92.38±0.65
ILM33	1.27±0.56	0.56±0.21	49.09±0.41	0.55±0.27	-	0.73±0.03	40.32±0.37	-	92.52±1.37
ILM34	0.66±0.14	0.60±0.05	45.61±0.74	0.64±0.20	-	0.71±0.13	39.83±1.85	-	88.06±2.53
ILM35	2.09±0.67	0.43±0.05	47.98±0.73	0.57±0.28	-	2.80±1.23	39.15±0.48	-	93.02±0.96
ILM36	0.56±0.21	0.50±0.08	46.97±0.80	0.41±0.06	-	0.65±0.17	41.32±1.14	-	90.41±0.38
ILM37	0.42±0.09	0.47±0.08	46.66±0.21	0.67±0.14	-	0.71±0.10	41.93±0.13	-	90.86±0.12
ILM38	1.15±0.21	0.60±0.07	48.51±0.41	0.47±0.12	-	0.77±0.26	39.93±0.05	-	91.43±0.44
ILM39	0.76±0.03	1.28±0.95	51.15±5.72	0.49±0.08	-	0.21±0.27	38.34±5.60	0.29±0.14	92.52±1.16
ILM40	1.80±0.37	0.48±0.04	47.35±0.41	0.56±0.17	-	0.71±0.34	45.31±0.91	-	96.21±0.60
ILM41	2.78±0.16	0.55±0.03	43.69±0.59	0.37±0.12	-	0.30±0.21	43.58±0.45	-	91.26±0.50
ILM42	0.69±0.54	0.73±0.24	46.92±0.87	0.20±0.07	-	0.71±0.18	41.64±1.34	-	90.89±0.80
ILM43	2.95±0.27	0.57±0.04	45.63±0.23	0.47±0.23	-	1.27±0.61	45.39±0.49	-	96.36±0.24
ILM44	3.15±0.13	0.45±0.02	45.71±0.54	0.23±0.11	-	1.21±0.18	44.50±1.31	-	95.26±1.43
ILM45	2.63±0.31	0.55±0.18	44.05±0.62	0.49±0.09	-	0.26±0.08	44.89±1.55	-	92.88±0.99
ILM46	0.91±0.55	0.49±0.03	50.73±0.72	0.49±0.15	-	0.75±0.33	38.62±1.98	-	91.99±1.11
ILM47	1.29±1.55	0.47±0.03	48.66±2.95	0.40±0.11	-	0.35±0.31	37.06±1.43	-	88.23±3.30
ILM48	2.85±0.42	0.56±0.10	50.53±4.04	0.42±0.10	-	0.25±0.04	38.07±2.72	-	92.69±2.57
Mean	1.58±0.86	0.59±0.18	48.97±2.91	0.50±0.14	-	0.75±0.48	41.46±2.41	0.02±0.08	93.93±4.41
Max.	3.30	1.40	54.86	1.06	0.57	2.80	46.31	0.39	104.38
Min.	0.39	0.41	42.80	0.20	-	0.16	35.38	-	81.15

GOL BOTTOM OTR

OTR1	1.31±1.63	0.43±0.10	62.20±1.72	0.39±0.06	1.36±1.45	37.33±1.26	103.02±2.77
OTR2	3.42±0.78	0.28±0.07	60.10±1.58	0.47±0.04	0.67±0.07	31.13±2.68	96.08±0.36
OTR3	0.49±0.45	0.42±0.04	56.79±1.63	0.42±0.09	0.76±0.58	34.56±3.15	93.45±1.90
OTR4	2.48±0.10	0.32±0.08	59.08±0.40	0.62±0.16	0.78±0.05	31.43±0.38	94.77±0.21
OTR5	1.09±0.50	0.34±0.02	54.77±1.96	0.23±0.17	0.61±0.25	33.16±4.05	90.21±2.21
OTR6	-	0.23±0.06	58.88±0.28	0.42±0.16	3.28±0.50	28.71±0.97	91.59±0.26
OTR7	1.15±1.31	1.83±1.12	51.70±5.72	0.54±0.21	0.10±0.07	33.51±6.09	88.81±0.42
OTR8	0.67±0.62	0.36±0.06	54.42±1.88	0.42±0.12	0.78±0.66	32.02±1.90	88.75±1.21
OTR9	0.97±0.31	0.46±0.06	56.02±3.59	0.36±0.18	0.48±0.21	32.44±2.70	90.73±0.72
OTR10	0.94±0.54	0.57±0.29	58.24±1.21	0.52±0.17	0.46±0.14	31.40±1.67	92.12±1.29
OTR11	0.36±0.37	0.48±0.08	61.59±2.80	0.45±0.22	0.40±0.11	32.12±1.48	95.41±4.34
OTR12	1.19±0.17	1.26±1.35	55.91±3.67	0.38±0.04	1.23±0.22	37.75±2.69	97.73±6.63
OTR13	1.24±0.88	0.38±0.03	58.05±1.03	0.42±0.18	0.40±0.13	32.35±1.75	92.84±0.19
OTR14	0.57±0.12	0.33±0.09	55.98±0.80	0.30±0.20	0.88±0.18	37.57±0.45	95.63±0.96
OTR15	1.24±0.94	0.58±0.05	50.96±1.57	0.32±0.28	0.31±0.26	28.99±2.14	92.38±0.54
OTR16	2.45±0.54	0.51±0.01	52.02±0.37	0.50±0.32	0.21±0.03	35.07±0.33	90.75±0.69
OTR17	1.15±0.24	0.48±0.06	54.83±0.93	0.27±0.04	1.17±0.32	38.37±1.12	96.27±1.00
OTR18	2.63±0.06	0.62±0.04	50.56±0.14	0.64±0.14	-	31.77±0.53	86.22±0.82
OTR19	2.69±0.37	0.44±0.01	51.30±0.98	0.51±0.18	0.27±0.10	33.23±0.86	88.49±1.54
OTR20	2.71±0.19	0.24±0.03	51.15±3.06	0.43±0.16	1.44±0.05	33.16±3.72	89.14±6.65
OTR21	1.12±0.15	0.38±0.08	54.43±0.52	0.31±0.09	1.22±0.72	37.13±2.30	94.59±1.23
Mean	1.42±0.93	0.52±0.37	55.67±3.57	0.42±0.11	0.80±0.71	33.49±2.80	92.81±3.87
Max.	3.42	1.83	62.20	0.64	3.28	38.37	103.02
Min.	-	0.23	50.56	0.23	-	28.71	86.22

* Below detection limit

Table 12. Average element concentration (wt. % and standard deviation (1 σ)) of grains from Puxi River sample Y9.

	MgO	Al ₂ O ₃	TiO ₂	V ₂ O ₃	Cr ₂ O ₃	MnO	FeO	ZnO	Total
Y9 EC									
EC 1	3.40±0.42	5.70±0.20	3.19±0.18	0.65±0.10	59.63±0.30	0.71±0.49	27.88±0.58	0.04±0.08	101.19±0.61
EC 2	4.19±1.49	6.45±0.52	3.39±0.35	0.70±0.04	61.48±0.65	0.71±0.64	28.05±1.47	0.11±0.20	105.07±1.46
EC 3	2.41±0.28	6.29±0.32	3.15±0.14	0.77±0.12	61.27±1.94	0.44±0.48	26.73±3.66	0.27±0.29	101.34±1.76
EC 4	2.91±0.21	6.42±0.39	3.25±0.44	0.70±0.09	59.42±0.29	0.94±0.32	29.80±0.49	0.06±0.12	103.48±0.55
EC 5	3.47±0.76	6.15±0.18	3.22±0.06	0.64±0.15	57.37±0.29	1.06±0.17	27.03±0.93	0.20±0.24	99.12±0.47
EC 6	3.53±0.32	5.70±0.31	2.99±0.09	0.73±0.05	56.67±0.43	1.11±0.14	26.83±0.37	0.52±0.38	98.06±0.53
EC 7	2.51±0.15	5.73±0.17	2.91±0.15	0.60±0.06	57.51±0.10	0.86±0.03	29.34±0.41	-*	99.17±0.05
EC 8	2.72±0.07	8.19±0.59	1.89±0.22	0.74±0.12	62.19±0.49	1.07±0.27	21.41±0.55	0.73±0.04	98.95±0.72
EC 9	6.82±2.41	6.18±0.12	2.87±0.35	0.70±0.10	60.04±1.37	0.19±0.39	23.96±3.98	0.31±0.51	101.08±0.71
EC 10	2.19±0.23	6.10±0.40	2.26±0.26	0.60±0.03	57.7±0.38	0.59±0.43	28.22±0.97	0.99±0.41	98.63±1.78
Mean	3.41±1.34	6.29±0.72	2.91±0.48	0.68±0.06	59.33±1.95	0.77±0.29	26.92±2.52	0.32±0.33	100.61±2.28
Max.	6.82	8.19	3.39	0.77	62.19	1.11	21.41	0.99	105.07
Min.	2.19	5.7	1.89	0.6	57.37	0.19	26.73	-	98.06
Y9 ILM									
ILM1	1.83±0.08	0.27±0.07	49.86±0.03	0.54±0.10		0.69±0.06	51.48±0.13		104.70±0.22
ILM2	1.53±0.11	0.30±0.07	47.74±0.13	0.58±0.10		0.50±0.12	50.69±0.47		101.30±0.40
ILM 3	1.49±0.11	0.44±0.08	35.43±0.46	0.57±0.19		0.76±0.12	57.35±0.36		96.04±0.58
Mean	1.62±0.19	0.34±0.09	44.34±7.79	0.56±0.02		0.65±0.13	53.17±3.64		100.68±4.36
Max.	1.83	0.44	49.86	0.58		0.76	57.35		104.70
Min.	1.49	0.27	35.43	0.54		0.50	50.69		96.04

* Below detection limit

Table 13. Average element concentration (wt. % and standard deviation (1 σ)) of grains from Puxi River sample P6a.

	MgO	Al ₂ O ₃	TiO ₂	V ₂ O ₃	Cr ₂ O ₃	MnO	FeO	ZnO	Total
P6a EC									
EC1	3.15±0.25	5.73±0.08	3.14±0.14	0.75±0.08	58.07±0.35	0.79±0.21	28.35±0.22	0.32±0.10	100.29±0.19
EC2	3.59±0.12	5.57±0.11	3.19±0.11	0.68±0.11	56.36±0.19	0.88±0.27	27.52±0.65	-*	97.79±0.41
EC3	2.40±0.24	6.33±0.18	2.96±0.09	0.73±0.05	56.46±0.32	0.95±0.11	28.41±0.51	0.35±0.21	98.60±0.46
EC4	3.05±0.18	6.07±0.19	3.17±0.04	0.71±0.03	58.87±0.31	0.93±0.22	26.45±0.40	0.66±0.04	99.92±0.80
EC5	2.84±0.41	6.01±0.10	3.09±0.20	0.71±0.10	57.21±0.36	0.85±0.09	26.91±0.94	0.68±0.08	98.29±1.17
Mean	3.01±0.44	5.94±0.30	3.11±0.09	0.72±0.03	57.39±1.07	0.88±0.06	27.53±0.87	0.40±0.28	98.98±1.08
Max.	3.59	6.33	3.19	0.75	58.87	0.95	28.41	0.68	100.29
Min.	2.40	5.57	2.96	0.68	56.36	0.79	26.45	-	97.79
P6a ILM									
ILM1	1.23±0.03	0.26±0.03	46.70±0.19	0.34±0.14		1.19±0.09	47.57±0.10		97.29±0.31

* Below detection limit

Table 14. Average element concentration (wt. % and standard deviation (1 σ)) of grains from the Massignano sample.

	MgO	Al ₂ O ₃	TiO ₂	V ₂ O ₃	MnO	FeO	Total
Massignano ILM.							
ILM 1	1.53±0.07	0.24±0.06	47.07±0.55	0.34±0.29	0.83±0.19	48.34±0.20	98.35±0.92
ILM 2	1.88±0.07	0.38±0.03	44.43±0.10	0.84±0.07	0.55±0.01	50.71±0.26	98.80±0.23
ILM 3	1.63±0.07	0.24±0.04	44.64±0.10	0.50±0.15	0.75±0.07	50.69±0.38	98.44±0.15
ILM 4	1.33±0.06	0.28±0.12	46.92±0.54	0.58±0.22	0.75±0.08	50.30±0.12	100.15±0.32
ILM 5	1.54±0.08	0.23±0.05	47.37±0.39	0.38±0.08	0.72±0.12	48.98±0.15	99.22±0.34
ILM 6	1.74±0.03	0.38±0.07	46.33±0.41	0.50±0.10	0.59±0.02	49.80±0.06	99.43±0.61
ILM 7	1.15±0.11	0.31±0.05	48.61±0.25	0.21±0.15	0.57±0.13	48.53±0.06	99.38±0.42
ILM 8	1.29±0.10	0.28±0.11	47.45±0.53	0.37±0.34	0.83±0.11	49.45±0.56	99.66±0.52
ILM 9	1.50±0.07	0.42±0.27	47.07±0.33	0.45±0.06	0.70±0.10	49.25±0.51	99.37±1.06
ILM 10	1.08±0.01	0.27±0.07	48.05±0.16	0.48±0.13	0.67±0.03	48.10±0.29	98.66±0.50
ILM 11	1.17±0.07	0.22±0.14	47.98±0.25	0.48±0.12	0.67±0.05	47.91±0.44	98.44±0.41
ILM 12	2.16±0.02	0.34±0.04	42.90±0.40	0.33±0.05	0.68±0.12	51.54±0.13	97.95±0.54
ILM 13	1.44±0.09	0.34±0.23	46.45±0.55	0.39±0.11	0.92±0.03	48.83±0.26	98.37±0.88
ILM 14	1.11±0.02	0.30±0.06	48.61±0.44	0.35±0.22	0.69±0.07	48.76±0.58	99.82±1.14
ILM 15	1.56±0.10	0.23±0.05	46.38±0.39	0.43±0.09	0.79±0.12	48.01±0.29	97.40±0.10
ILM 16	1.66±0.07	0.29±0.05	46.46±0.39	0.46±0.25	0.59±0.10	49.08±0.14	98.53±0.41
ILM 17	1.16±0.06	0.17±0.02	48.55±0.11	0.49±0.20	0.69±0.06	48.06±0.44	99.12±0.75
ILM 18	1.48±0.05	0.27±0.03	46.45±0.06	0.39±0.18	0.83±0.03	48.76±0.31	98.19±0.48
ILM 19	1.35±0.12	0.29±0.06	47.05±0.22	0.47±0.20	0.82±0.03	48.59±0.16	98.58±0.39
ILM 20	1.42±0.06	0.29±0.05	46.92±0.54	0.68±0.10	0.89±0.18	48.65±0.32	98.85±0.88
ILM 21	1.51±0.09	0.20±0.06	46.23±0.23	0.37±0.18	0.77±0.08	49.30±0.27	98.37±0.26
ILM 22	1.43±0.07	0.22±0.08	46.68±0.21	0.24±0.18	0.78±0.12	48.70±0.47	98.05±0.74
ILM 23	1.39±0.10	0.20±0.02	46.43±0.34	0.34±0.18	0.85±0.15	48.34±0.48	97.54±0.53
ILM 24	1.19±0.05	0.19±0.07	50.73±0.11	0.48±0.05	0.55±0.09	45.89±0.35	99.75±0.21
ILM 25	1.45±0.15	0.25±0.04	46.58±0.24	0.32±0.18	0.87±0.09	48.47±0.18	97.94±0.55
ILM 26	1.48±0.03	0.18±0.04	47.34±0.97	0.24±0.22	0.85±0.22	49.37±1.18	99.47±2.57
ILM 27	1.46±0.08	0.23±0.02	46.75±0.13	0.19±0.10	0.85±0.10	48.66±0.21	98.14±0.32
ILM 28	1.40±0.04	0.23±0.06	45.78±0.16	0.33±0.11	0.80±0.06	48.20±0.23	96.75±0.22
ILM 29	1.35±0.11	0.26±0.02	46.28±0.07	0.30±0.21	0.84±0.04	48.04±0.19	97.08±0.31
ILM 30	1.47±0.05	0.30±0.12	46.08±0.03	0.48±0.19	0.72±0.03	48.48±0.50	97.52±0.44
ILM 31	1.54±0.06	0.25±0.08	46.03±0.12	0.50±0.17	0.77±0.11	48.35±0.05	97.44±0.34
ILM 32	1.46±0.09	0.24±0.02	46.45±0.23	0.29±0.12	0.83±0.09	48.63±0.09	97.89±0.22
ILM 33	1.37±0.08	0.22±0.10	46.50±0.40	0.49±0.24	0.80±0.04	48.56±0.34	97.95±0.16
ILM 34	1.41±0.06	0.32±0.07	46.58±0.35	0.50±0.18	0.76±0.09	47.65±0.62	97.52±0.76

ILM 35	1.49±0.08	0.23±0.06	46.23±0.25	0.23±0.24	0.76±0.07	48.39±0.24	97.33±0.06
ILM 36	1.42±0.07	0.24±0.08	46.01±0.23	0.41±0.22	0.88±0.08	48.06±0.21	97.02±0.14
ILM 37	1.47±0.08	0.29±0.07	46.04±0.29	0.44±0.12	0.72±0.05	48.24±0.17	97.20±0.32
ILM 38	1.62±0.16	0.25±0.04	46.07±0.28	0.38±0.22	0.75±0.15	48.05±0.17	97.13±0.62
ILM 39	1.29±0.07	0.26±0.05	46.14±0.26	0.41±0.21	0.82±0.12	48.06±0.14	96.98±0.10
ILM 40	1.63±0.05	0.27±0.05	45.95±0.53	0.51±0.07	0.64±0.17	47.96±0.25	96.97±0.54
ILM 41	1.66±0.02	0.29±0.07	47.50±0.27	0.46±0.20	0.98±0.18	50.13±0.33	101.02±0.56
ILM 42	1.57±0.11	0.30±0.05	47.64±0.09	0.35±0.10	0.87±0.18	50.37±0.11	101.12±0.50
ILM 43	1.57±0.08	0.23±0.03	47.38±0.15	0.34±0.13	0.92±0.04	49.64±0.18	100.08±0.04
ILM 44	1.61±0.09	0.31±0.03	46.95±0.52	0.51±0.30	0.75±0.06	50.10±0.13	100.23±0.81
ILM 45	1.24±0.05	0.33±0.10	47.43±0.40	0.56±0.14	0.86±0.10	49.33±0.43	99.75±0.38
ILM 46	1.48±0.06	0.30±0.04	47.32±0.36	0.44±0.17	0.71±0.03	49.17±0.16	99.42±0.31
ILM 47	1.49±0.08	0.29±0.02	47.08±0.12	0.44±0.17	0.68±0.09	49.68±0.42	99.67±0.55
ILM 48	1.51±0.09	0.30±0.02	47.63±0.39	0.37±0.24	0.84±0.09	49.52±0.42	100.21±0.96
ILM 49	1.81±0.14	0.24±0.07	46.73±0.67	0.27±0.16	0.75±0.08	49.99±0.49	99.78±0.88
ILM 50	1.53±0.04	0.34±0.07	47.07±0.16	0.58±0.20	1.01±0.07	49.34±0.15	99.88±0.35
ILM 51	1.41±0.09	0.25±0.03	47.31±0.57	0.36±0.12	0.95±0.05	49.64±0.11	99.91±0.55
ILM 52	1.48±0.03	0.32±0.07	47.77±0.36	0.35±0.09	0.94±0.09	49.61±0.57	100.46±0.40
ILM 53	1.61±0.02	0.30±0.01	47.84±0.97	0.50±0.16	0.76±0.03	50.09±0.74	101.10±1.88
ILM 54	1.42±0.07	0.24±0.07	47.62±0.39	0.56±0.17	0.86±0.08	49.51±0.81	100.21±0.38
ILM 55	1.45±0.05	0.31±0.03	46.96±0.41	0.43±0.13	0.76±0.17	49.55±0.27	99.47±0.42
ILM 56	1.87±0.18	0.26±0.05	44.33±0.03	0.56±0.10	0.58±0.11	52.02±0.44	99.62±0.78
ILM 57	1.59±0.04	0.24±0.05	47.42±0.14	0.44±0.29	0.79±0.11	49.66±0.63	100.14±0.51
ILM 58	1.16±0.06	0.32±0.04	48.37±0.58	0.69±0.17	0.58±0.14	48.12±0.51	99.25±1.05
ILM 59	0.29±0.01	0.32±0.15	52.00±1.13	0.24±0.21	2.57±0.34	41.13±0.67	96.55±0.38
ILM 60	1.46±0.09	0.24±0.08	47.33±0.38	0.31±0.10	0.81±0.03	49.45±0.47	99.59±0.54
ILM 61	1.43±0.14	0.25±0.03	46.92±0.90	0.46±0.22	0.79±0.18	49.43±0.80	99.29±2.13
ILM 62	1.83±0.05	0.32±0.07	46.18±0.30	0.62±0.14	0.68±0.08	50.45±0.15	100.08±0.26
ILM 63	1.52±0.03	0.25±0.07	47.26±0.12	0.36±0.08	0.90±0.11	49.72±0.11	100.01±0.28
ILM 64	1.56±0.09	0.34±0.06	47.09±0.13	0.35±0.22	0.77±0.13	49.42±0.38	99.53±0.37
ILM 65	0.38±0.06	0.32±0.03	41.98±0.33	0.40±0.16	0.36±0.15	55.10±0.33	98.55±0.63
ILM 66	1.41±0.05	0.27±0.04	48.07±0.10	0.28±0.17	0.89±0.07	49.88±0.17	100.80±0.21
ILM 67	1.46±0.05	0.23±0.04	47.86±0.16	0.38±0.33	0.90±0.05	49.36±0.15	100.19±0.34
ILM 68	1.48±0.04	0.31±0.14	47.45±0.23	0.33±0.13	0.88±0.11	49.74±0.40	100.19±0.25
ILM 69	-*	0.14±0.02	53.81±0.37	0.13±0.13	2.46±0.06	45.12±0.63	101.70±0.22
ILM 70	-	-	53.90±0.94	0.40±0.26	1.82±0.21	42.14±1.19	98.26±0.15
ILM 71	1.58±0.02	0.28±0.08	47.60±0.51	0.36±0.05	0.83±0.09	49.97±0.09	100.63±0.69
ILM 72	1.52±0.05	0.25±0.04	47.94±0.27	0.32±0.16	0.84±0.10	49.82±0.20	100.68±0.40
ILM 73	1.52±0.07	0.25±0.04	48.01±0.38	0.31±0.17	0.81±0.12	50.14±0.03	101.04±0.48
ILM 74	1.63±0.02	0.25±0.01	47.43±0.36	0.55±0.31	0.66±0.08	50.84±0.53	101.36±0.83
ILM 75	1.98±0.05	0.26±0.05	46.90±0.17	0.38±0.11	0.87±0.07	50.96±0.33	101.36±0.44
ILM 76	1.36±0.03	0.28±0.04	48.44±0.27	0.46±0.27	1.01±0.19	50.30±0.66	101.86±0.47
ILM 77	1.61±0.04	0.21±0.15	47.55±0.22	1.03±0.26	0.62±0.04	50.46±0.15	101.48±0.13
ILM 78	1.91±0.06	0.40±0.03	47.84±0.29	0.33±0.21	0.65±0.04	49.99±0.31	101.11±0.35
ILM 79	1.47±0.06	0.24±0.03	47.55±0.29	0.33±0.30	0.96±0.17	49.86±0.47	100.41±0.49
ILM 80	1.33±0.11	0.27±0.09	47.36±0.29	0.54±0.19	0.88±0.11	49.86±0.35	100.23±0.65
ILM 81	1.52±0.05	0.27±0.04	47.33±0.34	0.58±0.22	0.76±0.04	50.36±0.57	100.82±1.12
Mean	1.43±0.35	0.27±0.06	47.17±1.69	0.42±0.14	0.83±0.32	49.10±1.74	99.23±1.35
Max.	2.16	0.42	53.90	1.03	2.57	55.10	101.86
Min.	-	-	41.98	0.13	0.36	41.13	96.55

* Below detection limit

Table 15. Average element concentration (wt. % and standard deviation (1 σ)) of grains from the fossil meteorite.

	MgO	Al ₂ O ₃	TiO ₂	V ₂ O ₃	Cr ₂ O ₃	MnO	FeO	ZnO	Total
<i>Fossil met. EC</i>									
EC1	2.37±0.32	6.46±0.24	2.77±0.08	0.84±0.19	61.77±0.37	-*	24.42±1.90	0.05±0.09	98.69±2.09
EC2	2.8±0.43	7.07±0.40	2.58±0.32	0.82±0.07	60.68±1.74	1.06±0.24	26.3±5.08	1.93±2.83	103.24±1.55
EC3	2.24±0.45	6.76±0.18	2.48±0.16	0.71±0.05	60.28±1.97	0.99±0.32	21.48±2.85	6.83±1.48	101.77±2.59
EC4	2.52±0.27	6.23±0.10	2.77±0.05	0.80±0.08	59.44±0.26	1.07±0.03	27.42±2.09	0.69±0.36	100.59±2.48
EC5	2.92±0.13	6.28±0.49	2.67±0.37	0.74±0.12	59.09±0.50	0.85±0.09	27.47±2.30	1.05±0.41	101.07±2.59
EC6	2.31±0.29	6.28±0.38	2.36±0.13	0.86±0.06	59.22±1.33	0.86±0.10	28.42±1.14	0.26±0.45	100.57±1.49
EC7	3.42±3.12	7.01±6.87	2.36±0.16	0.77±0.18	59.35±0.40	1.20±0.25	24.91±0.53	3.96±1.16	102.99±0.71
EC8	2.30±0.42	6.37±0.13	2.61±0.01	0.73±0.10	58.73±0.47	0.83±0.11	29.48±1.24	0.30±0.52	101.35±1.63
EC9	3.09±0.12	6.53±0.16	2.62±0.07	0.72±0.14	60.40±1.58	1.15±0.14	27.37±1.88	0.85±1.47	102.72±1.86
EC10	2.80±0.13	6.52±0.55	2.32±0.30	0.89±0.16	60.80±3.49	1.05±0.09	25.06±3.83	1.09±0.89	100.53±0.98
EC11	2.55±0.54	6.57±0.17	2.51±0.33	0.71±0.06	59.12±1.38	0.95±0.19	24.91±2.64	3.17±1.86	100.50±2.51
EC12	2.36±0.49	6.69±0.30	2.55±0.18	0.83±0.11	60.71±2.95	1.14±0.09	25.14±4.74	1.34±0.72	100.76±2.47
EC13	2.73±0.58	6.85±0.40	2.18±0.21	0.79±0.06	61.00±1.59	1.19±0.03	23.39±3.90	1.46±1.02	99.60±2.13
EC14	2.34±0.51	6.79±0.06	2.43±0.14	0.80±0.17	62.85±1.38	1.15±0.26	22.63±1.52	1.79±1.13	100.78±1.72
EC15	2.11±0.77	6.61±0.37	2.48±0.03	0.89±0.13	60.83±2.70	0.64±0.56	21.83±4.06	3.84±2.59	99.24±0.78
EC16	3.39±0.27	6.48±0.45	2.21±0.09	0.80±0.16	61.03±2.62	1.25±0.26	26.11±1.34	0.66±0.35	101.93±1.60
EC17	3.24±0.37	6.42±0.06	2.76±0.08	0.83±0.15	59.19±0.92	1.02±0.20	28.37±0.36	0.62±0.43	102.44±1.43
EC18	3.31±0.22	6.33±0.14	2.86±0.14	0.80±0.06	59.65±1.64	1.14±0.12	26.96±0.60	1.19±1.07	102.24±0.31
EC19	2.81±0.70	6.45±0.34	2.87±0.19	0.75±0.11	60.89±3.81	0.29±0.50	25.95±3.99	0.61±0.67	100.63±0.74
EC20	2.58±0.34	6.30±0.27	2.90±0.12	0.77±0.04	58.25±0.13	0.74±0.08	23.97±1.56	3.50±0.93	99.01±0.99
EC21	2.76±0.27	6.37±0.26	2.61±0.25	0.78±0.11	58.11±0.33	1.13±0.31	27.19±1.17	1.08±0.61	100.02±0.88
EC22	2.88±0.61	6.30±0.11	2.24±0.23	0.83±0.12	57.09±0.61	1.10±0.24	26.12±2.59	2.35±1.84	98.91±0.61
EC23	2.70±0.10	6.26±0.16	2.48±0.12	0.79±0.15	57.57±0.59	1.00±0.19	27.55±0.87	1.28±0.76	99.63±0.65
EC24	2.73±0.20	6.31±0.11	2.69±0.26	0.80±0.02	57.18±0.27	1.00±0.18	27.31±1.12	1.53±0.64	99.51±0.91
EC25	2.83±0.27	6.17±0.10	2.99±0.18	0.80±0.09	58.17±0.97	0.79±0.13	27.35±1.75	0.66±0.19	99.77±0.45
EC26	3.00±0.41	5.95±0.02	3.16±0.18	0.73±0.06	57.74±0.90	1.01±0.13	27.10±1.25	0.40±0.34	99.10±0.33
EC27	2.71±0.18	6.28±0.06	2.72±0.11	0.86±0.13	57.62±0.15	0.82±0.14	28.34±0.28	0.22±0.07	99.57±0.25
EC28	2.39±0.04	6.33±0.16	2.05±0.01	0.81±0.12	57.52±0.68	0.97±0.17	28.66±0.24	0.43±0.18	99.16±0.72
EC29	2.02±0.32	6.44±0.28	2.35±0.13	0.72±0.11	57.87±1.43	0.73±0.29	27.81±2.23	0.60±0.28	98.55±1.33
EC30	2.95±0.22	6.35±0.21	2.68±0.19	0.84±0.17	57.39±0.05	0.95±0.22	26.00±0.06	2.08±0.46	99.25±0.35
EC31	1.90±1.11	6.00±0.48	2.69±0.21	0.83±0.02	59.36±0.74	0.89±0.24	27.26±2.48	1.46±1.96	100.40±2.51
EC32	2.49±0.54	6.67±0.22	2.57±0.19	0.80±0.09	60.86±2.49	0.85±0.24	26.22±4.99	0.53±0.13	101.01±3.02
EC33	2.08±0.31	7.00±1.50	2.49±0.06	0.72±0.06	60.66±3.47	1.08±0.18	25.58±5.59	1.52±0.93	101.11±0.22
EC34	1.88±0.84	7.35±1.20	2.50±0.07	0.91±0.18	60.50±1.40	0.69±0.14	21.65±4.30	4.03±1.71	99.51±2.63
EC35	2.40±0.35	6.64±0.42	2.55±0.02	0.91±0.07	60.47±0.93	0.66±0.11	26.22±5.49	0.57±0.12	100.41±2.59
EC36	2.63±0.32	6.68±0.45	2.37±0.31	0.76±0.10	60.25±1.93	0.87±0.20	25.71±4.23	0.66±0.20	99.92±1.78
EC37	2.29±0.17	6.34±0.04	2.56±0.07	0.74±0.13	58.69±0.29	0.89±0.11	29.22±0.19	0.36±0.07	101.08±0.12
EC38	2.49±0.29	6.73±0.80	2.70±0.17	0.75±0.03	59.50±0.36	0.71±0.06	26.88±3.86	1.94±2.96	101.71±0.25
EC39	2.20±0.47	6.81±0.57	2.35±0.22	0.84±0.21	60.26±1.42	0.72±0.14	25.27±3.96	2.26±1.53	100.72±1.46
EC40	2.62±0.71	6.78±0.71	2.63±0.12	0.84±0.05	59.18±0.44	0.72±0.31	22.97±3.65	4.58±2.43	100.32±1.82
EC41	3.31±0.48	6.31±0.14	2.90±0.16	0.75±0.13	59.29±0.19	0.79±0.05	24.90±1.16	2.72±1.22	100.97±0.94
EC42	2.62±0.04	6.13±0.15	2.62±0.21	0.74±0.01	57.84±0.30	0.88±0.06	27.52±1.01	1.25±1.19	99.60±0.16
EC43	1.89±0.17	6.47±0.21	2.26±0.21	0.73±0.13	58.79±0.42	0.78±0.05	26.09±2.10	0.93±0.69	97.94±1.06
EC44	2.38±0.23	6.26±0.37	2.48±0.08	0.76±0.05	57.38±0.24	0.97±0.14	23.78±1.34	5.03±1.11	99.03±0.89
EC45	3.03±0.18	6.11±0.05	2.87±0.17	0.80±0.11	57.70±0.57	0.88±0.15	27.58±0.65	0.78±0.50	99.75±0.35
EC46	2.64±0.09	6.44±0.33	2.59±0.13	0.77±0.08	58.30±0.49	0.79±0.14	27.81±0.93	0.69±0.50	100.03±0.47
EC47	2.09±0.18	6.24±0.15	2.66±0.09	0.76±0.12	57.82±0.64	0.98±0.06	28.53±1.67	0.38±0.43	99.45±1.33
Mean	2.60±0.40	6.48±0.29	2.58±0.23	0.79±0.05	59.28±1.40	0.92±0.19	26.13±2.00	1.61±1.47	100.36±1.21
Max.	3.42	7.35	3.16	0.91	62.85	1.25	29.48	6.83	103.24
Min.	1.88	5.95	2.05	0.71	57.09	-	21.48	0.05	97.94
<i>F.MET. OTR</i>									
OTR1	1.73±0.10	-	69.57±2.95	-	-	0.41±0.36	25.50±2.84	-	97.21±0.84

* Below detection limit

**Tidigare skrifter i serien
”Examensarbeten i Geologi vid Lunds
Universitet”:**

188. Nilsson, Eva K., 2005: Extinctions and faunal turnovers of early vertebrates during the Late Silurian Lau Event, Gotland, Sweden.
189. Czarniecka, Ursula, 2005: Investigations of infiltration basins at the Vomb Water Plant – a study of possible causes of reduced infiltration capacity.
190. G³owacka, Ma³gorzata, 2005: Soil and groundwater contamination with gasoline and diesel oil. Assessment of subsurface hydrocarbon contamination resulting from a fuel release from an underground storage tank in Vanstad, Skåne, Sweden.
191. Wennerberg, Hans, 2005: A study of early Holocene climate changes in Småland, Sweden, with focus on the ‘8.2 kyr event’.
192. Nolvi, Maria & Thorelli, Gunilla, 2006: Extraterrestrisk och terrestrisk kromrik spinell i fanerozoiska kondenserade sediment.
193. Nilsson, Andreas, 2006: Palaeomagnetic secular variations in the varved sediments of Lake Goëci¹, Poland: testing the stability of the natural remanent magnetization and validity of relative palaeointensity estimates.
194. Nilsson, Anders, 2006: Limnological responses to late Holocene permafrost dynamics at the Stordalen mire, Abisko, northern Sweden.
195. Nilsson, Susanne, 2006: Sedimentary facies and fauna of the Late Silurian Bjärsjölagård Limestone Member (Klinta Formation), Skåne, Sweden.
196. Sköld, Eva, 2006: Kulturlandskapets förändringar inom röjningsröseområdet Yttra Berg, Halland - en pollenanalytisk undersökning av de senaste 5000 åren.
197. Göransson, Ammy, 2006: Lokala miljöförändringar i samband med en plötslig havsyteförändring ca 8200 år före nutid vid Kalvöviken i centrala Blekinge.
198. Brunzell, Anna, 2006: Geofysiska mätningar och visualisering för bedömning av heterogenitetens utbredning i en isälvsavlagring med betydelse för grundvattenflöde.
199. Erlfeldt, Åsa, 2006: Brachiopod faunal dynamics during the Silurian Ireviken Event, Gotland, Sweden.
200. Vollert, Victoria, 2006: Petrografisk och geokemisk karaktärisering av metabasiter i Herrestadsområdet, Småland.
201. Rasmussen, Karin, 2006: En provenansstudie av Kågerödformationen i NV Skåne – tungmineral och petrografi.
202. Karlsson, Jonnina, P., 2006: An investigation of the Felsic Ramiane Pluton, in the Monapo Structure, Northern Moçambique.
203. Jansson, Ida-Maria, 2006: An Early Jurassic conifer-dominated assemblage of the Clarence-Moreton Basin, eastern Australia.
204. Striberger, Johan, 2006: En lito- och biostratigrafisk studie av senglaciala sediment från Skuremåla, Blekinge.
205. Bergelin, Ingemar, 2006: ⁴⁰Ar/³⁹Ar geochronology of basalts in Scania, S Sweden: evidence for two pulses at 191-178 Ma and 110 Ma, and their relation to the break-up of Pangea.
206. Edvarsson, Johannes, 2006: Dendrokronologisk undersökning av tallbestånds etablering, tillväxtdynamik och degenerering orsakat av klimatrelaterade hydrologiska variationer på Viss mosse och Åbuamossen, Skåne, södra Sverige, 7300-3200 cal. BP.
207. Stenfeldt, Fredrik, 2006: Litostratigrafiska studier av en plåtformad sand- och grusavlagring i Skuremåla, Blekinge.
208. Dahlenborg, Lars, 2007: A Rock Magnetic Study of the Åkerberg Gold Deposit, Northern Sweden.
209. Olsson, Johan, 2007: Två svekofenniska graniter i Bottniska bassängen; utbredning, U-Pb zirkondatering och test av olika abrasionstekniker.
210. Erlandsson, Maria, 2007: Den geologiska utvecklingen av västra Hamrängesyklinallens suprakrustalbergarter, centrala Sverige.
211. Nilsson, Pernilla, 2007: Kvidingedeltat – bildningsprocesser och arkitektonisk uppbyggnadsmodell av ett glacifluvialt Gilbertdelta.
212. Ellingsgaard, Óluva, 2007: Evaluation of wireline well logs from the borehole Kyrkheddinge-4 by comparison to measured core data.

213. Åkerman, Jonas, 2007. Borrkärnekartering av en Zn-Ag-Pb-mineralisering vid Stenbrånet, Västerbotten.
214. Kurlovich, Dzmitry, 2007: The Polotsk-Kurzeme and the Småland-Blekinge Deformation Zones of the East European Craton: geomorphology, architecture of the sedimentary cover and the crystalline basement.
215. Mikkelsen, Angelica, 2007: Relationer mellan grundvattenmagasin och geologiska strukturer i samband med tunnelborrning genom Hallandsås, Skåne.
216. Trondman, Anna-Kari, 2007: Stratigraphic studies of a Holocene sequence from Taniente Palet bog, Isla de los Estados, South America.
217. Månsson, Carl-Henrik & Siikanen, Jonas, 2007: Measuring techniques of Induced Polarization regarding data quality with an application on a test-site in Aarhus, Denmark and the tunnel construction at the Hallandsås Horst, Sweden.
218. Ohlsson, Erika, 2007: Classification of stony meteorites from north-west Africa and the Dhofar desert region in Oman.
219. Åkesson, Maria, 2008: Mud volcanoes - a review. (15 hskp)
220. Randsalu, Linda, 2008: Holocene relative sea-level changes in the Tasiusaq area, southern Greenland, with focus on the Ta1 and Ta3 basins. (30 hskp)
221. Fredh, Daniel, 2008: Holocene relative sea-level changes in the Tasiusaq area, southern Greenland, with focus on the Ta4 basin. (30 hskp)
222. Anjar, Johanna, 2008: A sedimentological and stratigraphical study of Weichselian sediments in the Tvärkroken gravel pit, Idre, west-central Sweden. (30 hskp)
223. Stefanowicz, Sissa, 2008: Palynostratigraphy and palaeoclimatic analysis of the Lower - Middle Jurassic (Pliensbachian - Bathonian) of the Inner Hebrides, NW Scotland. (15 hskp)
224. Holm, Sanna, 2008: Variations in impactor flux to the Moon and Earth after 3.85 Ga. (15 hskp)
225. Bjärnberg, Karolina, 2008: Internal structures in detrital zircons from Hamrånge: a study of cathodoluminescence and back-scattered electron images. (15 hskp)
226. Noresten, Barbro, 2008: A reconstruction of subglacial processes based on a classification of erosional forms at Ramsvikslandet, SW Sweden. (30 hskp)
227. Mehlqvist, Kristina, 2008: En mellanjurassisk flora från Bagå-formationen, Bornholm. (15 hskp)
228. Lindvall, Hanna, 2008: Kortvariga effekter av tefranedfall i lakustrin och terrestrisk miljö. (15 hskp)
229. Löfroth, Elin, 2008: Are solar activity and cosmic rays important factors behind climate change? (15 hskp)
230. Damberg, Lisa, 2008: Pyrit som källa för spårämnen – kalkstenar från övre och mellersta Danien, Skåne. (15 hskp)
331. Cegrell, Miriam & Mårtensson, Jimmy, 2008: Resistivity and IP measurements at the Bolmen Tunnel and Ådalsbanan, Sweden. (30 hskp)
232. Vang, Ina, 2008: Skarn minerals and geological structures at Kalkheia, Kristiansand, southern Norway. (15 hskp)
233. Arvidsson, Kristina, 2008: Vegetationen i Skandinavien under Eem och Weichsel samt fallstudie i submoräna organiska avlagringar från Nybygget, Småland. (15 hskp)
234. Persson, Jonas, 2008: An environmental magnetic study of a marine sediment core from Disko Bugt, West Greenland: implications for ocean current variability. (30 hskp)
235. Holm, Sanna, 2008: Titanium- and chromium-rich opaque minerals in condensed sediments: chondritic, lunar and terrestrial origins. (30 hskp)



LUNDS UNIVERSITET